IN VITRO, ENZYME MEDIATED SYNTHESIS OF NANOPARTICLES – SIZE AND SHAPE CONTROL USING SYNTHETIC PEPTIDES AND THEIR APPLICATION

A THESIS SUBMITTED TO THE

UNIVERSITY OF PUNE

FOR THE DEGREE OF

DOCTOR OF PHILOSOPHY

(IN BIOTECHNOLOGY)

BY

ABU AYOOBUL ANSARY

UNDER THE GUIDANCE OF

DR. SUSHAMA M. GAIKWAD

DIVISION OF BIOCHEMICAL SCIENCES
NATIONAL CHEMICAL LABORATORY
PUNE – 411008 (INDIA)

AUGUST 2011

CONTENTS

CERTIFICATE

Certified that the work incorporated in the thesis entitled "**In vitro, enzyme mediated synthesis of nanoparticles – size and shape control using synthetic peptides and their application**" submitted by Mr. Abu Ayoobul Ansary was carried out under my supervision. Such material as has been obtained from other sources has been duly acknowledged in the thesis.

Dr. Sushama M. Gaikwad

Research Guide

DECLARATION OF THE CANDIDATE

I declare that the thesis entitled **"In vitro, enzyme mediated synthesis of nanoparticles – size and shape control using synthetic peptides and their application"** submitted by me for the degree of Doctor of Philosophy is the record of work carried out by me during the period from **1st of April, 2008 to 14th of February, 2011** under the guidance of **Dr. Sushama M. Gaikwad** and has not formed the basis for the award of any degree, diploma, associateship, fellowship, titles in this or any other University or other institute of Higher learning.

I further declare that the material obtained from other sources has been duly acknowledged in the thesis.

Signature of the Candidate Date:

Abu Ayoobul Ansary

ABSTRACT

Nanotechnology deals with the production, properties and manipulation of materials at the nanoscale. It gained importance because of the occurrence of novel properties when materials reach the nanoscale. Nanomaterials have found applications in a wide variety of fields ranging from energy storage, space sciences, biomedicine, catalysis, etc.

Nanoparticles have attracted lots of attention due to their shape and size-dependent properties. Investigation was carried out to study the role of enzyme reductases in the in vitro syntheses of fluorescent nanoparticles and the effect of synthetic peptides on the size and shape control of nanoparticles.

Chapter 1: Introduction

This chapter gives a brief introduction to nanotechnology with emphasis on quantum dots, the various methods of syntheses of nanomaterials and their applications.

Chapter 2: Materials and methods

This chapter presents the various materials and methods used during the course of the investigation. Optical properties were analysed using UV-Visible and fluorescence spectroscopy. Structural analyses of nanoparticles were performed using powder X-ray diffraction and X-ray photoelectron spectroscopy. Morphological analysis was done using transmission electron spectroscopy.

Chapter 3: Results

This chapter summarizes the various results obtained during the course of the investigation. The appearance of absorbance band indicated the in vitro enzyme mediated synthesis of fluorescent nanoparticles such as CdSe, PbS, Co_3S_4 and Ni_7S_6. The absence of absorbance band in the absence of enzyme reductase and synthetic peptides indicated the involvement of enzymes and peptides in the synthesis of nanoparticles. Size distribution analysis by dynamic light scattering technique revealed that synthetic peptides were responsible for the size control of fluorescent nanoparticles under study. Morphological analysis revealed that all the as-synthesized fluorescent nanoparticles were essentially quasi-spherical in shape with the exception of Ni_7S_6 which was found to be ‘tear-drop’ shaped. Analyses of optical properties revealed that the as-synthesized fluorescent nanoparticles possess large band gaps characteristics of semiconductor nanocrystals. Structural analyses revealed that all the as-synthesized nanoparticles were crystalline in nature and are pure-phased. As-synthesized

CdSe nanoparticles have been found to contain phases corresponding to the CdO phase. Chemical analyses of the nanoparticles matched well with the corresponding bulk materials. The as-synthesized nanoparticles have been found to possess free reactive amino groups on their surface. CdS and CdSe nanoparticles have been conjugated with bi/tri-antennary glycopeptides for potential biomedical applications. The conjugation of CdSe nanoparticles with glycopeptides resulted in the alteration of the optical properties towards lower wavelength of the spectrum.

Chapter 4: Discussion

Enzymes, nitrate reductase has been found to synthesize CdSe nanoparticles while sulphite reductase in the syntheses of metal sulphide nanoparticles such as PbS, Co_3S_4 and Ni_7S_6, in the presence of synthetic peptides. The synthetic peptides have been found to bind to the as-synthesized nanoparticles providing stability. The size, secondary structure and composition of amino acids have been found to play roles in the synthesis, control of size and shape of as-synthesized fluorescent nanoparticles. A hypothetical mechanism of the synthesis of nanoparticles using enzyme reductases and synthetic peptides has been proposed.

Chapter 5: Summary and conclusions

This chapter summarizes the key findings of the investigation and discusses the significance and scopes of the current study.

ABBREVIATIONS

QD	- Quantum dots
LASER	- Light absorption and stimulated emission of radiation
USP	- Ultrasonic spray pyrolysis
HDA	- Hexadecylamine
TDPO	- tetradecylphosphine oxide
TOPO	- tri-n-octylphosphine oxide
TBP	- tri-n-butylphosphine
DNA	- Deoxyribonucleic acid
RNA	- Ribonucleic acid
PD	- Phage display
CSD	- Cell surface display
FTIR	- Fourier transformed infrared
L-DOPA	- L-3,4-dihydroxyphenylalanine
NADPH	- Nicotinamide Adenine Dinucleotide Phosphate, reduced
t-RNA	- transfer RNA
PVP	- Poly-Vinyl-Pyrrolidone
CTAB	- Cetyl Tri-methyl ammonium bromide
CTAC	- Cetyl Tri-methyl ammonium chloride
ACA	- 1- adamantanecarboxylic acid
OLA	- Oleylamine
AA	-1-adamantaneamine
FMBMN	- Fluorescent-magnetic-biotargeting multifunctional Nanobioprobes
OLET	- Organic light emitting transistors
PDA	- Potato dextrose agar

DEAE	- Di-ethyl-amino-ethane
MES	- 2-(N-Morpholino) Ethanesulphonic acid
EDTA	- Ethylene-di-amine tetraacetic acid
CM	- Carboxymethyl
BSA	- Bovine Serum Albumine
SDS	- Sodium dodecyl sulphate
PAGE	- Polyacrylamide electrophoresis
CP	- Capping peptide
EDC	- N-Ethyl-N′-(3-dimethylaminopropyl)carbodiimide
NTEE	- Nitro-tyrosine ethyl ester
HEPES	- (4-(2-hydroxyethyl)-1-piperazineethanesulfonic acid)
TNBS	- Tri-nitrobenzene sulphonic acid
TCA	- Trichloro Acetic Acid
CD	- Circular Dichroism
DLS	- Dynamic light scattering
FFT	- Fast fourier transformed
SAED	- Selected Area Electron Diffraction
FWHM	- full-width-half-maximum
XRD	- X-ray diffraction
XPS	- X-ray photoelectron spectroscopy
PAA	- Poly-(acrylic acid)
BAGP	- Bi-antennary glycopeptide
TAGP	- Tri-antennary glycopeptide

ACKNOWLEDGEMENT

I take this opportunity to gratefully acknowledge my guide ***Dr. Sushama M. Gaikwad*** *for her guidance and keen interest during the course of this investigation. She gave me the freedom to think, and work; and I shall cherish my learning experience under her guidance.*

I am grateful to Late ***Dr. M. I. Khan*** *for his unparalleled guidance, love and care during the course of this study. I derive a great deal of enthusiasm and courage from his astounding knowledge of science, extraordinary thinking and consummate problem solving skills.*

The love and care shown by ***Mrs. Kausar Khan*** *is fondly remembered.*

I find no words to express my gratefulness for my ***Parents*** *whose patience and unconditional support made me achieve this feat. I am also thankful to my* ***Brothers, Sister, Cousins*** *and other* ***Family members****, who have been a moral support to me, standing by me and boosting my morale in times of stress. I am grateful to my* ***Wife*** *for her extreme patience and love that helped me accomplish this work with ease.*

I am thankful to ***Dr. Sumedha S. Deshmukh*** *for her kind nature and guidance.*

I am grateful to ***Dr. Siddharth H. Bhosle*** *for his technical help.*

I am also grateful ***Dr. M. V. Krishnasastry*** *and* ***Dr. C. G. Suresh*** *for their valuable suggestions during the course of investigation.*

I would also like to extend my sincere thanks to:

Dr. K. N. Ganesh*, Organic Chemistry, NCL, for permission to use the CD facility*

Dr. P. A. Joy*, Physical Chemistry Division, NCL, for permitting to use the powder X-Ray diffraction facility*

Dr. Kashinath Patil*, Centre for materials characterization for XPS analyses*

Dr. Krishna Gholap*,* ***Mr. Narendar, Mr. Pandiaraj*** *and* ***Mr. Anuj****, Centre for materials characterization for HR-TEM analyses*

I am grateful to ***Farid bhai, Mulla sir, Kotwal sir*** *and* ***Imran sir*** *for their encouragement and moral support during my stay at NCL.*

Special thanks are due to my labmates, ***Avinash Kumar, Madhurima, Sonali*** *and* ***Sayali*** *for their continuous support.*

I am indebted to my friends ***Sajid Khan, Imran, Mujahid, Saravanan, Madhu,*** *and* ***Geetha,*** *who were my pillars of strength.*

I express my deep feelings and love for my ex-labmates and friends ***Drs. Feroz Khan, Atul Thakur, Anil Kumar, Sajid Khan, Nagaraj, Shabab, JP, Shashi, Sreekanth, Rohtas,*** *for their relentless help, support and company during my stay at NCL.*

My friends ***Chetan, Azfar, Faisal, Atul, Asad, Vicky, Meera, Dipti, Fazal, Avinash, Manisha, Ruby, Shadab, Raju, Poonam, Ravi, Prasad, Santhosh Jadhav, Santhosh Kumar, Ishwar, Merlyn, Vishnu, Deepti, Ali Azarifar, Muhammed Ali, Ramya, Sagar Bhat, Elmira, Amol, Ruchita*** *and* ***Vaibhav*** *are second to none.*

Finally, I thank ***Head****, Division of Biochemical Sciences and the* ***Director****, National Chemical Laboratory, for permitting me to submit this work in the form of the thesis, and the Council of Scientific and Industrial Research, India for financial assistance.*

Abu Ayoobul Ansary

CHAPTER: 1

INTRODUCTION

Nanotechnology is an enabling technology that deals with the manipulation of matter in the scale ranging from 1 to 100 nm[1]. It is a collection of technologies, devices and process that enable us to synthesize, manipulate, characterize and utilize matter by controlling the size and shape of materials at the nanoscale[2]. Hence any technology or method or design that enables us to understand and study the property of matter at the nanoscale is called as Nanotechnology[3]. At this range of size, matter tends to have properties that are different from those attributed to bulk matter of the same material. The properties of matter at the nanoscale are explained based on the laws of quantum mechanics rather than the laws of classical mechanics that is used to explain bulk materials. Nanomaterials tend to have exquisite mechanical, electronic, thermal, catalytic and magnetic properties that are not characteristics of the corresponding bulk matter. Due to these new found properties, nanomaterials have found potential applications in a wide range of industries from space science, electronics, catalysis, cosmetics, medicine, energy, automobile, etc.

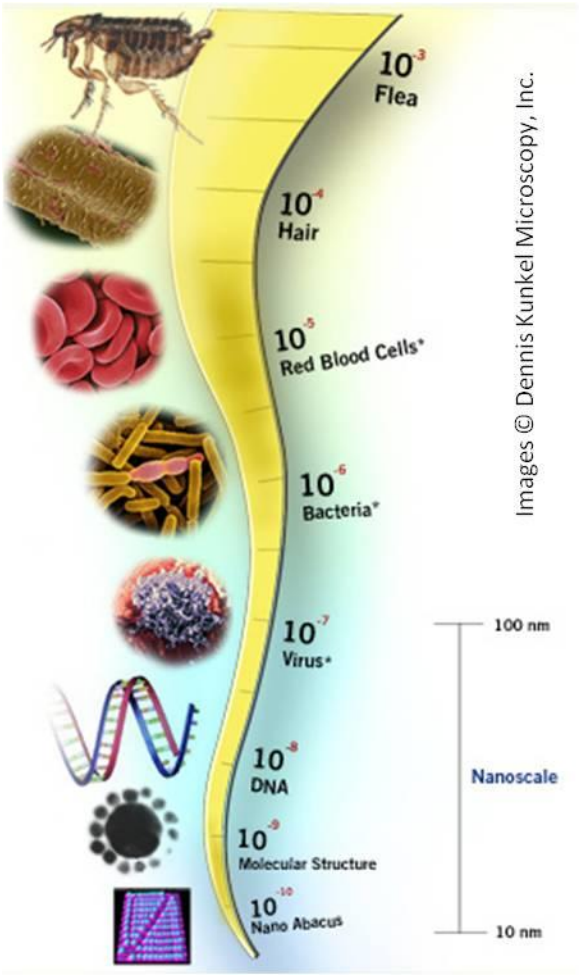

Fig. 1.1: *Size comparison of materials – natural and man-made*

Moreover, a vast majority of the components found in nature that are involved in a variety of functions ranging from maintaining homeostasis of living systems to extraction of metals, operate at the nano scale. These natural entities are highly ordered and function with very high efficiency and specificity. Hence, the scientific interest in this interface of biology and technology is based on the perception that

nanotechnology can lead to the development of potentially interesting and useful functional nanosystems.

Quantum confinement

As the size of matter approaches the nanoscale, the properties of the materials are governed by the laws of quantum mechanics. The change in the properties of nanomaterials can be understood by studying the electronic structure and quantum confinement of nanomaterials. Since quantum dots are smaller than the Bohr's radius, quantum confinement effects predominate their properties. The basic concept of quantum confinement comes from the interplay of two fundamental principles of quantum mechanics; namely the electronic system must obey the Schrödinger equation and also follow the de Broglie momentum-wavelength relationship.

In order to qualify for a quantum structure, the material should have at least one dimension smaller than the de Broglie's wavelength, λ;

$$\lambda = h/p,$$

where, h – planck's constant, $p = hk/2\pi$ is the momentum of the electron in the sample at temperature T. If we take $E = 3/2\ kt = p^2 / 2m$, E the kinetic energy, k Boltzmann's constant and m the mass of the electron (or hole) we find at room temperature (~300 K) to be ~6 nm. This means that for the spherical crystal of diameter D < 6 nm the electrons (or holes) wave packet is squeezed somewhat unnaturally into a space smaller than it normally likes to have. The result is, the electron takes a higher energy than it would normally have in its host structure. Another way of looking at this effect is to say that the natural exciton Bohr radius is larger than the host crystal structure. Such small host crystals are called quantum dots

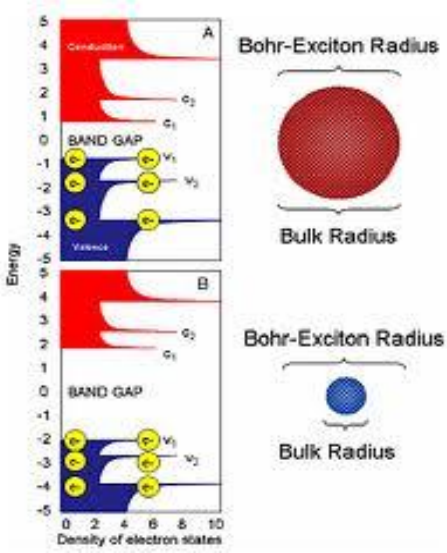

Fig.1.2: *Schematic comparison of band gap structures of bulk and quantum confined semicondcutors*

and the resulting physical state is called quantum confinement. Fig.1.2 represents the comparison of band gap structures of bulk and quantum confined semiconductors.

Quantum dots

Quantum dots (QDs) are semiconductor nanocrystals typically in the size range of 1 – 20 nm. They contain as few as 100 to 100,000 atoms per particle. QDs exhibit novel properties that are between bulk counterparts and discrete molecules due to their confinement in all the three dimensions. Technically, they are crystal structures whose natural Bohr radius is larger than those of the host crystal structure. The properties of a traditional semiconductor are fixed. This is due to the shortcoming that their optical and electronic properties are difficult to manipulate since their intrinsic band gap is hardly tunable. QDs exhibit discrete and quantized electronic energy levels due to their extremely small size. The energy difference between the energy levels is dependent on the diameter of the nanocrystal and hence can be manipulated by varying the size of the nanocrystal. Fig.1.3 provides a over-view of emission properties achieved for quantum dots of various sizes.

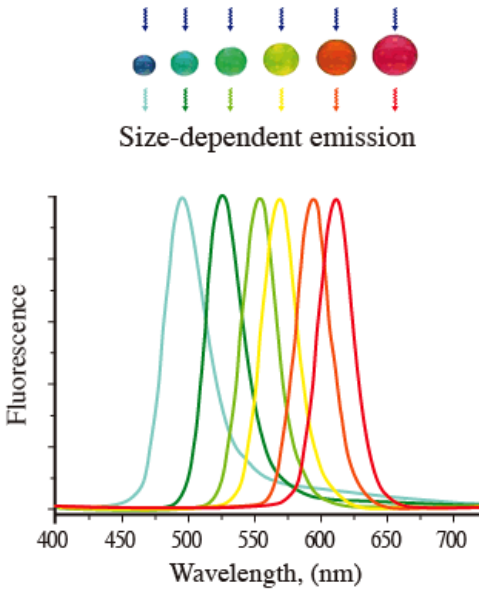

Fig.1.3: *Size-dependent emission properties of quantum dots*

The most common QDs are the binary semiconductor compounds consisting of II-VI elements, i.e., cadmium sulfide (CdS), cadmium selenide (CdSe), cadmium telluride (CdTe), zinc selenide (ZnSe), lead sulfide (PbS), and mercury sulfide (HgS), etc. There are also some QDs comprising III-V elements, i.e., indium phosphide (InP), gallium nitride (GaN), indium arsenide (InAs), etc. Moreover, some QDs composed of single element (such as silicon), or of ternary elements with two of them in either cation or anion site (such as CdZnS, CdSSe, InNP, etc.) have also been reported. The bulk counter parts with the above composition of QDs are semiconductors typically with a band gap of less than 4 eV. In order to study the variation in the properties of QDs with corresponding change in particular size and shape, reliable methods of synthesis have

to be developed. An ideal method would be one that addresses all the shortcomings with reference to particle size, shape and distribution. Yet each method has its own advantages and disadvantages. These methods serve as a preliminary approach towards the development of efficient synthesis protocols and subsequent manipulation of nanomaterials.

Synthesis of Quantum dots

Quantum dots have found use in a wide range of applications. To date, numerous synthesis methods have been developed for the synthesis and manipulation of quantum dots. All these methods are broadly classified into

i. Physical methods
ii. Chemical methods
iii. Biosynthetic methods

i. Physical methods:

Physical methods of synthesis of nanomaterials mostly employ the Top-down approach where in the parent material is cut into the desired end-product by using mechanical means such as LASERs, ball mills, pyrolysis, etc. In this approach, the stoichiometry of the material remains unaltered from the parent material to the end-product since there is no chemical reaction involved in this process. Some of the most commonly used physical methods for the synthesis of nanomaterials are discussed here. Table 1 summarizes the various physical and chemical methods for the synthesis of nanomaterials.

a. Nanolithography

The most commonly used top down fabrication technique is nanolithography. In this process, required material is protected by a mask and the exposed material is etched away. Depending upon the level of resolution required for features in the final product, etching of the base material can be done chemically using acids or mechanically using ultraviolet light, x-rays or electron beams. This technique is widely used for the manufacture of microchips.

Some of the variations of this technique and the resolutions achieved are:

i. Photolithography micro contact printing - 200 nm
ii. Particle lithography - 90 nm

iii. X-Ray, electron and ion-beam lithography - 10 nm

iv. AFM based lithography - 1 nm

v. STM based lithography - 1 angstrom

b. LASER ablation

In laser ablation, high-power laser pulses are used to evaporate matter from a target surface such that the stoichiometry of the material is preserved in the interaction. A supersonic jet of particles (plume) is ejected normal to the target surface and the ablated species condense on the substrate placed opposite to the target. The ablation process takes place either in vacuum or in the presence of some background gas such as oxygen for oxides. In addition, the substrate temperature has to be sufficiently large (700-800°C) to obtain epitaxial films.

Semiconductor nanowires, metal nanoparticles such as Silver, Gold, Nickel, colloidal metal nanoparticles and ceramics have been reported using this technique[4-9]. Quantum dots such as GaAs and CdS, β-SiC and PbTe have been synthesized using LASER ablation technique[10-11].

c. Spray pyrolysis

Spray pyrolysis is a process in which a thin film is deposited by spraying a solution on a heated surface, where the constituents react to form a chemical compound. The chemical reactants are selected such that the products other than the desired compound are volatile at the temperature of deposition. The process is particularly useful for the deposition of oxides and has long been a production method for applying a transparent electrical conductor of SnOx to glass[12]. Sha Liu et al reported the synthesis of cubic ZnS nanoparticles from a low-cost single-source precursor in a continuous spray pyrolysis reactor[13]. Sensitized-type solar cells based on ZnO photoanode and CdS quantum dots (QDs) as sensitizers have been fabricated using ultrasonic spray pyrolysis (USP) deposition technique[14].

ii. Chemical methods:

In addition to the physical methods discussed above, there are numerous purely chemical methods for the production of nanoparticles. Chemical methods can be used for the production of nanoparticles in large quantities where as physical methods lack this attribute severely. Meanwhile nanomaterials produced through chemical methods

are prone to contain impurities while in physical methods purity can be maintained to a higher degree. Some of the most common chemical methods for the production of nanoparticles are as follows.

a. Wet chemical process

This class of chemical methods typically involves the reduction of metal ions into their corresponding metal. The so-formed reduced metal coalesces to form nanoparticles. The basic components of this method are metal salts, reducing agents and capping molecules. Typically metal halides are preferred as the metal ion donor; Sodium citrate, $NaBH_4$, Ascorbic acid, etc act as reducing agent and Thiols, citrates and polymers such as PVP and PVA act as capping agents.

CdSe quantum dots (QDs) were obtained by wet chemical synthesis route, using cadmium oxide and pure selenium as precursors, hexadecylamine (HDA), tetradecylphosphine oxide (TDPO) and tri-n-octylphosphine oxide (TOPO) as complexing agents in tri-n-butylphosphine (TBP) solvent in the reactor with an argon protection atmosphere[15]. Bakar et al reported the synthesis of CdSe-CdTe core shell quantum dots using a wet-chemical process at a moderate temperature (300 °C) following two-steps process of core and shell synthesis[16].

b. Thermolysis

This method involves the decomposition of solids or liquids at high temperature having metal cations or molecular anions or organometallic compounds. Nanoparticles synthesized by this method are found as a mixture with the surrounding organic material. These nanoparticles are isolated by conventional chemical methods by dissolving the organic compounds and recovery of the nanoparticles.

Li et al described the production of CdS quantum dots and nanorods by thermolysis using a single precursor, $(Me_4N)_4[S_4Cd_{10}(SPh)_{16}]$, in hexadecylamine (HAD)[19,20]. CdS quantum dots and nano-rods were synthesized at 230°C and 220°C respectively, under vacuum.

Pros and cons of physical and chemical routes

Each and every method applied for the synthesis of quantum dots has its own merits and demerits. The option for a particular method depends on the advantages the

methods offers over others in terms of utility, ease of use, economy, the properties of the end product, etc. Some of the advantages associated with the physical and chemical routes for the synthesis of quantum dots are outlined below.

Table 1. Summary of various nanoparticles synthesized using different physical and chemical routes

Method	Nanomaterial synthesized	Reference
Nanolithography	GaN, SiGe, GaAs/AlGaAs, SiGe, InAs	21, 22, 23, 17, 18
Condensation methods	Fe, ZnS, ZnO, CdSe	24, 25, 26, 27
Spray pyrolysis	ZnS, SiO_2/ZnO, ZnO, Y_2O_3-ZrO_2, CeO_2	28, 29, 30, 31
Reduction	Co, $Fe(CO)_5$, PbSe, CdTe	32, 33, 34, 35
Thermal decomposition	ε-Co, Ag, Fe_3O_4	36, 37, 38
Polyol process	Hcp Co, Co/Ni alloy, CdSe/CdS	39, 40, 41
Sonochemical deposition	Fe, α-HgS & β-HgS, CdSe/ZnS, In_2S_3	42, 43, 44, 45

Advantages:

Physical routes:

1. In physical routes, the stoichiometry of the starting material remains unaltered till the end-product.
2. High degree of purity is achievable.
3. Angstrom level precision can be achieved in scanning tunneling microscopy based lithography.
4. Any form of shape can be fabricated

Chemical routes:

1. Ideal for large scale production of nanoparticles
2. Economical

3. Requires basic laboratory set-up
4. Better control over shape and size of nanoparticles

Disadvantages:

1. Requires sophisticated laboratory set-up and highly skilled work force.
2. Not suited for large scale production.
3. High production cost
4. Chemical routes are prone to produce impurities in the product.
5. End products require additional functionalization steps to render them aqueous soluble.
6. Employ extreme conditions such as high temperature and pressure.
7. Utilize toxic precursors and produce toxic by-products.
8. Hazardous to the environment

iii. Biosynthetic routes:

The disadvantages associated with the physical and chemical routes have prompted researchers to look for possible alternatives for the synthesis of quantum dots. One of the major draw backs of the physical and chemical routes is the involvement of ecologically hazardous reagents and chemicals, which require extreme caution during usage as well as disposal. In order to overcome this hurdle, researchers looked at nature for inspiration and have started to utilize the natural processes for the synthesis of nanoparticles in general and also of quantum dots. Nature produces and processes numerous materials for millions of years with the utmost sophistication and atomic precision. **Biomineralization** is a very good example of the processes that nature utilizes to assemble complex structures.

Some of the examples of biominerals found in nature include hard structures such as teeth, bones and shells of marine animals. These materials follow an intricate mode of synthesis and assembly, to produce materials, that is controlled at the genetic level[46-48]. The genera of diatoms present the best example of biomineralization in which macroscopic structures are formed in the intracellular or extracellular matrix by the ordered assembly of nanometer sized building blocks of mineral crystals[49].

Magnetotactic bacteria produce intracellular magnetic nanoparticles called **magnetosomes** which they utilize to align themselves along the geomagnetic field[50].

Magnetosomes are in the size range of 35-120 nm and are made of mono-dispersed crystals of magnetic iron mineral, often Fe_3O_4. More than ten different proteins have been identified so far to be present in the membrane of magnetosome[51].

In addition to the above observations, microbes are used for chemical conversion of metals as exemplified by the **bioleaching** of metals such as copper, iron, nickel, zinc, etc[52-54]. A variety of microbes including bacteria, yeast, algae, fungi, protozoa, etc has been reported to be used in bioleaching[53-56]. Microbes bring about mobilization of metals by the secretion of organic acids or inorganic acids such as sulfuric acid, oxidation or reduction reactions or secretion of metal chelating agents[57]. Microbes have evolved complex machineries to manipulate materials with high efficiency and specificity which make them attractive targets for use as nanoparticle fabricators.

The ability of biological systems to fabricate structural and functional inorganic materials of precise dimensions and controlled morphology in an eco-friendly manner has led nanotechnologists to explore the use of biological systems for the fabrication of nanomaterials. A variety of microorganisms and biomolecules such as enzymes, DNA, RNA, peptides, plant extracts, have been reported to synthesize quantum dots of different shapes, sizes and properties.

a. Microorganisms mediated synthesis:

Microorganisms mediated syntheses of quantum dots have gained prominence because of their economy, scalability, utilization of environmentally benign synthetic conditions and ease of use. Microbes have evolved over the years to produce highly ordered nanomaterials. Microorganisms when exposed to unfavorable conditions such as extreme temperatures, high metal ions concentration or extreme pH, tend to produce factors to maintain the homeostasis of the organism. Some of the main reasons for the production of nanoparticles by microbes are,

i. production of energy by chemolithotrophy – metabolism of inorganic substrates to obtain reducing equivalents for use in biosynthetic processes or energy storage
ii. utilization of nanoparticles in special functions – synthesis of inorganic materials and their integration as special components

iii. survival by detoxification of the environment - microbes employ several strategies for detoxification such as enzymatic reduction/oxidation, sorption on the cell wall, chelating with extracellular peptides or polysaccharides.

A wide variety of microbes spanning both prokaryotes and eukaryotes have been reported for the synthesis of different classes of quantum dots. The nanoparticles are produced either extracellularly or intracellularly. Microorganisms mediated synthesis of nanoparticles has been extensively reviewed by several authors[58-59]. Tables 2 & 3 list the various nanoparticles synthesized using microbes.

i. Bacteria

Bacteria mediated synthesis of nanoparticles in general has been explored in detail during the past decade[60]. Haefeli et al were the first to report the synthesis of silver nanocrystals using *Pseudomonas stutzeri* A259[61]. The strain was isolated from silver mine and the ability of the bacteria to form silver nanocrystals, was attributed to the presence of plasmids in the strain. Even bacteria such as *Lactobacillus* sp. found in butter milk that have not been previously exposed to toxic metals have been reported to crystallize silver ions[62-63].

Gold ions which are comparatively less toxic have been crystallized by bacteria. *Pedomicrobium*-like bacteria have been reported to produce gold nanoparticles at 24-carats quality[64]. Other bacteria also have been reported to crystallize Gold and silver nanoparticles. The nanoparticles have been biosynthesized either extracellularly or intracellularly. The intracellular accumulation of nanoparticles has been reported in cell wall, bacterial envelope, periplasmic space, membrane vesicles, cell surface and inside the cell[65-72].

Extracellular synthesis of nanoparticles is observed when the reductive components of the cell are found in the cell wall and/or when they are secreted as soluble fractions in solution. Extracellular synthesized nanoparticles have found broader applications as compared to their intracellular counterparts. The recovery of nanoparticles synthesized by this route is easier. He at al observed that *Rhodopseudomonas capsulate* reduced gold ions to form spherical nanoparticles of 10-20nm at pH 7.0 and a mixture of spherical and triangular nanoparticles at pH 4.0[73]. *Bacillus megaterium* produced silver nanoparticles in the range of 10-20 nm, extracellularly, when challenged with

Table 2: Summary of different nanoparticles synthesized using microbes - I

	Nanoparticle	Name of microorganism	Reference
Bacteria	**Silver**	*Pseudomonas stutzeri*	37
		Pseudomonas stutzeri A259	61
		Shewanella oneidensis	106
		Lactobacillus sp.	62-63
		Bacillus megaterium	74
		Bacillus sp.	214
	Gold	*Bacillus subtilis*	107
		Shewanella algae	40
		Bacillus cereus	62
		Thermomonospora	215
		Rodococcus	101
	CdS	*Clostridium thermoaceticum*	75
		Klebsiella pneumoniae	76-77
		E. coli	112
		Glucanobacter xylinus	116
		Klebsiella aerogenes	114
	Fe_3O_4	*Magnetospirillum* sp.	117
		Aquaspirillum sp.	118
		Thermoanaerobacter ethanolicus	119
	PbS	*Rhodobacter sphaeroides*	121
		Desulfotomaculum sp.	216
	$SrCaO_4$	*Pseudomonas fluorescens*	122
	Fe_3S_4	Magnetotactic bacteria	123
	Co_3O_4	*Brevibacterium casei*	124
	UO_2	*Shewanella oneidensis* – MR1	125

silver ions[74].

In addition to nanoparticles of noble metals, bacteria have been used for the synthesis of semiconductor nanoparticles such as CdS, ZnS, Se and Te. *Clostridium thermoaceticum* used cysteine-hydrochloride as the sulfide source for the extracellular synthesis of CdS quantum dots with a large size distribution of 20-200nm[75]. CdS crystallites were formed when *Klbesiella pneumoniae* were incubated with Cadmium ions in solution[76-77]. Fesharaki et al reported the synthesis of Selenium nanoparticles using *Klebsiella pneumoniae*[78].

i. Algae

There are very few reports on the synthesis of nanomaterials using algae. Singaravelu et al reported the use of marine algae, *Sargassum wightii* for the biosynthesis of gold nanoparticles extracellularly[79]. Palladium nanoparticles of different sizes and shape were synthesized when Palladium (II) Chloride complex was reacted with the biomass of cyanobacteria, *Plectonema boryanum* UTEX 485)[80]. In addition to the synthesis of metal nanoparticles, algae have been implicated in the synthesis of nanobiomaterials found in coccoliths and diatoms[62].

ii. Fungi

Fungi have been extensively studied for the synthesis of nanomaterials of different elemental composition, shapes and sizes. They are preferred over other microbes because of their robustness, eukaryotic nature, ease of handling and their wide availability. Since fungi have robust cell wall they are capable of withstanding harsh physical conditions to some extent. Hence they are ideal for use in flow cultures. Fungi being eukaryotic are highly developed and possess sophisticated biological machineries which could be exploited for the synthesis of nanomaterials.

Sastry et al have extensively studied the use of fungi for the synthesis of metal and metal sulfide nanoparticles[82]. Fungi were used to synthesize metal and metal sulfide nanoparticles which are attributed to the presence of a variety of enzymes. *Fusarium oxysporum* was used to synthesize Gold, Silver, Ag-Au alloy, CdS, CdSe and Zr nanoparticles[83-88]. Other fungi that were used for the synthesis of nanoparticles include but not limited to, *Colletotrichum* sp., *Trichothecium* sp., *Verticillium* sp., *Aspergillus niger, Penicillium fellutanum,* etc[89-93]. In addition, fungi were used to synthesize

nanoparticles of a variety of shapes[94-99].

iii. Actinomycetes

Actinomycetes possess features of both prokaryotes as well as eukaryotes that make them attractive targets for use as microbial nanofactories. They are the major producers of secondary metabolites. *Thermomonospora* sp., an extremophile has been reported to produce monodisperse Gold nanoparticles[100]. The presence of amide bonds in the nanoparticles is indicative of the involvement of proteins bound to the nanoparticles. *Rhodococcus* sp. crystallized reduced gold nanoparticles on the cell wall and cytoplasmic membranes utilizing enzymes present on the cell wall[101]. *Streptomyces* sp. was used to synthesize metal oxide nanoparticles that offered antimicrobial properties to the fabric they were coated with[102].

iv. Yeast

Eukaryotic microbes possess highly advanced metabolic machineries which provide them advantage over prokaryotic microbes. Among the eukaryotic microbes that are used for the synthesis of nanoparticles, Yeast has been studied in detail for their ability to synthesize nanoparticles of different compositions. Dameron et al were the first to report the use of Yeast to synthesize semiconductor nanoparticles. *Candida glabrata* and *Schizosaccharomyces pombe* when cultured in the presence of Cadmium salts resulted in the synthesis of monodisperse CdS quantum dots of size 2 nm[103]. These nanoparticles were found to be coated with short chelating peptides produced by the yeast. Kowshik et al showed that silver nanoparticles can be synthesized when a silver tolerant yeast strain MKY3 was incubated in silver salt solution[104]. Gold nanoparticles were produced in the cell wall of *Yarrowia lipolytica* NCIM 3589 when the biomass was suspended in a solution of $HAuCl_4$[105].

i. Virus

Viruses have also been used for the synthesis of nanoparticles either as templates or to display molecules such as peptides that bind to specific surfaces such as metal salts[126]. The ability of a phage to display a biomolecule such as peptide or protein on the surface with corresponding change in its genotype has been exploited in the selection of peptides that bind selectively to specific target surfaces. Phage display and Cell surface display are the most common display methods used in the bio-panning of

Table 3: Summary of different nanoparticles synthesized using microbes - II

	Nanoparticle	Name of microorganism	Reference
Fungi	**Silver**	*Trichoderma asperellum*	66
		Trichoderma viride	72
		Fusarium oxysporum	217
		Phaenerochaete chrysosporium	218
		Fusarium semitectum	219
		Aspergillus fumigates	96
	Gold	*Helminthosporum solani*	109
		Verticillium luteoalbum	110
		Volvariella volvaceae	111
		Trichothecium sp.	90
		Colletotrichum sp.	89
	Magnetite	*Fusarium oxysporum*	99
		Verticillium sp.	99
	Si	*Fusarium oxysporum*	220
	Ti	*Fusarium oxysporum*	220
	CdSe	*Fusarium oxysporum*	87
	$BaTiO_3$	*Fusarium oxysporum*	221
	Bi_2O_3	*Fusarium oxysporum*	222
Yeast	**Ag**	Yeast strain MKY3	104
	Au	*Schizosaccharomyces cerevisiae*	223
		Pichia jadinii	110
		Yarrowia lipolytica NCIM 3589	105
	CdS	*Candida glabrata*	103
		Schizosaccharomyces pombe	224
		Fusarium oxysporum	86
	PbS	*Torulopsis* sp.	225
	Sb_2O_3	*Schizosaccharomyces cerevisiae*	226

peptides that crystallize nanoparticles. In Phage display, much of the work has been done using filamentous phages such as M13, fd and f1 and bacteriophages such as T7, T4 and λ. Flynn et al isolated A7, a constrained peptide sequence CNNPMHQNC that binds to ZnS and two 12-mers that bind to CdS nanoparticles[127]. PD and CSD have been used successfully for the isolation of a variety of nanoparticles[128-134]. Basindale et al reported an improved methodology for the use of phage display to crystallize inorganic nanoparticles[135]. They retained 10% of the wild type genome of the phage, in addition to the introduction of rolling cycle amplification strategy for the amplification of phage DNA bound to inorganics.

b. Plant extracts bases synthesis

Plant extracts are complex mixtures that contain a variety of biochemicals ranging from proteins, alkaloids and phenolics. In their quest for environmentally safe protocol

Table 4: Summary of different nanoparticles synthesized using plant extracts

	Nanoparticle	Source of extract	Reference
	Ag	*Cinnamon zeylanicum*	138
		Carica papaya	227
		Azadirachta indica	228
		Pelargonium graveolens	229
		Mangifera indica	233
		Desmodium triflorum	234
	Au	Lemon grass	136
		Cinnamon leaf	137
		Terminalia cattappa	230
		Azadirachta indica	231
		Sesbania drummondi	232
	Pt	*Diapyros kaki*	139
	Cu	Magnolia	235
	In_2O_3	*Aloe vera*	236

for the synthesis of nanoparticles, researchers explored extracts from a variety of plants and were successful in reporting the synthesis of metal nanoparticles. Shankar

et al reported the synthesis of thin, flat, gold nanotriangles using extracts from lemon grass[136]. They hypothesized that the process involves rapid reduction, assembly and sintering of liquid-like spherical gold nanoparticles. Table 4 summarizes the various sources of plants extracts used for the synthesis of nanomaterials. Gold nanoparticles were produced when chloroauric acid solution was treated with extracts of cinnamon leaf[137]. Silver nanoparticles were produced using the extract and powder of the bark of the tree, *Cinnamon zeylanicum*[138]. Pt nanoparticles were synthesized when cholroplatinic acid was added to the leaf extract of *Diapyros kaki* at 95°C[139]. FTIR analysis has revealed that no enzymes were involved in the synthetic process. One of the major advantages of the plant extract based syntheses is that they are good for instant in vitro production of nanoparticles. Moreover, they can be scaled up easily given the simple methodology they are associated with.

c. Enzyme based synthesis

Biosynthesis of nanoparticles using microbes has fulfilled the quest for an eco-friendly approach for the synthesis of nanomaterials to a considerable extent. Yet these methods lack heavily in the ability to produce nanomaterials of desirable shapes and sizes which is very important to realize the full potential of these nanomaterials. In order to understand the mechanisms that underlie the synthesis of nanomaterials, researchers have resorted to biomolecules to synthesize nanomaterials thereby simplifying the method.

By ascertaining the role of each and every component of the process, the possibility of manipulating the method for a better product is high. Researchers scoured the sources that produced nanoparticles for biomolecules that are responsible for the production of nanoparticles. They found that the biomolecules responsible for the production of nanoparticles are primarily enzymes except for some plant extract based synthesis methods. Enzymes bring about the synthesis of nanoparticles primarily by reduction of corresponding metal ions in solution. The reduced metal ions are in turn bound by capping molecules thereby preventing agglomeration.

There is considerable amount of reports that demonstrate the use of enzymes for the synthesis of metal nanoparticles. Reduction of gold ions using enzymes leading to the synthesis/growth of gold nanoparticles has been well documented. This method has been used to quantify the enzyme present in a given sample by following the relative

Table 5: Summary of different biomolecules involved in the synthesis of nanoparticles (reproduced with permission from Ref.58 with slight modifications)

Nanoparticle	Biomolecule(s) responsible	Reference
Au	Carotenoids and NADPH-dependent enzymes	241
	66 and 10 kDa protein	83
	α-NADPH dependent sulfite reductase and phytochelatin	143
	Glutathiones	89
	80 and 10 kDa protein	100
	Peptidoglycans and reducing sugars	223
Ag	Nitroreductase	242
	α-NADPH dependent sulfite reductase and phytochelatin	142
	Nitrate reductase	92
	Compactin	243
CdS	J140 fusion proteins	244
	Glutamate and aspartate	126
Zr	24-28 kDa protein	88
Pt	Dimeric hydrogenase	
Sb_2O_3	Quinine or pH-dependent oxidoreductase	226
ZnS	Peptide A7	246

difference in the surface plasmonic resonance of gold nanoparticles. Glucose oxidase produces H_2O_2 upon action on its substrate. The evolved H_2O_2 reduces $AuCl_4^-$ thereby producing Au nanoparticles, which is in turn correlated with the activity of glucose oxidase[140]. Tyrosine is converted to L-DOPA by Tyrosinase using O_2 as the source of oxygen. L-DOPA generates gold nanoparticles, which is used to quantify L-DOPA[141]. The use of enzymes for the synthesis of semiconductor nanoparticles remains a fairly unexplored area of nanotechnology. Several reports focus on the probable role of endogenous reductase enzymes responsible for the synthesis of semiconductor nanoparticles using microbes. Yet there are only a handful of reports that document the use of enzymes for the in vitro synthesis of semiconductor nanoparticles. Khan and

co-workers purified enzymes, NADPH dependent-sulfite and nitrate reductases from the extracellular broth of the fungus, *Fusarium oxysporum* that has been reported to produce metal, metal sulfide and CdSe nanoparticles and demonstrated the use of enzymes for the in vitro synthesis of gold, silver and CdS nanoparticles[142-144]. They also purified capping molecules that served as the templates for the crystallization of these nanoparticles. Hence, the use of enzymes for the in vitro synthesis of nanoparticles holds great potential for becoming an alternative strategy for the synthesis of a wide variety of nanoparticles of different compositions.

Advantages

Some of the hallmarks of enzyme mediated syntheses of nanoparticles are economy, eco-friendliness, and simplicity. Enzymes can be purified from natural resources and can be recovered and reused by immobilization on solid support. Spent enzymes are easily disposable and hence do not cause environmental hazard. The process requires ambient conditions. They have the potential to be highly specific and efficient given the specificity and efficiency of enzymes. The process can be scaled for bulk production as is the characteristics of majority of enzyme based processes.

SIZE CONTROL OF NANOPARTICLES

One of the most predominant characteristics of nanoparticles is the change in the properties with reference to the corresponding bulk material of same structure and composition. Since materials at the nanoscale are quantum confined, they follow the rules of quantum mechanics and hence exhibit novel properties that are not attributed to their bulk counterpart. These novel properties hold the key for applications of nanoparticles in each and every field of science. The novel optical and electronic properties of nanocrystals are highly dependent on the size of the crystals. In order to study the novel properties of these nanocrystals, nanocrystals of monodisperse nature have to be synthesized. A monodisperse sample is one that contains identical nanocrystals in terms of size, shape, surface chemistry and internal structure. In case of nanocrystals, the definition of monodispersity is slightly relaxed and is used to describe a sample with a mean deviation of less than 5% in diameter. This need for size controlled nanocrystals has resulted in a quest for synthetic protocols that

produces nanocrystals of defined sizes and shapes by modifying the existing synthetic protocols. Colloidal or chemical methods for the synthesis of nanocrystals have emerged as the predominant methods for the synthesis of size controlled nanocrystals. Yet other methods are also available that have specific advantages over the remaining methods to a certain extent. Some of the methods to produce size controlled nanocrystals are as follows:

i. In micellar solutions

Surfactants when dissolved in organic solvents form spherical aggregates called reverse micelles. These reverse micelles are thermodynamically stable nanospheres of the surfactant employed and enclose nanodroplets of water inside. This allows a variety of polar and ionic species to be dissolved into the water cores. The size of the micelles can be controlled by adjusting the ratio of surfactant to organic solvents. Gold nanoparticles were size controlled synthesized using diblock copolymer of Poly(styrene)-b Poly(ethylene oxide)[145]. Size controlled CdS quantum dots of 4-8 nm synthesized using reverse micellar system showed improved luminescence characteristics due to surface modifications when refluxed[146]. The photoluminescence properties of CdSe quantum dots were altered by size controlled synthesis using reverse micelles[147]. Vakurov et al controlled the size of acrylamide/bisacrylamide - based functionalized polymeric nanoparticles of size 20 – 90 nm using reverse micellar system of dioctyl-sulfosuccinate (AOT)/octane and toluene as template[148].

ii. In presence of templates

Template mediated synthesis of nanoparticles involve the use of ligands that are integrated into the nanoparticles thereby maintaining the nanoparticles within the nano regime by preventing the nanoparticles from forming aggregates. A wide variety of templates ranging from polysaccharides, nucleotides, peptides, surfactants, etc have been used for the synthesis of nanoparticles. Anisotropic metal structures have been synthesized using both soft and rigid templates. DNA is an interesting template because of its linear structure and negatively charged phosphate backbone. Gearheart et al functionalized citrate stabilized gold nanoparticles with DNA oligomers using ligand exchange thereby replacing the citrate ligands on the surface of nanoparticles[149]. Levina et al reported the synthesis of highly efficient PbS quantum

dots, that emits in the IR region, using DNA as the template[150]. Aptamers were used to synthesize PbS quantum dots rendering them water solubility while still retaining the

Table 6: Summary of various factors involved in the size control of nanoparticles

	Nanoparticle	Factor responsible	Reference
Micellar	**Au**	Poly(styrene)-b Poly(ethylene oxide)	145
	CdSe	AOT/heptanes	147
	Acrylamide/bisacr-ylamide polymer	Dioctyl-sulfosuccinate (AOT)/octane	148
	Cu	Sodium bis-(2-ethylhexyl)-sulphosuccinate	236
	$CaCO_3$	Sodium bis-(2-ethylhexyl)-sulphosuccinate	237
	YF_3	Water/Cyclohexane	238
	Fe_3O_4	Sodium dodecylbenzenesulfonate/xylene	239
	$CoFe_2O_4$	Water/oil	240
Template mediated	**Au**	DNA	149
		Cow chlorotic mottle virus	81
	PbS	DNA	150
		Aptamers	151
	Ag	Bacterial cellulose nanofibers	247
	FePt	PAMAM-dendrimers	248
	GaOOH	Surfactant vesicles	249
	Tb-doped $CePO_4$	Polycarbonate membranes	250
	Hydroxyapatite	Chondroitin sulfate	251

secondary structure required for binding to the target molecule[151]. Kelly and co-workers documented the role of three dimensional structure of t-RNA in the aqueous synthesis of CdS nanocrystals. They found that a folded 3D structure of t-RNA templated the synthesis of spherical CdS nanocrystals of 5 nm and an unstructured t-RNA produced CdS nanocrystals in the range of 5-10nm[152].

Carbohydrates and surfactants present yet another classes of ligands used as templates for the size control of nanocrystals. The addition of *Undaria pinnatifida* polysaccharides to the redox system of selenite and ascorbic acid resulted in the size

controlled synthesis of Se nanoparticles[153]. Liu et al controlled the growth of gold nanoparticles using a new class of surfactants, geminis, as templates and modifying the length of spacer[154].

Some of the most important biomolecules used for the size control of nanomaterials are peptides. Peptides score over other molecules such as DNA due to the possibility of creating numerous combinations of peptides of different lengths and structures thereby influencing the growth of nanocrystals. Slocik et al reported the use of histidine rich peptides such as AHHAHHAAD, for the synthesis of Ag and Au nanostructures[155]. These peptides made the nanoparticles recognizable by antibodies indicating the presence of peptide in its native form. Banerjee et al employed histidine-rich peptide nanotubes to synthesize Cu nanotubes[156]. When the pH was altered the sizes of the Cu nanoparticles were restricted to 10-30 nm. Lu et al exploited the ordered surface positive charges of self-assembled amyloid β-peptide as templates for metal nanoparticles such as gold and palladium[157]. They found that under acidic conditions, individual segments of the amyloid β-peptide self assemble in to robust peptide nanotubes and exploited this property for the synthesis of metal nanoparticles.

iii. Under physical confinements

Restricting the size of nanoparticles by physical methods involve the use of microcavities to restrict the growth of nanoparticles. The microcavities are large enough to accommodate ions and small enough to restrict the growing nanoparticles in the nano regime. This method works on the principle of steric hindrance between the growing nanoparticles and the physical confinement with in which it is present. Large proteins with globular structure have been used as nanofactories to produce nanoparticles of defined sizes. Meldrum et al demonstrated the use of iron-storage protein as nanocage for to restrict the growth of iron sulfide nanoparticles[158]. The growth of manganese and uranium-oxo species can also be restricted using this method. In a similar approach, Allen et al synthesized nano-sized iron oxide nanoparticles using recombinant ferritin-like protein from *Listeria innocua*[159]. Other examples include use of peptide assembled nanotubes or nanorings[160-162]. Ogale et al reported the size control of gold nanoparticles synthesized by plant extract using percolative microcavity synthesis[163]. Glass micro beads were used to physically

restrict the growth of gold nanoparticles.

SHAPE CONTROL OF NANOPARTICLES

The properties of nanomaterials depend not only on the size, but also on the shape of the material. Novel properties have been exhibited by nanomaterials when they are restricted to a particular shape. Fascinating properties have been reported to be exhibited by 1D nanomaterial such as wires, rods, multipod structures, facetted particles, etc such as emission of polarized light by nanorods of CdSe and aggregation of silver nanoparticles mediated by light[164]. Similarly, other shapes such as rods, triangular prisms and cubes exhibit multiple scattering peaks due to charge localization at edges and corners of these nanostructures[165-166]. The reactivity of material is highly dependent on the surface characteristics. The morphology of the surface as well as ratio of surface-area to volume greatly influences the chemical reactivity of a material. Palladium and Platinum exhibit size and shape dependent catalytic properties utilized in specific catalysis[167]. This has led to the quest for producing nanomaterials of specific shapes in order to understand the influence of shape in the properties of nanomaterials.

i. DNA and protein mediated:

Numerous approaches have been reported for the shape controlled synthesis of nanomaterials. Wang et al reported the one pot synthesis of Au nanoflowers using 30-mer DNA as template[168]. 30-mer sequences of poly-A and poly-C templated the synthesis of Au nanoflowers where as poly-T produced Au nanospheres. They concluded that the difference in affinity of DNA to Au nanoparticles is responsible for the difference in morphology. Yang and co workers demonstrated the use of colloidal synthesis for the shape controlled synthesis of single crystalline Ag, Au and Pt nanocrystals bound exclusively by {100} and {111} crystal planes such as cubes, cuboctohedral and octahedral geometries[169-171]. In addition to DNA, proteins have also been reported to be used for the size control of nanoparticles. Sun et al reported the use of Type-1 collagen, a structural protein for the synthesis of networks of noble metals such as Au, Ag, Pt and Pd[172].

Table 7: Summary of synthesis of different shapes of nanoparticles

Nanoparticle	Factor(s) responsible	Shape	Reference
Au	DNA	Nanoflower	168
	Small seed gold particles	Nanodogbones	253
	Poly(vinyl pyrrolidone)	Triangle	171
	CTAC CTAB	Triangles Spheres	176
Ag	Poly(vinyl pyrrolidone)	Cube	254
	Poly(vinyl pyrrolidone)	Cube, sphere, wire	255
	Poly(vinyl pyrrolidone)	Polyhedran	169
	Surfactant daxad 19	Monodisperse	175
	Addition of Pt nanoparticles	Nanowires	173
Pd	RNA	Hexagon	252
	Tetranuclear Pd clusters	Tetrahedron	256
β-In_2S_3	Time of reaction	Nanotubes	257
Pt	Sodium polyacrylate or poly(N-vinyl-2-pyrrolidone)	Tetrahedron, Octhedran, Cubic	177
	Addition of Ag^+ ions	Cubes, octahedra	170
CdTe	Source of precursor	Sphere and Rod	258
Au, Ag, Pt, Pd	Type-1 Collagen	Networks	172
Fe_3O_4	pH, temperature	Octahedran & sphere	179
	1- adamantanecarboxylic acid & oleylamine (OLA)	Star-like	180
	1- adamantanecarboxylic acid & 1-adamantaneamine	Flower-like	
Co	Polymer	Spheres and rods	178
FePt	Precursors, temperature solvents, surfactants,	Spheres, cubes, rods	181
ZnO	Alkyl amines	Nanoparticles & rod	182

ii. Surfactant mediated:

Some of the reports suggest the use of surfactants for the synthesis of nanomaterials with controlled shape. Sun et al reported a soft solution phase approach for the synthesis of Ag nanowires of 30-40nm diameter[173]. They used Pt nanoparticles for the heterogenous nucleation and growth of Ag nanowires in the presence of PVP. Johnson et al prepared gold nanorods using a seed mediated sequential growth process in the presence of cationic surfactant CTAB[174]. Lah et al used daxad 19, a surfactant for the stabilization and shape control of monodisperse anisotropic Ag nanoparticles[175]. They observed that the desired shape is produced by controlling the temperature and weight ratios of the reactants. Gold nanotriangles were produced when gold ions were reduced by tryptophan in the presence of CTAB while CTAC mediated the synthesis of spherical gold nanoparticles[176]. Pt nanoparticles were shape controlled synthesized by adjusting the rate of reduction of Pt^{4+} ions in the presence of PVP or PAA. Teranishi et al observed that the slow reduction of Pt^{4+} by H_2 resulted in the formation of tetrahedral particles while the use of methanol as the reducing agent produced truncated tetrahedran irrespective of the choice of polyol used[177].

iii. Polymer mediated:

Lu et al controlled the size and shape of water soluble magnetic Co nanoparticles using alkyl thioether end functionalized poly (methacrylic acid) [178]. The concentration of the polymer used affected the size of the Co nanoparticles. Using this synthetic approach, large nanoparticles of 80 nm as well as nanorods were synthesized. Magnetite nanoparticles of a variety of sizes and shapes such as octahedral, irregular or spherical morphologies were synthesized by varying the synthetic parameters such as types of reagents, their concentrations, pH, temperature and the synthesis atmosphere[179]. In another report, star-like and flower-like magnetite nanoparticles were synthesized using surfactants such as 1- adamantanecarboxylic acid (ACA) and oleylamine (OLA), ACA and 1-adamantaneamine (AA) as the combined surfactants, respectively[180]. FePt nanoparticles of a variety of morphology such as spherical, cubic, rod-shaped can be achieved to the order of 1nm by varying the synthetic parameters such as precursors, solvents, quantity of surfactants and heating conditions[181]. Kahn et

al used a novel organometallic synthetic method for the size and shape control of crystalline ZnO nanoparticles[182]. Isotropic ZnO nanoparticles of 3-6nm and nanorods of 3-4 nm diameters were produced by this method which utilizes long alkyl chain amines as the stabilizing agent. Kruszynska et al used colloidal chemistry for the synthesis of Cu_2S-$CuInS_2$ hybrids as well as pure $CuInS_2$ nanorods, dimeric nanorods, hexagonal discs and P-shaped nanoparticles by varying the reaction conditions[183]. They observed that Cu_2S-$CuInS_2$ forms as an intermediate during the synthesis and Cu_2S play a role in the shape control. They extended the synthetic protocol for the synthesis of $CuInS_2$-ZnS alloys as well.

In addition to the methods described above for the control of shape, there are other methods which bring about the change of shape using induced formation of shape from one to another. Jin et al described the transformation from spherical to triangular shaped nanoparticles of silver by photoirradiation whereas, a thermally induced transformation was employed for the conversion of spherical gold clusters to nanocubes[184-185]. Li et al used chemically induced transformation to convert gold spheres into planar forms[186]. In an interesting approach, Roorda et al synthesized gold nanorods by ion beam irradiation of spherical gold-silica core-shell nanoparticles[187]. The ion beam irradiation is shown to deform the silica shell leading to the deformation of the core spherical gold nanoparticle. Similarly shape transformation by laser irradiation was shown to be responsible for the formation of Φ-shaped nanoparticles from nanorods[188].

APPLICATIONS OF NANOMATERIALS

Novel properties exhibited by nanomaterials due to miniaturization have resulted in the application of nanomaterials in a wide range of fields of science and technology ranging from medicine to cosmetics to space sciences. The new found properties of nanomaterials have evoked a lot of expectation from the field of nanotechnology to answer some of the toughest challenges that mankind faces. The field of nanotechnology has so far offered some of the best solutions to fulfil the shortcomings that have prevailed so far.

i. Nanomedicine

Nanomaterials have found lots applications in the field of medicine.

- Nanometer sized titania and alumina enhanced the proliferation of osteoblasts and chondrocytes paving way for the use of these materials as bone prosthetic materials[189]. It was observed that size was the only difference between these materials and the conventional materials used as bone prosthetic materials.
- Titanium, even though, is a very good bone repairing material, it lacks bioactivity and hence does not support cell adhesion and growth well. Biomimetic deposition of apatite of 60 nm thickness increases bioactivity while remaining stable[190].
- Special dyes that generate oxygen that kill the cancer cells when irradiated with LASER produce side effects. Hydrophobic version of this dye encapsulated by porous nanoparticles shows no side effects[191].
- Song et al reported the use of mAb coupled Fluorescent-magnetic-biotargeting multifunctional nanobioprobes (FMBMNs) for the detection of multiple types of cancer cells from a large population of normal cells with 96% efficiency[192]. The approach is characterized by economy and simplicity.
- Vemula et al reported the use of thin layer of glycerine emollient containing nanoparticles of either calcium carbonate or calcium phosphate that prevents the penetration of nickel ions into the skin[193]. The nanoparticles captured nickel ions by ion exchange and remained on the surface of the skin facilitating easier removal by simple washing with water.
- In addition, nanomaterials have been used for a variety of purposes such as fluorescent bio-labels, detection of pathogens and proteins, hyperthermia, MRI contrast enhancement, etc[194-198].

ii. Catalysis

Catalysis is a purely surface phenomenon. The bulk of the atoms present on the surface, decides the catalytic ability of a given material. Nanomaterials are characterized by the presence of large surface to volume ratio i.e. the number of atom present on the surface. A nanomaterial is phenomenally large as compared to the bulk material of same volume. Hence, nanomaterials have been found to have excellent catalytic properties. Supported metal nanoparticles have been found to possess excellent catalytic properties.

- Gold being a noble metal is inert in its bulk form. But, Au nanoparticles possess excellent catalytic properties evident from their usage in numerous applications. Au nanoparticles of size 3nm showed optimum catalytic activity in the oxidation of CO[199]. Au nanoparticles of various sizes are used in numerous other catalytic applications[200-203].
- Pd nanoparticles supported on polyaniline nanofibers were used for the Suzuki coupling of aryl chlorides and phenylboronic acids[204]. The catalyst had excellent stability and can be used for up to 10 times in the Suzuki reaction.
- Other supported metal nanocatalysts with high efficiency include Ag, Rh, and Ru[205-207].
- Tedsree et al developed a catalyst, by coating thin layer of Pd atoms onto Ag nanoparticles that efficiently catalyzes the formation of H_2 from formic acid under ambient temperature[208]. The nanocatalyst has a core shell structure with the shell containing 1-10 layers of Pd atoms. This catalyst has the potential to be used in the development of portable micro polymer electrolyte membrane fuel cells.
- Hydrogen is a promising candidate for cleaner energy. But efficient storage of hydrogen is still a problem. Jeon et al have developed air stable nanocomposite made of Mg nanocrystals in a gas barrier polymer matrix that enables the storage of high density of hydrogen without the use of catalysts[209].

iii. Molecular electronics

Molecular electronics is the use of a molecule or group of molecules as an electronic device in a circuit. Molecular structures have several advantages towards use in electronics such as size, assembly and recognition, dynamical stereochemistry and synthetic tailorability[210].

- Schulz et al reported the control of spin polarization of extracted charge carriers from an organic semiconductor by the inclusion of a thin interfacial layer of polar materials[211]. The highest occupied molecular orbital of the OSC with respect to the Fermi energy of the ferromagnetic contact shifts due to the electric dipole moment brought about by this layer. The spin band appropriate for charge carrier extraction can be controlled by this approach leading to the

development of new spintronics device concepts.

- Capelli et al reported the production of highly efficient organic light emitting transistors (OLET) that out performed any currently available OLETs and OLEDs[212]. They used a p-channel/emitter/n-channel trilayer semiconducting heterostructure in OLETs that prevented exciton-charge annihilation and electrode photon losses.
- Matyba et al demonstrated the *in-situ* formation of a dynamic p-n junction within an organic semiconductor through electrochemistry[213]. This opens up the possibility of the production of low-cost and flexible devices that revolutionize the field of electronics.

PRESENT INVESTIGATION

The unique properties observed by the miniaturization of bulk materials have resulted in the investigation of nanomaterials for their both basic as well as applied aspects. One of the major challenges that the field of nanotechnology faces is the development of reliable, eco-friendly, economical and efficient synthesis of nanomaterials. Physical and chemical methods for the synthesis of nanomaterials are expensive, utilize and produce toxic chemicals and hazardous to the environment. Biological routes for the synthesis of nanomaterials using microbes and plant extracts under ambient conditions have resulted in the exploration of biological systems for the efficient synthesis of nanomaterials. The basic mechanism underlying the synthesis of nanomaterials is the oxidation/reduction of metal ions. Since enzymes are capable of these reactions, an attempt was made to investigate the role of oxido/reductase enzymes for the synthesis of nanomaterials. In addition, as observed in majority of the synthetic processes, nanomaterials require a template that affects the growth characteristics of the nanomaterials. The morphological characteristics of nanomaterials have been found to be dependent on the template employed. Since peptides have been implicated in the synthesis of nanomaterials using enzymes, an attempt has been made to investigate the role of peptides in the size and shape control of quantum dots.

References

1. Feynman, R. P. (1991) Science **254,** 1300-1301.
2. Bamford, D. H. (2000) Curr. Biol. **10**, R558-561.
3. Mirkin, C. A. (2005) Small **1**, 14-16.
4. Morales, A. M., Liebe, C. M., (1998) Science **297**, 208-211.
5. Mafune, F; Kohno, J; Takeda, Y; Kondow, T; (2000) J. Phys. Chem. B **104**, 9111–9117
6. Shafeev, G. A; Freysz, E; Bozon-Verduraz, F; (2004) Appl. Phys. A **78**, 307–309
7. Kabashin, A. V; Meunier, M; (2003) J. Appl. Phys. **94**, 7941–7943
8. Liu, B; Hu, Z; Che, Y; Cheng, Y; Pan, X; (2007) Appl. Phys. Lett. **90**, 044103
9. Barsch, N; Jakobi, J; Weiler, S; Barcikowski, S; (2009) Nanotechnology 445603
10. Lalayan, A. A; (2005) Appl. Surf. Sci. **248**, 209-212
11. Yang, S; Cai, W; Zeng, H; Xu, X; (2009) J. Mater. Chem., **19**, 7119-7123
12. Mochel, J. M. (1951) US Patents 2,564,707; 2,564,987; 2,564,709; 2,564,710; 2,564,708; 2,564,706
13. Liu, S; Zhang, H; Swihart, M. T; (2009) Nanotechnology **20**, 235603.
14. Zhu, G; Lv, T; Pan, L; Sun, Z; Su, C; (2011) J. Alloy Compd. **509**, 362-365
15. Louh, R. F; Chang, A. C; Wang, R; Hsiao, C. H; (2008) Adv. Sci. Technol. **57**, 37-43
16. Bakar, N. A; Umar, A. A; Salleh, M. M; Yahay, M; (2010) Sains Malaysiana **39**, 473-477
17. Li, Z; Cai, W; Sui, J; (2008) Nanotechnology **19**, 035602
18. Bo, X, -Z; Rokhinson, L. P; Yao, N; Tsui, D. C; Stur, J. C; (2006) J. Appl. Phys. **100**, 094317
19. Martín-Sánchez, J; Alonso-González, P; Herranz, J; González, Y; González, L; (2009) Nanotechnology **20**, 125302
20. Li, Z; Sui, J; Li, X; Ca, W; (2011) Langmuir (In press)
21. Crozier, P. A; Tolle, J; Kouvetakis, J; Ritter, C; (2004) *Appl. Phys. Lett.* **84**, 3441-3443

22. Bo, X. –Z; Rokhinson, L. P; Yao, N; Tsui, D.C; Sturm, J. C; (2006) *J. Appl. Phys.* **100**, 094317
23. Keyser, U.F; Schumacher, H.W; Zeitler, U; Haug, R. J; Eberl, K. (2001) **224**, *Phys. Status Solidi B* 681-684
24. de Heer, W. A; Milani, P; Chatelain, A; (1990) *Phys. Rev. Lett.* **65**, 488-491
25. Sánchez-López, J. C; Fernández, A; (1998) *Thin Solid Films* **317**, 497-499
26. Schwartz, D. A; Norberg, N. S; Nguyen, Q. P; Parker, J. M; Gamelin, D. R; (2003) *J. Am. Chem. Soc.* **125**, 13205-13218
27. Kopping, J. T; Patten, T. E; (2008) *J. Am. Chem. Soc.* **130**, 5689-5698
28. Liu, S; Zhang, H; Swihart, M. T; (2009) *Nanotechnology* **20**, 235603
29. Mikrajuddin, Iskandar, F; Okuyama, K; Shi, F. G; (2001) *J. Appl. Phys.* **89**, 6431-6434
30. Xia, B; Lenggoro, I. W; Okuyama, K; (2001). *Adv. Mater.* **13**, 1579–1582
31. Xia, B; Lenggoro, I. W; Okuyama, K; (2001) *J. Mater. Chem.* **13**, 2925–2927
32. Sun, S; Murray, C. B; (1999) *J. Appl. Phys*. **85**, 4325-4330
33. Sun, S; Murray, C. B; Weller, D; Folks, L; Moser, A; (2000) *Science*, **287**, 1989-1992
34. Joo, J; Pietryga, J. M; McGuire, J. A; Jeon, S. –H; Williams, D. J; Wang, H. L; Klimov, V. I; (2009) *J. Am. Chem. Soc.* **131**, 10620-10628
35. Duan, J; Song, L; Zhan, J; (2009) *Nano Res.* **2**, 61-68
36. Dinega, D. P; Bawendi, M. G; (1999) *Angew. Chem., Int. Ed.*, **38**,1788-1791
37. Lee, D. K; Kang, Y. S; (2004) *ETRI J.* **26**, 252-256
38. Yu, W. W; Falkner, J. C; Yavuz, C. T; Colvin, V. L; (2004) *Chem. Commun.* 2306-2307
39. Murray, C. B; Sun, S; Doyle, H; Betley, T. A; (2001) *MRS Bull.*, **26**, 985-991
40. Murray, C. B; Sun, S; Gaschler, W; Doyle, H; Betley, T. A; Kagan, C. R; (2001) *IBM J. Res. & Dev.*, **45**, 47-56
41. Zhai, C; Zhang, H; Du, N; Chen, B; Huang, H; Wu, Y; Yang, D; (2011) *Nanoscale Res. Lett.* **6**, 31-35
42. Suslick, K. S; Fang, M; Hyeon, T; (1996) *J. Am. Chem. Soc.* **118**, 11960-11961
43. Wang, H; Zhu, J; (2003) *Ultrason. Sonochem.* **11**, 293-300

44. Murcia, M. J; Shaw, D. L; Woodruff, H; Naumann, C. A; Young, B. A; Long, E. C; (2006) *Chem. Mater*. **18**, 2219-2225
45. Biljana, P; Ivan, G; (2006) *Czech. J. Phys.* **56**, 75-84
46. S. Mann, (2000) Angew. Chem. 2000, **112**, 3532-3548
47. Mann, S; (2000) Angew. Chem. Int. Ed. **39**, 3392-3406
48. Fincham, A. G; Moradian-Oldak, J; Simmer, J. P; (1999) J. Struct. Biol. **126**, 270-299
49. Round, F. E; Crawford, R. M; Mann, D. G; The Diatoms: Biology and Morphology of the Genera, Cambridge University Press, Cambridge, **1990**
50. Schüler, D; Frankel, R. B; (1999) Appl. Microbiol. Biotechnol. **52**, 464-473
51. Niemeyer, C. M; (2001) Angew. Chem. Int. Ed. **40**, 4128-4158
52. Rao, D. V; Shivannavar, C. T; Gaddad, S. M; (2002) Indian J. Exp. Biol. **40**, 319-324
53. Bayraktar, O; (2005) World J. Microb. Biot. **21**, 661-665
54. Bayat, O; Sever, E; Bayat, B; Arslan, V; Poole, C; (2009) Appl. Biochem. Biotechnol. **152**, 117-126
55. Rezzaa, I; Salinasa, E; Elorzaa, M; Sanz de Tosettia, M; Donatib, E; (2001) Process Biochem. **36**, 495-500
56. Calmoi, R; Cecal, A; (2007) Environ. Eng. Manag. J. **6**, 27-30
57. Rehm, H.-J; Reed, G; (2008) Biotechnology: Special Processes, Vol. 10, Second Edition, Pg. 191–224, Wiley-VCH.
58. Narayanan, K. B; Sakthivel, N; (2010) Adv. Colloid. Interfac. **156**, 1-13
59. Krumov, N; Perner-Nochta, I; Oder, S; Gotcheva, V; Angelov, A; Posten, C; (2009) Chem. Eng. Technol. **32**, 1026–1035
60. Mandal, D; Bolander, M. E; Mukhopadhyay, D; Sarkar, G; Mukherjee, P; (2006) Appl. Microbiol. Biotechnol. **69**, 485-492
61. Haefeli, C; Franklin, C; Hardy, K; (1984) J. Bacteriol., **158**, 389-392.
62. Slocik, J. M; Knecht, M. R; Wright, D. W; (2004) Encyclopedia Nanosci.Nanotechnol. **1**, 293-308
63. Nair, B; Pradeep, T; (2002) Cryst. Growth Des. **2**, 293-298
64. Mann, S; (1992) Nature, **357**, 358-360
65. Beveridge, T. J; Murray, R. G. E; (1980) J. Bacteriol. **141**, 876-887

66. Southam, G; Beveridge, T. J; (1994) Geochim. Cosmochim. Acta **58**, 4527-4530
67. Lengke, M; Southam, G; (2006) Geochim. Cosmochim. Acta **70**, 3646-3661
68. Kashefi, K; Tor, J. M; Nevin, K. P; Lovley, D. R; (2001) Appl. Environ. Microbiol. **67**, 3275-3279
69. Konishi, Y; Tsukiyama, T; Tachimi, T; Saitoh, N; Nomura, T; Nagamine, S; (2007) Electrochim. Acta **53**, 186-192
70. Lengke, M; Fleet, M. E; Southam, G; (2006) Langmuir **22**, 2780-2787
71. Lengke, M; Ravel, B; Fleet, M. E; Wanger, G; Gordon, R. A; Southam, G; (2006) Environ. Sci. Technol. **40**, 6304-6309
72. Du, L; Jiang, H; Xiaohua, H; Wang, E; (2007) Electrochem. Commun. **9**, 1165-1170
73. He, S; Guo, Z; Zhang, Y; Zhang, S; Wang, J; Gu, N; (2007) Mater. Lett. **61**, 3984-3987
74. Prakash, A; Sharma, S; Ahmad, N; Ghosh, A; Sinha, P; (2010) Intl. Res. J. Biotechnol. **15**, 71-79
75. Cunningham, D. P; Lundie, Jr. L. L; (1993) Appl. Environ. Microbiol. **59**, 7-14
76. Smith, P. R; Holmes, J. D; Richardson, D. J; Russell, D. A; Sodeau, J. R; (1998) J. Chem. Soc. Faraday Trans. **94**, 1235-1241
77. Holmes, J. D; Richardson, D. J; Saed, S; Evans Gowing, R; Russell, D. A; Sodeau, J. R; (1997) Microbiol. UK **143**, 2521-2530
78. Fesharaki, P. J; Nazari, P; Shakibaie, M; Rezaie, S; Banoee, M; Abdollahi, M; Shahverdi, A. R; (2010) Braz. J. Microbiol. **41**, 461-466
79. Singaravelu, G; Arockiamary, J. S; Kumar, V. G; Govindaraju, K; (2007) Colloid Surface B **57**, 97-101
80. Lengke, M. F; Fleet, M. E; Southam, G; (2007) Langmuir **23**, 8982-8987
81. Slocik, J. M; Naik, R. R; Stone, M. O; Wright, D. W; (2005) *J. Mater. Chem.* **15**, 749-753
82. Sastry, M; Ahmad, A; Khan, M. I; Kumar, R; (2003) Curr. Sci. India **85**, 162-170
83. Mukherjee, P; Senapati, S; Mandal, D; Ahmad, A; Khan, M. I; Kumar, R; Sastry, M; (2002) Chembiochem, **3**, 461-463

84. Ahmad, A; Mukherjee, P; Senapathi, S; Mandal, D; Khan, M. I; Kumar, R; Sastry, M; (2003) Colloids Surf. B Biointerf. **28**, 313 – 318

85. Senapati, S; Ahmad, A; Khan, M. I; Sastry, M; Kumar, R; (2005) Small, **1**, 517-520

86. Ahmad, A; Mukherjee, P; Senapathi, S; Mandal, D; Khan, M. I; Kumar, R; Sastry, M; (2002) J. Am. Chem. Soc. **124**, 12108-12109

87. Kumar, S. A; Ansary, A. A; Ahmad, A; Khan, M. I; (2007) J. Biomed. Nanotechnol. **3**, 190-194

88. Bansal, V; Rautaray, D; Ahmad, A; Sastry, M; (2004) J. Mater. Chem. **14**, 3303-3305

89. Shankar, S. S; Ahmad, A; Pasricha, R; Sastry, M; (2003) J. Mat. Chem. **13**, 1822-1826

90. Ahmad, A; Senapati, S; Khan, M. I; Kumar, R; Sastry, M; (2005) J. Biomed. Nanotechnol. **1**, 47-53

91. Mukherjee, P; Roy, M; Mandal, B. P; Dey, G. K; Mukherjee, P. K; Ghatak, J; (2008) Nanotechnology **19**, 075103

92. Gade, A. K; Bonde, P. P; Ingle, A. P; Marcato, P; Duran, N; Rai, M. K; (2008) J. Biobased Mater. Bioenergy **2**, 1-5

93. Kathiresan, K; Manivanan, S; Nabeel, M. A; Dhivya, B; (2009) Colloids Surf. B: Biointerf. **71**, 133-137

94. Mukherjee, P; Ahmad, A; Mandal, D; Senapati, S; Sainkar, S. R; Khan, M. I; (2001) Angew. Chem. Int. Ed. **40**, 3585-3588

95. Gericke, M; Pinches, A; (2006) Hydrometallurgy 83, 132-140

96. Bhainsa, K. C; D'Souza, S. F; (2006) Colloids Surf B: Biointerf. **47**, 160-164

97. Fayaz, M; Balaji, K; Girilal, M; Yadav, R; Kalaichelvan, P. T; Venketesan, R; (2010) Nanomedicine **6**, 103-109

98. Riddin, T. L; Gericke, M; Whiteley, C. G; (2006) Nanotechnology **17**, 3482

99. Bharde, A; Rautaray, D; Bansal, V; Ahmad, A; Sarkar, I; Yusuf, S. M; Sanyal, M; Sastry, M; (2006) Small **2**, 135-141

100. Ahmad, A; Senapati, S; Khan, M. I; Kumar, R; Sastry, M; (2003) Langmuir **19**, 3550-

101. Ahmad, A; Senapati, S; Khan, M. I; Kumar, R; Ramani, R; Srinivas, V; Sastry, M; (2003) Nanotechnology **14a**, 824

102. Usha, R; Prabu, E; Palaniswamy, M; Venil, C. K; Rajendran, R; (2010) Global J. Biotech. Biochem. **5**, 153-160

103. Dameron, C. T; Reese, R. N; Mehra, R. K; Kortan, A. R; Carroll, P. J; Steigerwald, M. L; Brus, L. E; Winge, D. R; (1989) Nature **338**, 596-597

104. Kowshik, M; Ashtaputre, S; Kharrazi, S; Vogel, W; Urban, J; Kulkarni, S. K; Paknikar, K. M; (2003) Nanotechnology **14**, 95

105. Agnihotri, M; Joshi, S; Kumar, A. R; Zinjarde, S; Kulkarni, S; (2009) Mater. Lett. **63**, 1231-1234

106. Kumar, S. A; Wang, W; Pelletier, D; Gu, B; Moon, J; Mortensen, N; Allison, D; Joy, D; Phelps, T; Doktycz, M. J; (2010) *Environ. Sci. Technol.* **44**, 5210-5215

107. Konishi, Y; Nomura, T; Tskukiyama, T; Saitoh, N; (2004) *Trans.Mater. Res. Soc. Jpn.* **29**, 2341-2343

108. Suresh, A. K; Pelletier, D. A; Wang, W; Broich, M. L; Moon, J; Gu, B; Allison, D. P; Joy, D. C; Phelps, T. J; Doktycz, M. J; (2011) *Acta Biomater.* (**In press**)

109. Kumar, S. A; Peter, Y; Nadeau, J; (2008) *Nanotechnology*, **19**, 495101

110. Gericke, M; Pinches, A; (2006) Gold Bull. **39**, 22-28

111. Philip, D; (2009) Spectrochim. Acta A **73**, 374-381

112. Sweeney, R. Y; Mao, C. B; Gao, X. X; Burt, J. L; Belcher, A. M; Georgiou, G; Iverson, B. L; (2004) *Chem. Biol.* **11** 1553-1559

113. Scarano, G; Morelli, E; (2003) *Plant Sci.* **165**, 803-810

114. Holmes, J. D; Smith, P. R; Evans-Gowing, R; Richardson, D. J; Russell, D. A; Sodeau, J. R; (1995) *Arch. Microbiol.* **163**, 143-147

115. Lovley, D.R; Phillips, E. J. P; Gorby, Y. A; Landa, E. R; (1991) Nature **350**, 413-416

116. Li, X; Chen, S; Hu, W; Shi, S; Shen, W; Zhang, X; Wang, H; (2009) Carbohyd. Poly. **76**, 509-512

117. Balkwill, D. L; Maratea, D; Blakemore, R. P; (1980) *J. Bacteriol.* **141**, 1399-1408

118. Philipse, A; Maas, D; (2002) *Langmuir* **18,** 9977-9984

119. Roh, Y; Lauf, R. J; McMillan, A. D; Zhang, C; Rawn, C. J; Bai, J; Phelps, T. J; (2001) *Solid State Commun.* **118**, 529-534

120. Slawson, R. M; Van Dyke, M. I; Lee, H; Trevors, J. T; (1992) *Plasmid* **27**, 72-79

121. Bai, H. J; Zhang, Z. M; Guo, Y; Yang, G. E; (2009) *Coll. Surf. B* **70**, 142-146

122. Anderson, S; Appanna, V. D; (1994) *FEMS Microbiol. Lett.* **116**, 43-48

123. Mann, S; (1992) *Nature* **357**, 358-360

124. Kumar, U; Shete, A; Harle, A. S; Kasyutich, O; Schwarzacher, W; Pundle, A; Poddar, P; (2008) *Chem. Mater*. **20**, 1484-1491

125. Marshall, M. J; Beliaev, A. S; Dohnalkova, A. C; Kennedy, D. W; Shi, L; Wang, Z; Boyanov, M. I; Lai, B; Kemner, K. M; McLean, J. S; Reed, S. B; Culley, D. E; Bailey, V. L; Simonson, C. J; Saffarini, D. A; Romine, M. F; Zachara, J. M; Fredrickson, J. K; (2006) *PLoS Biol*. **4**, 1324-1333

126. Shenton, W; Douglas, T; Young, M; Stubbs, G; Mann, S; (1999) Adv. Mater. **11**, 253-256

127. Flynn, C. E; Mao, C; Hayhurst, A; Williams, J. L; Georgiou, G; Iverson, B; Belcher, A. M; (2003) J. Mater. Chem. **13**, 2414-2421

128. Brown, S; (1997) Nature Biotechnol. **15,** 269–272

129. Brown, S; Sarikaya, M; Johnson, E; (2000) J. Mol. Biol. **299,** 725–732

130. Whaley, S. R; English, D. S; Hu, E. L; Barbara, P. F; Belcher, M. A; (2000) Nature **405,** 665–668

131. Naik, R. R; Brott, L; Carlson, S. J; Stone, M. O; (2002) J. Nanosci. Nanotechnol. **2,** 1–6

132. Naik, R. R; Stringer, S. J; Agarwal, G; Jones, S. E; Stone, M. O; Nature Mater. **1,** 169–172

133. Gaskin, D. J. H; Starck, K; Vulfson, E. N; (2000) Biotech. Lett. **22,** 1211–1216

134. Brown, S. (1992) Proc. Natl Acad. Sci. USA **89,** 8651–8655

135. Bassindale, A. R; Codina-Barrios, A; Frascione, N; Taylor, P. G; (2007) Chem. Commun. 2956–2958

136. Shankar, S. S; Rai, A; Ankamwar, B; Singh, A; Ahmad, A; Sastry, M; (2004) Nature Mater. **3**, 482-488

137. Narayanan, K. B; Sakthivel, N; (2008) Mater. Lett. **62**, 4588-4590

138. Sathishkumar, M; Sneha, K; Won, S. W; Cho, C. -W; Kim, S; Yun, Y. -S; (2009) Colloid. Surf. B **73**, 332–338

139. Song, J. Y; Kwon, E, Y; Kim, B. S; (2010) Bioprocess Biosyst. Eng. 33, 159–164

140. Zayats, M; Baron, R; Popov, I; Willner, I; (2005) Nano Lett. **5**, 21-25

141. Baron, R; Zayats, M; Willner, I; (2005) Anal. Chem. **77**, 1566-1571

142. Kumar, S. A; Kazemian, M; Gosavi, S. W; Kulkarni, S; Parischa, R; Ahmad, A; Khan, M. I; (2007) Biotechnol. Appl. Bioc. **47**, 191-195

143. Kumar, S. A; Kazemian, M; Gosavi, S. W; Kulkarni, S; Parischa, R; Ahmad, A; Khan, M. I; (2007) Biotech. Lett. **29**, 439-445

144. Ansary, A. A; Kumar, S. A; Krishnasastry, M. V; Abyaneh, M. K; Kulkarni, S. K; Ahmad, A; Khan, M. I; (2007) J. Biomed. Nanotechnol. **3**, 406-413

145. Spatz, J. P; Roescher, A; Moller, M, (1996) Adv. Mater. **8**, 337-340

146. Zhang, J; Sun, L; Liao, C; Yan, C; (2002) Solid State Commun. **124**, 45–48

147. Chandrasekharan, N; Kamat, P. V; (2002) Res. Chem. Intermediat. **28**, 847-856

148. Vakurov, A; Pchelintsev, N. A; Forde, J; O'Fagain, C; Gibson, T; Millner, P; (2009) Nanotechnology **20**, 295605

149. Gearheart, L. A; Ploehn, H. J; Murphy, C. J; (2001) J. Phys. Chem. B **105**, 12609–12615

150. Levina, L; Sukhovatkin, V; Musikhin, S; Cauchi, S; Nisman, R; Bazett-Jones, D. P; Sargent, E. H; (2005) Adv. Mater. **17**, 1854-1857

151. Choi, J. H; Chen, K. H; Strano, M. S; (2006) J. Am. Chem. Soc. **128**, 15584-15585

152. Ma, N; Dooley, C. J; Kelley, S. O; (2006) J. Am. Chem. Soc. **128**, 12598-12599

153. Chena, T; Wonga, Y; Zhengb, W; Huang, Y. B. L; (2008) Colloid. Surf. B **67**, 26-31

154. Liu, Q; Guo, M; Nie, Z; Yuan, J; Tan, J; Yao, S; (2008) Langmuir **24**, 1595-1599

155. Slocik, J. M; Moore, J. T; Wright, D. W; (2002) Nano Lett. **2**, 169-173

156. Banerjee, I. A; Yu, L; Matsui, H; (2003) Proc. Natl. Acad. Sci. U. S. A. **100**, 14678-14682

157. Lu, K; Conticello, V. P; Lynn, D. G; (2004) Mater. Res. Soc. Synp. Proc. 826E, eds. V1.6

158. Meldrum, F. C; Wade, V. J; Nimmo, D. L; Heywood, B. R; Mann, S; (1991) Nature, **349**, 684-687

159. Allen, M; Willits, D; Mosolf, J; Young, M; Douglas, T; (2002) Adv. Mater. **14**, 1562-1565

160. Reches, M; Gazit, E; (2003) Science, **300**, 625-627

161. Nuraje, N; Su, K; Haboosheh, A; Samson, J; Manning, E. P; Yang, N; Matsui, H; (2006) Adv. Mater. **18**, 807-811

162. Lee, S. -Y; Gao, X; Matsui, H; (2007) J. Am. Chem. Soc. **129**, 2954-2958

163. Ogale, S. B; Ahmad, A; Pasricha, R; Dhas, V. V; Syed, A; (2006) App. Phys. Lett. **89**, 263105

164. Jin, R; Cao, Y; Mirkin, C. A; Kelly, K. L; Schatz, G. C; Zheng, J. G; (2001) Science **294**, 1901-1903

165. Yu, Y. Y; Chang, S. S; Lee, C. L; Wang, C. R. C; (1997) J.Phys. Chem. B **101**, 6661-6664

166. Sun, Y; Xia, Y; Science 2002, 298, 2176-2179

167. Ahmadi, T. S; Wang, Z. L; Green, T. C; Henglein, A; El-Sayed, M. A; (1996) Science **272**, 1924-1926

168. Wang, Z; Zhang, J; Ekman, J. M; Kenis, P. J. A; Lu. Y; (2010) Nano Lett. **10**, 1886-1891

169. Tao, A. R; Sinsermsuksakul, P; Yang, P; (2006) Angew.Chem. **118**, 4713–4717

170. Song, H; Kim, F; Connor, S; Somorjai, G. A; Yang, P; (2005) J. Phys. Chem. B **109**, 188-193

171. Kim, F; Connor, S; Song, H; Kuykendall, T; Yang, P; Angew. Chem. 2004, 116, 3759–3763

172. Sun, Y; Sun, L; Zhang, B; Xu, F, Liu, Z, Guo, C; Zhang, Y; Li, Z; (2009) Talanta. **79**, 562-569

173. Sun, Y; Gates, B; Mayers, B; Xia, Y; (2002) Nano Lett. **2**, 165-168

174. Johnson, C. J; Dujardin, E; Davis, S. A; Murphy, C. J; Mann, S; (2002) J. Mater. Chem. 12, 1765-1770

175. Lah, N. A. C; Johan, M. R; (2011) Appl. Surf. Sci. (In press)

176. Kasture, M; Sastry, M; Prasad, B. L. V; (2010) Chem. Phy. Lett. **484**, 271-275

177. Teranishi, T; Kurita, R; Miyake, M; (2000) J. Inorg. Organomet. P. **10**, 145-156

178. Lu, L. T; Tung, L. D; Robinson, I; Ung, D; Tan, B; Long, J; Cooper, A. I; Fernig, D. G; Thanh, N. T. K; (2008) J. Mater. Chem. **18**, 2453-2458

179. Nyiro-Kosa, I; Nagy, D. C; Posfai, M; (2009) Eur. J. Mineral. **21**, 293-302

180. Zhang, L; Dou, Y; Gu, H; (2006) J. Cryst. Growth **296**, 221-226

181. Nandwana, V; Elkins, K. E; Poudyal, N; Chaubey, G. S; Yano, K; Liu, J. P; (2007) J. Phys. Chem. C **111**, 4185-4189

182. Kahn, M. L; Monge, M, Colliere, V, Senocq, F; Maisonnat, A; Chaudret, B; (2005) Adv. Funct. Mater. **15**, 458-468

183. Kruszynska, M; Borchert, H; Parisi, J; Kolny-Olesiak, J; (2010) J. Am. Chem. Soc. **132**, 15976-15986

184. Jin, R; Egusa. S; Scherer. N. F; (2004) J. Am. Chem. Soc. **126**, 9900-9901

185. Jin, R; Cao, C; Hao, E; Metraux, G. S; Schatz, G. C; Mirkin, C. A; (2003) Nature **425**, 487-490

186. Li, D., Li, J. (2003) Chem. Phys. Lett. **372**, 668-673

187. Roorda, S; van Dillen, T; Polman, A; Graf, C; van Blaaferen, A; Kooi, B; (2004) Adv. Mater. **16**, 235-237

188. Link, S; Burda. C; Nikoobakht El-Sayed. M. A. J. (2000) Phys. Chem. B **104**, 6152-6163

189. Gutwein, L. G; Webster, T. J; (2003) American Ceramic Society: 26th Annual Meeting Conference Proceedings Vol. 23, Issue 4

190. Ma, J; Wong, H; Kong, L. B; Peng, K. W; (2003) Nanotechnology **14**, 619-623

191. Roy, I; Ohulchanskyy, T. Y; Pudavar, H. E; Bergey, E. J; Oseroff, A. R; Morgan, J; Dougherty, T. J; Prasad, P. N; (2003) J. Am. Chem. Soc. **125**, 7860-7865

192. Song, E; Hu, J; Wen, C; Tian, Z; Yu, X; Zhang, Z; Shi, Y; Pang, D; Dai-Wen Pang; (2011) ACS Nano **5**, 761-770

193. Vemula, P. K; Anderson, R. R; Karp, J. M; (2011) Nat. Nanotechnol. (**In press**)

194. Bruchez, M; Moronne, M; Gin, P; Weiss, S; Alivisatos, A. P; (1998) Science **281**, 2013-2016

195. Edelstein, R. L; Tamanaha, C. R; Sheehan, P. E; Miller, M. M; Baselt, D. R; Whitman. L. J; Colton, R. J; (2000) Biosensors Bioelectron. **14**, 805-813

196. Nam, J. M; Thaxton, C. C; Mirkin, C. A; (2003) Science **301**, 1884-1886

197. Yoshida, J; Kobayashi, T; (1999) J. Magn. Magn. Mater. **194**, 176-184

198. Weissleder, R; Elizondo, G; Wittenburg, J; Rabito, C. A; Bengele, H. H; Josephson, L; (1990) Radiology **175**, 489-493

199. M. Haruta, (2002) CATTECH **6**, 102-115

200. Su, F. Z; Liu, Y. M; Wang, L. C; Cao, Y; He, H. Y; Fan, K. N; (2008) Angew. Chem. **120**, 340–343; (2008) Angew. Chem. Int. Ed. **47**, 334–337

201. Okumura, M; Akita, T; Haruta, M; (2002) Catal. Today **74**, 265–269

202. Taarning, E; Madsen, A. T; Marchetti, J. M; Egeblad, K; Christensen, C. H; (2008) Green Chem. **10**, 408–414

203. Willis, N. G; Guzman, J; (2008) Appl. Catal. A: Mol. **339**, 68–75

204. Gallon, B. J; Kojima, R. W; Kaner, R. B; Diaconescu, P. L; (2007) Angew. Chem. **119**, 7389–7392; (2007) Angew. Chem. Int. Ed. **46**, 7251–7254

205. Zhao, H; Zhou, J; Luo, H; Zeng, C; Li, D; Liu, Y; (2006) Catal. Lett. **108**, 49-54

206. Evangelisti, C; Panziera, N; Vitulli, M; Pertici, P; Balzano, F; Uccello-Barretta, G; Salvadori, P; (2008) Appl. Catal. A: Mol. **339**, 84–92

207. Pan, J; Li, J; Wang, C; Yang, Z; (2007) React. Kinet. Catal. Lett. **90**, 233–242

208. Tedsree, K; Li, T; Jones, S; Chan, C. W. A; Yu, K. M. K; Bagot, P. A. J; Marquis, E. A; Smith, G. D. W; Tsang, S. C. E; (2011) Nat. Nanotechnol. (**In Press**)

209. Jeon, K; Moon, H. R; Ruminski, A. M; Jiang, B; Kisielowski, C; Bardhan, R; Urban, J. J; (2011) **10**, 286-290

210. Heath, J. R; Ratner, R. A; (2003) Phy. Today 46-49

211. Schulz, L; Nuccio, L; Willis, M; Desai, P; Shakya, P; Kreouzis, T; Malik, V. K; Bernhard, C; Pratt, F. L; Morley, N. A; Suter, A; Nieuwenhuys, G. J; Prokscha, T; Morenzoni, E; Gillin, W. P; Drew, A. J; (2011) Nat. Nanotechnol. (**In press**)

212. Capelli, R; Toffanin, S; Generali, G; Usta, H; Facchetti, A; Muccini, M; (2010) Nat. Nanotechnol. **9**, 496-503

213. Matyba, P; Maturova, P; Kemerink, M; Robinson, N. D; Edman, L; (2009) Nat. Mater. **8**, 672-676

214. Pugazhenthiran, N; Anandan, S; Kathiravan, G; Prakash, N. K. U; Crawford, S; Ashokkumar, M; (2009) *J. Nanopart. Res.* **11**, 1811-1815

215. Ahmad, A; Senapati, S; Khan, M. I; Kumar, R; Sastry, M; (2003) *Langmuir* **19**, 3550-3553

216. Jun, G; ZhaoMing, Z; HongJuan, B; Guane, Y; (2007) *Sci. China Ser. B* **50**, 302-307

217. Senapati, S; Mandal, D; Ahmad, A; Khan, M. I; Sastry, M; Kumar, R; (2004) *Ind. J. Phys.* **78 A**, 101-105

218. Vigneshwaran, N; Kathe, A. A; Varadarajan, P. V; Nachane, R. P; Balasubramanya, R. H; (2006) *Coll Surf B: Interf.* **53**, 55-59

219. Basavaraja, S, Balaji, S. D; Lagashetty, A; Rajasab, A. H; Venkataraman, A; (2008) *Mat. Res. Bull.* **43**, 1164-1170

220. Bansal, V; Rautaray, D; Bharde, A; Ahire, K; Sanyal, A; Ahmad, A; Sastry, M; (2005) *J. Mater. Chem.* **15**, 2583-2589

221. Bansal, V; Poddar, P; Ahmad, A; Sastry, M; (2006) *J. Am. Chem. Soc.* **128**, 11958-11963

222. Uddin, I; Adyanthaya, S; Syed, A; Selvaraj, K; Ahmad, A; Poddar, P; (2008) *J. Nanosci. Nanotechnol*. **8**, 3909-3913

223. Lin, Z; Wu, J; Xue, R; Yang, Y; (2005) *Spectrochimica Acta Part A* **61**, 761-765

224. Kowshik, M; Vogel, W; Urban, J; Kulkarni, S. K; Paknikar, K. M; (2002) *Adv. Mater*. **14**, 815-818

225. Kowshik, M; Deshmukh, N; Vogel, W; Urban, J; Kulkarni, S. K; Paknikar, K. M; (2002) *Biotechnol. Bioeng.* **78**, 583-588

226. Jha, A. K; Prasad, K; Prasad, K; (2009) *Biochem. Eng. J.* **43**, 303-306

227. Jain, D; Daima, H, K; Kachhwaha, S; Kothari, S. L; (2009) *Dig. J. Nanomater. Bios.* **4**, 557-563

228. Shankar, S. S; Rai, A; Ahmad, A; Sastry, M; (2004) *J. Colloid. Interface Sci.* **275**, 496-502

229. Shankar, S. S; Ahmad, A; Sastry, M; (2003) *Biotechnol. Prog.* **19**, 1627-1631

230. Ankamwar, B; (2010) E-J. Chem. **7**, 1334-1339

231. Thirumurugan, A; Jiflin, G. J; Rajagomathi, G; Tomy, N. A; Ramachandran, S; Jaiganesh, R; (2010) *Int. J. Biol. Technol.* **1**, 75-77

232. Sharma, N. C; Sahi, S. V; Nath, S, Parsons, J. G; Torresdey, J. L. G; Pal, T; (2007) *Environ. Sci. Technol.* **41**, 5137-5142

233. Philip, D; (2011) *Spectrochim. Acta A: Mol. Biomol. Spectrosc.* **78**, 327-331

234. Ahmad, N; Sharma, S; Singh, V. N; Shamsi, S. F; Fatma, A; Mehta, B. R; (2011) Biotech. Res. Int. (In press)

235. Maensiri, S; Laokul, P; Klinkaewnarong J, Phokha, S; Promarak, V; Seraphin, S; (2008) *J. Optoelec. Adv. Mater.* **10**, 161-165

236. Cason, J. P; Roberts, C. B; (2000) *J. Phys. Chem.* **104**, 1217-1221

237. Dagaonkar, M. V; Mehra, A; Jain, R; Heeres, H. J; (2004) *Chem. Engg. Res. Des.*, **82**, 1438-1443

238. Lemyre, J; Ritcey, A. M; (2005) *Chem. Mater.* **17**, 3040-3043

239. Lee, Y; Lee, J; Bae, C. J; Park, J; Noh, H; Park, J; Hyeon, T; (2005) *Adv. Funct. Mater.* **15**, 503-509

240. Doker, O; Bayratkar, E; Mehmetoglu, U; Calimli, A; (2003) *Rev. Adv. Mater.* **5**, 498-500

241. Feng, Y; Yu, Y; Wang, Y; Lin, X; (2007) *Curr. Microbiol.* **55**, 402-408

242. Shahverdi, A. R; Minaeian, S; Shahverdi, H. R; Jamalifar, H; Nohi, A. A; (2007) *Proc. Biochem.* **42**, 919-923

243. Shaligram, N. S; Bule, M; Bhambure, R; Singhal, R. S; Singh, S. K; Szakacs, G; (2009) *Proc. Biochem.* **44**, 939-943

244. Mao, C; Flynn, C. E; Hayhurst, A; Sweeney, R; Qi, J; Georgiou, G; (2003) *Proc. Natl. Acad. Sci.* USA **100**, 6946-6951

245. Govender, Y; Riddin, T. L; Gericke, M; Whiteley, C. G; (2010) *J. Nanopart. Res.* **12**, 261-271

246. Lee, S. W; Mao, C; Flynn, C. E; Belcher, A. M; (2002) *Science* **296**, 892-

247. Ifuku, S; Tsuji, M; Morimoto, M; Saimoto, H; Yano, H; (2009) *Biomacromolecules* **10**, 2714-2717

248. Bai, L; Wan, H; Street, S. C; (2009) *Colloid Surface A* **349**, 23-28

249. Wang, J; Li, Q; Qiu, X; He, Y; Liu, W; (2010) *J. Nanosci. Nanotechnol.* **10**, 4308-4311

250. Zhang, F; Wong, S. S; (2010) *ACS Nano* **4**, 99-112

251. He, D; Xiao, X; Liu, F; Liu, R; (2008) *Appl. Surf. Sci.* **255**, 361-364

252. Gugliotti, L. A; Feldheim, D. L; Eaton, B. E; (2004) *Science* **304,** 850-852

253. Chiu, P. H; Hunag, C. J; Wang, Y. H; Chen, C. H; (2008) *Adv. Mater. Res.* **55-57**, 665-668

254. Sun, Y; Xia, Y; (2002) *Science* **298**, 2176-2179

255. Pothukuchi, S; Li, Y; Wong, C. P; 54th Electronic components and technology conference, 2004 Vol.2, pp.1965-1967

256. Norimatsu, F. Y; Mizokoshi, Y; Mori, K; Mizugaki, T; Ebitani, K; Kaneda, K; (2006) *Chem. Lett.* **35**, 276-277

257. Kim, Y. H; Lee, J. H; Shin, D. –W; Park, S. M; Moon, J. S; Nam, J. G; Yoo, Ji. –B; (2010) *Chem. Commun.* **46**, 2292-2294

258. Mntungwa, N; Rajasekhar, P. V. S. R; Revaprasadu, N; (2011) *Mater. Chem. Phys.* **126**, 500-506

CHAPTER: 2

MATERIALS AND METHODS

MATERIALS

Nitrate reductase and sulphite reductase were purified from the extracellular broth of fungus, *Fusarium oxysporum*, using the method described by Anil et al[1-2].

Chromatography matrices were from Sigma Chemicals (USA).

Capping peptides were procured from Geno Mechanix, Florida, U.S.A.

Cadmium chloride, selenium tetrachloride, sodium nitrate, lead nitrate, cobalt nitrate, nickel chloride, sodium sulphite, α-NADPH were from Sigma chemicals, U.S.A. All other chemicals used were of analytical grade.

Carbon coated copper grids, for HR-TEM analysis, were procured from Ted pella, Inc. (USA).

Bi-antennary and tri-antennary glycopeptides were purified from fibrinogen and fetuin respectively, from Sigma Chemicals (USA).

METHODS

i. Purification of enzymes, sulphite reductase and nitrate reductase:

Both the enzyme sulphite reductase and nitrate reductase were purified from the extra-cellular broth of fungus, *Fusarium oxysoprum* as described by Anil et al[1-2].

Microorganism and growth:

Fusarium oxysporum was maintained on PDA slants (potato 20% w/v, dextrose 2% w/v and agar 2% w/v) at 25°C. The fermentation was carried out by inoculating a 1 cm diameter mycelium from 7 day old PDA slant, into a 100 ml liquid MGYP medium (0.3% w/v malt extract, 1.0% w/v glucose, 0.3% w/v, yeast extract and 0.5% w/v peptone), in 500 ml Erlenmeyer flasks, followed by incubation at 26±1°C on a rotary shaker (200 rpm) for 96 h. After the fermentation period, the mycelia was collected by centrifugation (4500 *g*, 10°C, 20 min) washed with distilled water under sterile conditions and then suspended in 100 ml sterile distilled water, in 500 ml Erlenmeyer flask for 48 h under shaking (200 rpm). The supernatant was collected by centrifugation (4500 *g*, 20 min), concentrated by lyophilization, dialyzed extensively against Milli-Q water followed by dialysis against 20 mM phosphate buffer, pH 7.2 and used as the source of enzymes.

a. Sulphite reductase

DEAE-Sephadex chromatography:

The concentrated and dialyzed sample obtained from the above step was loaded on to a DEAE-Sephadex column (2.5x25 cm) pre-equilibrated with 20 mM phosphate buffer, pH 7.2, at a flow rate of 30 ml/h. The column was then washed with the above buffer till A_{280} was < 0.1. The bound protein was then eluted with a step wise gradient of NaCl (100-500 mM) in the same buffer at a flow rate of 30 ml/h. Fractions of 3 ml were collected and assayed for sulphite reductase activity and protein. The 100 mM eluates containing the sulphite reductase activity were pooled, lyophilized, dissolved in minimum amount of Milli Q water and dialyzed extensively against Milli Q water followed by 20 mM phosphate buffer, pH 7.2 containing 150 mM NaCl and used for the next step.

Gel filtration on Sephacryl S-300:

The fractions containing sulphite reductase obtained from the above step was loaded on to a Sephacryl S-300 column (2x100 cm) pre-equilibrated with 20 mM phosphate buffer, pH 7.2 containing 150 mM NaCl at a flow rate of 12 ml/h. Fractions of 2 ml were collected and checked for enzyme activity and protein. Active fractions were pooled, concentrated by lyophilization, dialyzed against Milli Q water and stored at 4°C till further use.

Sulfite reductase activity:

This was carried out according to Yashimoto et al[3]. The total reaction mixture 1.4 ml contained 1.0 mM of freshly prepared sodium sulfite, in 200 mM MES buffer pH 6.0, containing 1.0 mM EDTA, 0.15 mM NADPH and appropriately diluted enzyme. The reaction was initiated by the addition of NADPH followed by incubation at 25°C. The oxidation of NADPH was monitored spectrophotometrically at 340 nm. Enzyme samples incubated in the absence of sodium sulfite served as blank. One unit of sulphite reductase activity is defined as the amount of enzyme required to oxidize 1 mole of NADPH/min under the assay conditions.

b. Nitrate reductase

***DEAE-Sephadex chromatography*:**

The extracellular broth was loaded on to a DEAE-Sephadex column (2.5x25 cm) pre-equilibrated with 20 mM phosphate buffer, pH 7.2, at a flow rate of 30 ml/h. The un-adsorbed fractions containing nitrate reductase activity were pooled, concentrated by lyophilization and dialyzed extensively against Milli Q water followed by 20 mM sodium acetate buffer, pH 4.5 and used for the next step.

CM-Sephadex column chromatography:

The enzyme from the above step was chromatograped on a CM-Sephadex column (25x2.5 cm) pre-equilibrated with 20 mM sodium acetate buffer, pH 4.5. The column was then washed with the same buffer till A280 was < 0.1.The bound protein was then eluted with a step wise gradient of NaCl (100-500 mM) in the above buffer at a flow rate of 30 ml/h. Fractions of 2 ml were collected and assayed for nitrate reductase activity and protein. The 200 mM eluate containing nitrate reductase activity was lyophilized, dissolved in minimum amount of Milli Q water and then dialyzed extensively against Milli Q water followed by 20 mM phosphate buffer containing 150 mM NaCl, pH 7.2 and used for gel filtration.

Gel filtration on Sephacryl S-300:

The fractions containing nitrate reductase obtained from the above step was loaded on to a Sephacryl S-300 column (2x100 cm) pre-equilibrated with 20 mM phosphate buffer containing 150 mM NaCl, pH 7.2, at a flow rate was 12 ml/h. Fractions of 2 ml were collected and those with nitrate reductase were pooled, concentrated, dialyzed against Milli Q water and stored at 4°C till further use.

Determination of nitrate reductase activity:

This was performed as described by Snell et al[4]. The total reaction mixture of 1.5 ml, in one side arm of a Thunberg tube, contained 10mM of sodium nitrate in 200mM of phosphate buffer pH 7.0 and appropriately diluted enzyme. The other arm of the Thunberg tube contained 1mg of freshly prepared sodium dithionate and 1 mM α-NADPH, in 1ml of 200mM phosphate buffer pH 7.0. Subsequently the tubes were evacuated and the reaction was initiated by the addition of α-NADPH and sodium

dithionate followed by incubation at 55°C for 10 min. The reaction was terminated by opening the Thunberg tube to oxidize excess α-NADPH. To 1 ml of the above reaction mixture, 1ml of sulfanilamide reagent (1% w/v in 1 M HCl) and 1 ml of N-(1-napthyl)-ethylenediamine dihydrochloride (0.02% w/v in water) was added and left at room temperature for 10 min. The red color developed was measured at 540 nm after making up the volume to 9.5 ml with water. One unit of the enzyme is defined as the amount of enzyme required to produce 100 nmole of nitrite under the assay conditions. Reaction mixture incubated in the absence of enzyme served as blank.

Protein determination

Protein concentration was determined according to Lowry et al. using BSA as standard[5]. However, during enzyme purification steps protein concentrations were determined using the formula $1.55*A_{280} - 0.76*A_{260}$ = protein (mg/ml)[6].

Electrophoresis

PAGE of the purified enzymes was carried out in denaturing conditions in 8% (w/v) polyacrylamide gel, pH 4.3, with 10% SDS, according to Reisfeld et al. and the gels were stained with Coomassie Brilliant Blue R-250. SDS-PAGE was performed in 15% (w/v) polyacrylamide gel at pH 7.2 according to Weber and Osborn [7-8]. After electrophoresis the gels were visualized by silver staining according to Blum et al[9].

ii. Purification of bi/tri-antennary glycopeptides

One gm of the glycoprotein was dissolved in 100 ml of 20 mM Tris-HCl (containing 150 mM NaCl, 0.5 % w/v sodium azide), pH 7.2 and digested by 50 mg of pronase-E at 37 °C for 72 h, 20 mg of pronase was added after every 24 h. The digest was lyophilized, dissolved in 5 ml of 100 mM acetic acid, centrifuged (10000 g, 20 min), supernatant was collected. The pellet was re-extracted five times in 1 ml of 100 mM acetic acid. Two ml of clear supernatant was loaded on Sephadex G-25 column (1.5 · 100 cm) pre-equilibrated with 20 mM acetic acid, and eluted with the same buffer at the flow rate of 20 ml/h. The fractions (2 ml) were collected and those showing presence of sugar were pooled and further digested by carboxypeptidase (10 U at pH 7.0 and 25 °C for 24 h) and aminopeptidase (10 U at pH 8.5 and 25 °C for 24 h). The

residual peptides were removed by chromatography on Dowex-50 column (1.5*4 cm) in 20 mm acetic acid[10-11].

Neutral sugar estimation

The sugar solutions (400µl) were incubated with 400 µl of 5% (w/v) phenol for 10 min at room temperature. Two ml of sulfuric acid was then added and the mixture was allowed to cool for 20 min at room temperature. The colour developed was then measured spectrophotometrically, at 490 nm, using galactose-mannose (4:3) as standard[12].

iii. Enzyme mediated synthesis of fluorescent nanoparticles

CdSe nanoparticles:

The total reaction mixture of 3 ml contained 1.0 mM each of freshly prepared Cadmium chloride and Selenium tetrachloride, 5 mM Sodium nitrate, 100 µg of capping peptide (CP_n) of general structure γ-(Glu-Cys)$_n$-Gly (where n = 2,3,4 or 5), 1.0 mM α-NADPH and 1.66 U (100 µg protein) of nitrate reductase was incubated for 4 hours, under anaerobic conditions, at 25°C. On completion of the reaction, the as-synthesized CdSe nanoparticles were subjected to extraction with 50% (v/v) 1, 4-dioxane to remove the unbound proteins and used for further characterization.

Metal sulphide nanoparticles:

CdS nanoparticles were synthesized as described by Ansary et al[13]. Other metal sulphide nanoparticles were synthesized as follows. Under anaerobic condition, 3 mL of reaction mixture (0.2 M phosphate buffer (pH 7.2)) containing 1.0 mM of the appropriate metal salt viz., Cobalt nitrate, Nickel chloride or Lead nitrate and 1.0 mM of Na_2SO_3, 100 µg of capping peptide (CP_n), of general structure (γ-Glu-Cys)$_n$-Gly (where n = 2, 3, 4 or 5), 1.0 mM NADPH and 100 µg of sulphite reductase was incubated at 25°C for 4 h. On completion of the reaction, the as-synthesized metal sulfide nanoparticles were subjected to treatment with 50% v/v of 1,4 Dioxane to remove the unbound proteins and used for further characterization.

iv. Materials characterization of nanoparticles

All the nanoparticles synthesized using the enzymatic routes were characterized using the following techniques.

a. Absorbance spectroscopy

This method deals with the study of electronic transitions between orbitals or bands of atoms, ions or molecules in gaseous, liquid and solid state[14]. Metallic nanoparticles are known to exhibit characteristic colors. Mie, for the first time, explained the origin of colour by solving Maxwell's equation for the absorption and scattering of electromagnetic radiation by small metallic particles[15]. The absorption of electromagnetic radiation by metallic nanoparticles originates from the coherent oscillation of the valence band electrons induced by an interaction with the electromagnetic field[16]. These resonances are known as surface plasmons and occur only with nanoparticles[17]. Hence, UV-Vis can be utilized to study the unique optical properties of nanoparticles[18-19].

UV-Vis spectrophotometric measurements were performed on a Shimadzu dual beam spectrophotometer (model UV-1601 PC) operated at a resolution of 1 nm.

b. Fluorescence spectroscopy

In this technique, an incident light of a fixed wavelength is directed onto the specimen, prompting the transition of electron from the ground to excited state. The excited state of the molecule then undergoes a non-radiative internal relaxation and the excited electron moves to a more stable excited level. After a characteristic lifetime in the excited state, the electron returns to the ground state by emitting photons in the process with a characteristic wavelength in the form of light. This emitted energy can be used to obtain qualitative and quantitative information like, chemical composition, structure, impurities, kinetic process and energy transfer.

Fluorescence measurements were carried out on a Perkin-Elmer LS 50B luminescence spectro-fluorimeter, with slit width of 2 nm for both the monochromators and scan speed of 100 nm/min. Samples were excited at the wavelength corresponding to the absorbance maxima and the emission spectra recorded.

c. X-Ray diffraction (XRD) analysis

X-ray diffraction is used for the determination the crystal structure of solids, including lattice constants and geometry, orientation of single crystals, defects, etc[20]. Bragg's equation obtained on measurement of the diffraction pattern of the crystals relates to the distance between two *hkl* planes (*d*) and the angle of diffraction (2θ) as: $n\lambda$ =

$2d\sin\theta$, where, λ = wavelength of X-rays, n = an integer is known as the order of reflection (*h*, *k* and *l* which represents Miller indices of the respective planes[21]. Moreover, the mean size of the nanoparticles can be determined using the Debye–Scherrer equation: $D = k\lambda / \beta\cos\theta$, where *D* = thickness of the nanocrystal, *k* is a constant, λ = wavelength of X-rays, β = width at half maxima of (111) reflection at Bragg's angle 2θ[22–23].

Thin films of as-synthesized nanoparticles were prepared on Si (111) substrates by drop-coating with nanoparticles suspension. The films on Si wafers were then subjected to X-ray diffraction (XRD) using Philips X'PERT PRO instrument equipped with X'celerator, a fast solid-state detector with a total number of active channels of 121. Iron-filtered Cu Kα radiation (λ=1.5406 Å) was used. XRPD patterns were recorded in the 2θ range of 20°- 80° with a step size of 0.02° and a time of 5 seconds per step.

d. X-ray photoelectron spectroscopy (XPS)

X-ray photoelectron spectroscopy is widely used for probing the electronic structure of atoms, molecules and condensed matter. When an X-ray photon of energy ($h\nu$) is incident on a solid matter, the kinetic energy (E_k) and the binding energy (E_b) of the ejected photoelectrons can be related as follows: $E_k = h\nu - E_b$. This kinetic energy distribution of the photoelectrons forms a series of discrete bands, which symbolizes the electronic structure of the sample. The core level binding energies of all the elements (other than H and He) in different oxidation states are unique which provides information about the chemical composition of the sample. However, to account for the multiplet splitting and satellites accompanying the photoemission peaks, the photoelectron spectra should be interpreted in terms of many-electron states of the final ionized state of the sample, rather than the occupied one-electron states of the neutral species[24].

Chemical analysis of a drop-coated film of CdSe nanoparticles on a conductive substrate was carried out on a ESCALAB MK II X-ray photoelectron spectrometer (V. G. Scientific, UK) with A1 k_α as the excitation source ($h\gamma$ = 1486.6 e V) operating at an accelerating voltage of 10 kV and 20 m A at a pressure of approximately 10^{-8} Pa.

e. Dynamic light scattering measurements

Dynamic light scattering and zeta potential measurements for the nanoparticles samples were performed on a Brookhaven 90 Plus/BI-MAS Instrument (Brookhaven Instruments, New York), equipped with a 15 mW solid state laser at a wavelength of 657 nm and scattering signals were collected at 90°, placed in the measurement cell in a 1-cm path cuvette at an average of 6 runs per scan.

f. High resolution transmission electron microscopy (HRTEM)

Transmission electron microscopy is typically used for high resolution imaging of thin films of solid samples for structural and compositional analysis. The technique involves: (i) irradiation of a very thin film by a high-energy electron beam, which is then diffracted by lattices of the crystalline or semicrystalline material and propagated in different directions, (ii) imaging and angular distribution analysis of the forward-scattered electrons and (iii) energy analysis of the emitted X-rays[25]. The topographic information obtained by TEM, in the vicinity of atomic resolution, can be utilized for structural characterization and identification of various forms of nanomaterials, viz., hexagonal, cubic or lamellar[26]. One of the limitations of TEM is that the electron scattering information on TEM originates from a three-dimensional image which is then projected onto a two dimensional detector. Therefore, structural information along the electron beam direction is superimposed at the image plane.

Samples were prepared by drying a drop of nanoparticles suspension on carbon pre-coated TEM copper grids followed by analysis on a FEI Tecnai 30 Transmission electron microscope operated at an accelerating voltage of 300 kV.

v. Biochemical characterization of nanoparticles

a. Estimation of free amino group

Total reaction volume of 1 ml containing 100 μg of CdS/CdSe nanocrystals, 500 μl of 4% sodium carbonate buffer pH 8.4, 50 μl of 0.1 % TNBS was incubated in dark at 30°C for 2 hours. The number of amino groups modified was determined spectrophotometrically at 335nm using a molar absorption coefficient of 9950 $M^{-1}cm^{-1}$ [27].

b. Estimation of carboxyl group

The total reaction mixture 3 ml containing 100 μg of CdS/CdSe nanoparticles in 50 mM MES/HEPES buffer (75:25 v/v) pH 6.0, 50 mM EDC and 30 mM NTEE were incubated at 30°C for 45 minutes. Subsequently the reaction was arrested with the addition of 1 ml of 10% TCA and the precipitated CdSe-peptide complex was collected by centrifugation, washed extensively with chilled acetone, air-dried and re-dissolved in 1 ml of 100 mM NaOH. The number of nitro-tyrosyl group incorporated was determined spectrophotometrically at 430 nm using a molar absorption coefficient of 4600 $M^{-1}cm^{-1}$ [28].

vi. Conjugation of glycopeptides with nanoparticles

A modification of the method used to estimate the carboxyl group was used for the conjugation of CdS/CdSe nanoparticles with bi/tri-antennary glycopeptides. The total reaction mixture of 3 ml containing 100 μg of CdS/CdSe nanoparticles, 50 μg of bi/tri-antennary glycopeptide in 50 mM MES/HEPES buffer (75:25 v/v) pH 6.0 and 50 mM EDC was incubated at 30°C for 45 minutes. The CdS/CdSe-bi/tri-antennary glycopeptides conjugates were purified by passing the mixture through Sephadex G-25 matrix pre-equilibrated with 20 mM phosphate buffer pH 7.2 containing 150 mM NaCl.

vii. Structure elucidation of synthetic peptides

Circular dichroism spectra were collected on a Jasco J-715 spectropolarimeter. Far UV CD spectra (200-250nm) were collected with 0.1 mg/ml of the peptides placed in a path length of 1cm. The final spectrum was an average of 5 accumulations measured at a rate of 100nm/min at 1nm resolution. Secondary structure elements were calculated using CD pro software[29].

REFERENCES

1. Anil Kumar, S., Majid Kazemian, Gosavi, S. W., Kulkarni S. K., Renu Pasricha, Absar Ahmad, Khan M. I., (2007) *Biotechnol. Lett.* **29**, 439-445
2. Anil Kumar, S., Majid Kazemian, Gosavi, S. W., Kulkarni, S., Absar Ahmad, Khan, M. I., (2007) *Biotechnol. Appl. Bioc.* **47**, 191-195
3. Yoshimoto, A., Sato, R. (1968) *Biochim. Biophys. Acta.* **153**, 555-575
4. Snell, F. P., Snell, C. T. (1949) *Colorimetric methods of analysis* **3**, 804-805
5. Lowry, O. H., Rosenbrough, N. H., Farr, A., Randall, R. J. (1951) *J. Biol. Chem.* **193**, 265-275
6. Stoscheck, C. M. (1990) *Methods Enzymol.* **182**, 50-68
7. Reisfeld, R. A., Lewis, U. J. and William, A. G. (1962) *Nature* **195**, 281-283
8. Weber, K. and Osborn, M. (1969) *J. Biol. Chem.* **214**, 4406-4412
9. Blum, H., Beier, H. and Gross, H. J. (1987) *Electrophoresis* **8**, 93-99
10. Lis, H., Sharon, N. and Katchalski (1996) *J. Biol. Chem.* **241**, 684-689
11. Townsend, R. R., Hardy, M. R., Wong, T. C. and Lee, Y. C. (1986) *Biochemistry* **25**, 5716-5725
12. Dubois, M., Gills, K. K., Hamilton, J. K., Rebers, P. A. and Smoth, F. (1956) *Anal. Chem.* **28**, 350-356
13. Ansary, A. A.; Kumar, S. A.; Krishnasastry, M. V.; Abyaneh, M. K.; Kulkarni, S. K.; Ahmad, A.; Khan, M. I.; (2007) *J. Biomed. Nanotechnol.* **3**, 406-413
14. Jorgensen, K. (1962) Absorption Spectra and Chemical Bonding in Complexes, Pergamon, New York
15. Mie, G. (1908) *Ann. Physik*. **25,** 377-445
16. Faraday, M. (1857) *Philos. Trans.* **147,** 145-181
17. Papavassiliou, G. C. (1980) *Prog. Solid State Chem.* **12,** 185-193
18. Wang, Z. L., Mohamed, M. B., Link, S., El-Sayed, M. A. (1999) *Surf. Sci.* **440,** L809
19. Burda, C., Green, T., Landes, C., Link, S., Little, R., Petroski, J., El-Sayed, M. A. Characterization of Nanophase Materials, Ed, Z. L. Wang, Wiley-VCH, (2000) Weinheim, , Chapter 7, pp. 197
20. Wang, Z. I., Poncharal, P., De Heer, W. A. (2000) *J. Phys. Chem. Solids* **61,** 1025-1030

21. Bragg, W. H., Bragg, W.L., The Crystalline State, McMillan, (1949) New York, Vol.**1**
22. Birks, L. S., Friedman, H. (1946) *J. Appl. Phys.* **17**, 687-692
23. Rau, R. C. (1962) Advances in X-ray Analysis, Ed, W. M. Mueller, Sir Isaac Pitman and Sons Ltd., London, , Vol. **5**, pp. 104–116
24. Egelhoff Jr., W. F. (1987) *Surf. Sci. Rep.* **6**, 253-415
25. Fryer, J. R. (1979) Chemical Applications of Transmission Electron Microscopy, Academic Press, San Diego
26. Wang, Z. L. Characterization of Nanophase Materials, Ed, Z. L. Wang, (2000) Wiley-VCH, Weinheim, Ch 3, pp. 37
27. Habeeb, A. F. S. A. (1966) *Anal. Biochem.* **14**, 328-336
28. Pho, D. B., Roustan, C., Tot, A. N. T. and Pradel, L. A. (1977) *Biochemistry* 16, 4533-4537
29. Sreerama, N; Venyaminov, S. Y; Woody, R. W; (1999) *Protein Sci.* 370-380

CHAPTER: 3

RESULTS

This chapter discusses the various results obtained during the course of the current investigation on the synthesis and size control of quantum dots such as CdSe, Co_3S_4, PbS and CdS, and shape control studies of Ni_7S_6. It discusses in detail the synthetic procedures involved in the synthesis of fluorescent quantum dots viz. CdSe, and metal sulphide nanoparticles such as Co_3S_4, PbS, Ni_7S_6. The detailed characterization of the as-synthesized nanoparticles using dynamic light scattering, transmission electron microscopy, X-ray diffraction, absorbance and fluorescence spectroscopies and X-ray photoelectron spectroscopy is also presented. In addition, this chapter encompasses the results of the conjugation of CdS and CdSe nanoparticles with bi-/tri-antennary glycopeptides and their characterization.

i. Enzyme mediated synthesis of fluorescent nanoparticles

Ideally, under anaerobic conditions, 3ml of the reaction mixture, in 200mM Phosphate buffer (pH 7.2) containing 1 mM of appropriate precursor metal salt(s), 5mM of the appropriate substrate, 100µg of capping peptide of general structure $(\gamma\text{-Glu-Cys})_n\text{-Gly}$, where n – 2, 3, 4 or 5, 0.1 mM NADPH (Nicotinamide Adenine Di-nucleotide

Precursor(s)	Enzyme	Nanoparticle product
$CdCl_2$ & $SeCl_4$	Nitrate reductase	CdSe
$CdCl_2$	Sulphite reductase	CdS
$CoCl_2$	Sulphite reductase	Co_3S_4
$PbCl_2$	Sulphite reductase	PbS
$Ni(NO_3)_3$	Sulphite reductase	Ni_7S_6

Table 3.1: *Precursor metal salts and enzymes involved in the synthesis of different quantum dots*

Phosphate-Sodium Salt, reduced) and 100µg of enzyme reductase, was incubated at 25°C for 4 hours which resulted in the formation of fluorescent quantum dots. The

enzymes nitrate reductase and sulphite reductase, were purified from the extra-cellular broth of fungus, *Fusarium oxysporum.* The synthesis was monitored by following the increase in absorption band that arises with the synthesis of quantum dots. The precursor metal salts and the corresponding enzyme reductase utilized for the synthesis of various quantum dots are presented in the Table 3.1. Sulphite and nitrate reductases utilized sodium sulphite and sodium nitrate as the substrates, respectively. Both the enzymes are NADPH dependent i.e. they require NADPH for their activity that serves as a co-factor. The absence of absorption band in the absence of either the enzyme reductase or NADPH or the synthetic peptides or the addition of denatured enzyme (data not shown) indicated the involvement of enzyme in the synthesis of quantum dots. The synthesis of quantum dots is hypothesized to be due to the reduction of metal ion (M^{+}) to stable metal M^{0}, utilizing the substrate and NADPH as the cofactor, with the so-formed nanoparticles bound by the synthetic peptides. A number of studies report the formation of nanoparticles by the reduction of metal ions to form stable nanoparticles[1]. Eq. 1 & 2 describe schematically the syntheses of CdSe and metal sulphide nanoparticles respectively under investigation.

$$Cd^{2+} + Se^{4+} + NO_3^- \xrightarrow[\text{Nitrate reductase}]{\text{NADPH, } CP_n} CdSe + NO_3^- \qquad (1)$$

$$M^{+} + SO_2^- \xrightarrow[\text{Sulphite reductase}]{\text{NADPH, } CP_n} MS \qquad (2)$$

The as-synthesized nanocrystals were treated with ethanol to remove the unbound protein and used for further characterization. In an earlier study, we reported the synthesis of CdSe quantum dots using the same fungus, *Fusarium oxysporum*, which served as the source of the enzyme nitrate reductase[2]. We also reported the use of sulphite reductase purified from the extra-cellular broth of fungus, *Fusarium oxysporum,* for the in vitro synthesis of CdS quantum dots and gold nanoparticles[3-4].

ii. Control of size of particles

The synthesis protocol described above was used for the determination of the role of synthetic peptides in the size and shape control of nanoparticles under investigation

such as CdSe, Co_3S_4, PbS and Ni_7S_6. The size control of CdS nanoparticles was studied by modifying the synthesis method reported by Ansary et al[3]. The length of the synthetic peptides was varied to study the influence of these peptides in the size and shape control of the nanoparticles under investigation. The as-synthesized nanoparticles suspensions, after the removal of unbound proteins, were subjected to dynamic light scattering analysis to determine the size distribution of nanoparticles in individual reaction mixtures. Size distribution analyses of all the individual reaction mixtures using dynamic light scattering (DLS) are summarized in Table 3.2.

Peptide	CdSe	Co_3S_4	PbS	Ni_7S_6	CdS
ECECG (1)	**~5.5 nm**	~158 nm	~67 nm	~30 nm	~27 nm
ECECECG (2)	~ 78nm	~78 nm	~25 nm	**~ 20 nm**	~32 nm
ECECECECG (3)	~ 218nm	**~9 nm**	**~5 nm**	~ 35 nm	~77 nm
ECECECECECG (4)	~ 278nm	~45 nm	~90 nm	~ 75 nm	**~6 nm**

Table 3.2: *Summary of the size distribution of nanoparticles synthesized using different lengths of synthetic peptides. (The numerals in brackets indicate the serial number of reaction mixture)*

DLS analysis of individual reaction mixtures showed that the different peptides had varying effects on the size control of nanoparticles under study.

In case of CdSe, the reaction mixture with the shortest of all the peptides under study, of structure $(\gamma\text{-Glu-Cys})_2$-Gly, contained CdSe nanoparticles in the size range of 3.9 – 9.0 nm with a mean size of ~5.5 nm. The reaction with larger peptides yielded larger nanoparticles.

In case of Co_3S_4 and PbS, the synthetic peptides of sequence $(\gamma\text{-Glu-Cys})_4$-Gly, were efficient in restricting the growth of both the nanoparticles below 10nm with an average size of ~9 and ~5nm respectively. The rest of the peptides produced larger nanoparticles.

The synthetic peptides of sequence $(\gamma\text{-Glu-Cys})_5$-Gly were responsible for the synthesis of CdS nanoparticles having a mean size of ~6nm. Our previous study reported the synthesis of CdS nanoparticles of mean size of ~27nm utilizing (γ-Glu-

Cys)$_2$-Gly as the template[3]. Of all the 5 nanoparticles under study, Ni_7S_6 nanoparticles had the largest size restricted particles at ~20nm. The peptide involved had a sequence of (γ-Glu-Cys)$_3$-Gly. The results showed no consensus with regards to the peptide sequence and restriction of nanoparticles. The results prompted further characterization to validate the results of DLS analysis. Of all the reaction mixtures with different peptides, only the nanoparticles with lowest size distribution as discussed above were selected for further characterization.

iii. Transmission electron microscopic analysis

In order to confirm the results of DLS analyses of all the nanoparticles under study, the nanoparticles samples were subjected to transmission electron microscopy (TEM) analysis. TEM analyses provide valuable information on the crystallinity, morphology and size distributions of the samples under study. The images were acquired in the transmission mode. All the images were acquired at different magnifications from different parts of the surface of grid to obtain a complete picture of the morphological features of the as-synthesized nanoparticles.

a. CdSe nanoparticles

CdSe nanoparticles synthesized using enzyme nitrate reductase in the presence of (γ-Glu-Cys)$_2$-Gly as the template was subjected to TEM analysis. This reaction mixture has been found to contain CdSe nanoparticles of the smallest size of all the other reaction mixtures with other capping peptides. HR-TEM observations showed that the crystals are essentially spherical in shape with the size distribution of nanocrystals in the range of 3.9 to 9.0 nm (Figure 3.1.A & C). The CdSe nanocrystals also showed good crystallinity, with the lattice fringes clearly visible, that agrees well with that of the X-Ray diffraction measurements. The corresponding reduced FFT images of the nanocrystals could be indexed to CdSe nanocrystals. Fig.3.1.A shows the transmission electron micrograph of CdSe nanocrystals synthesized using capping peptide of structure (γ-Glu-Cys)$_2$-Gly with the {112} and {101} phases exposed, which corresponds to d-spaces of 1.83 and 3.31 Å respectively. Fig. shows a single CdSe nanocrystal with the exposed {102} phase (d-spacing 2.56 Å). The size distribution of as-synthesized CdSe nanoparticles were calculated by counting ~100 individual nanoparticles from the images acquired from different parts of the copper grid

(Fig.3.1.B). CdSe nanoparticles of 5 nm in size were found in large numbers. TEM analysis indicated that the as-synthesized CdSe nanoparticles have a markedly narrow size distribution.

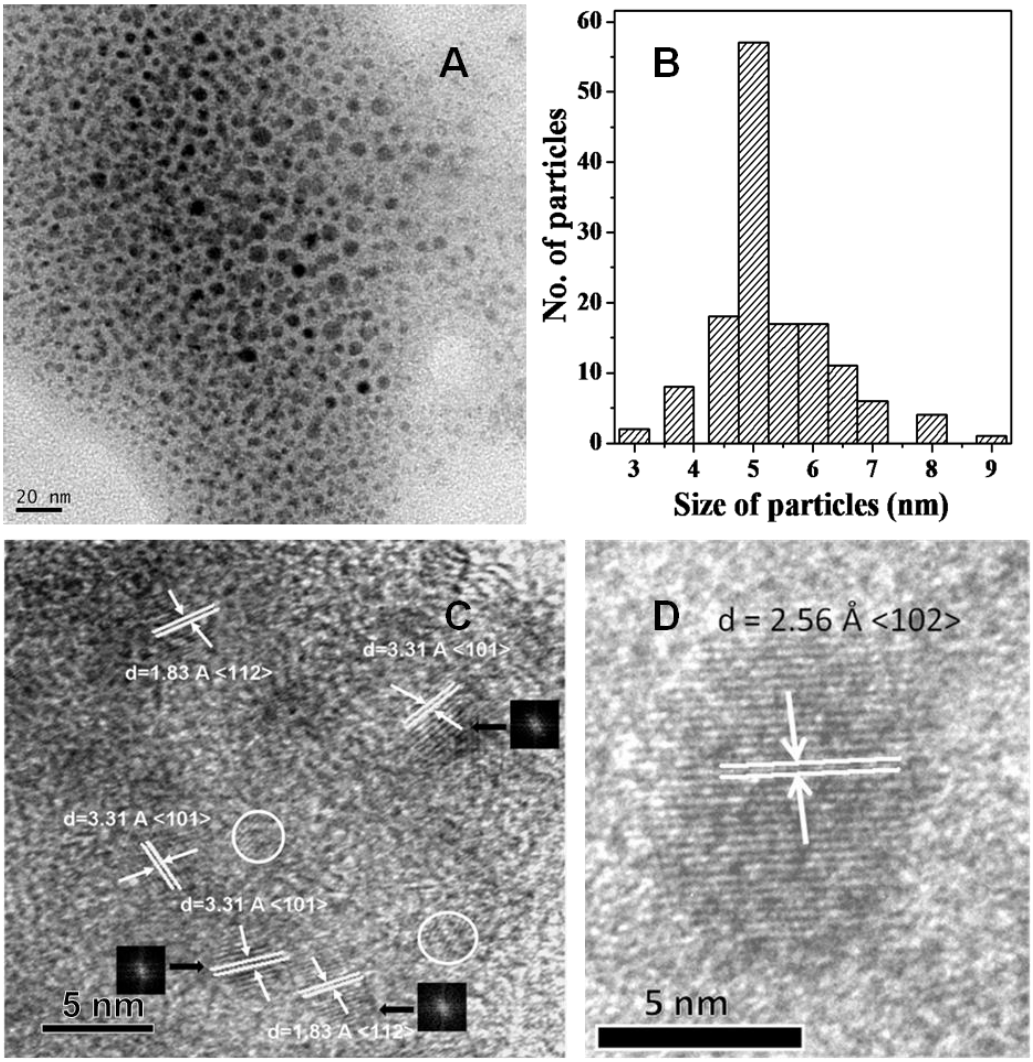

Fig. 3.1: *Transmission electron micrographs of CdSe quantum dots synthesized using enzyme nitrate reductase and CP_2 (A) TEM images taken at different magnifications from different areas of the grid (B) Histogram of size distribution of particles from TEM images (C) HRTEM image of as-synthesized CdSe quantum dots. Reduced FFT images are placed beside individual nanocrystal (D) HRTEM image of an individual CdSe quantum dot*

b. Co_3S_4 nanoparticles

Co_3S_4 nanoparticles synthesized using enzyme sulfite reductase in the presence of $(\gamma\text{-Glu-Cys})_4$-Gly as the template was subjected to TEM analysis. Of all the synthetic peptides under study, $(\gamma\text{-Glu-Cys})_4$-Gly produced the smallest Co_3S_4 nanoparticles.

TEM analysis at different magnifications revealed that the as-synthesized Co_3S_4 nanoparticles have a spherical morphology and agreed well with the distribution of particle size calculated using dynamic light scattering technique (Fig.3.2.A). HR-TEM analysis of the sample showed the crystal plane of the nanoparticles indicating good crystallinity (Fig.3.2.B). The crystal planes could be indexed to {311} phase of the Co_3S_4 nanoparticle with a corresponding d-spacing of 2.841 Å.

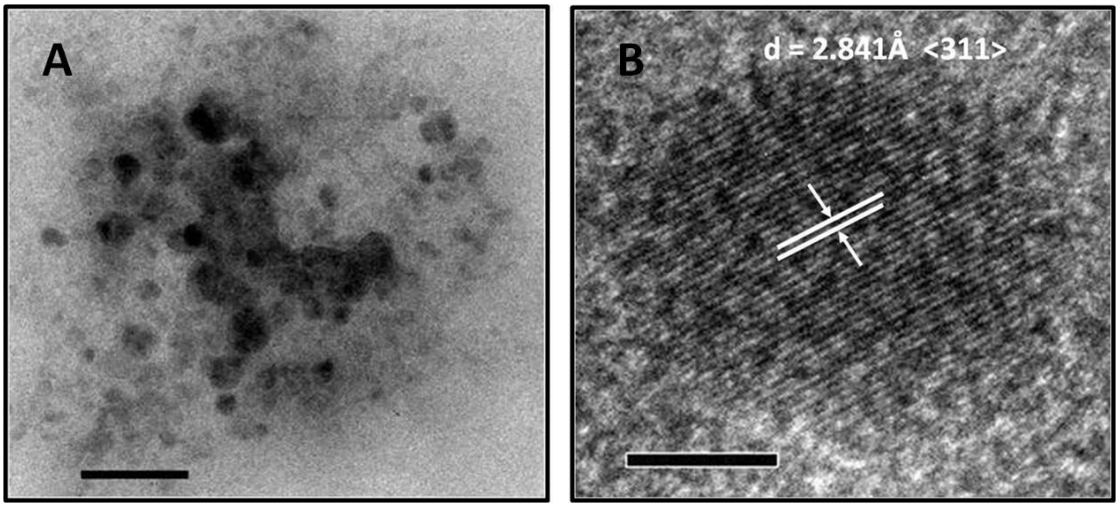

Fig.3.2: *A. Transmission electron micrograph of as-synthesized Co_3S_4 nanoparticles (Scale bar – 50 nm), B. HR-TEM of an individual Co_3S_4 nanoparticle (Scale bar – 5 nm)*

c. PbS nanoparticles

PbS nanoparticles synthesized using enzyme sulfite reductase in the presence of $(\gamma\text{-Glu-Cys})_4$-Gly as the template was subjected to TEM analysis. Of all the synthetic peptides under study, $(\gamma\text{-Glu-Cys})_4$-Gly mediated the synthesis of the smallest PbS nanoparticles. TEM analysis of the as-synthesized PbS nanoparticles at lower magnifications revealed that the morphology of the nanoparticles are essentially spherical with a narrow size distribution (Fig.3.3.A, C & D) HR-TEM analysis of the as-synthesized PbS nanoparticles showed crystal planes corresponding to the {112} plane with a d-value of 2.83 Å reported for PbS crystals (Fig.3.3.B). The crystallinity of the nanoparticles was also confirmed by the above analysis. The size distribution of the as-synthesized PbS nanoparticles obtained from different TEM images show that majority of the PbS nanoparticles are of 5 nm in size even though the size of nanoparticles ranges from 3 – 7 nm.

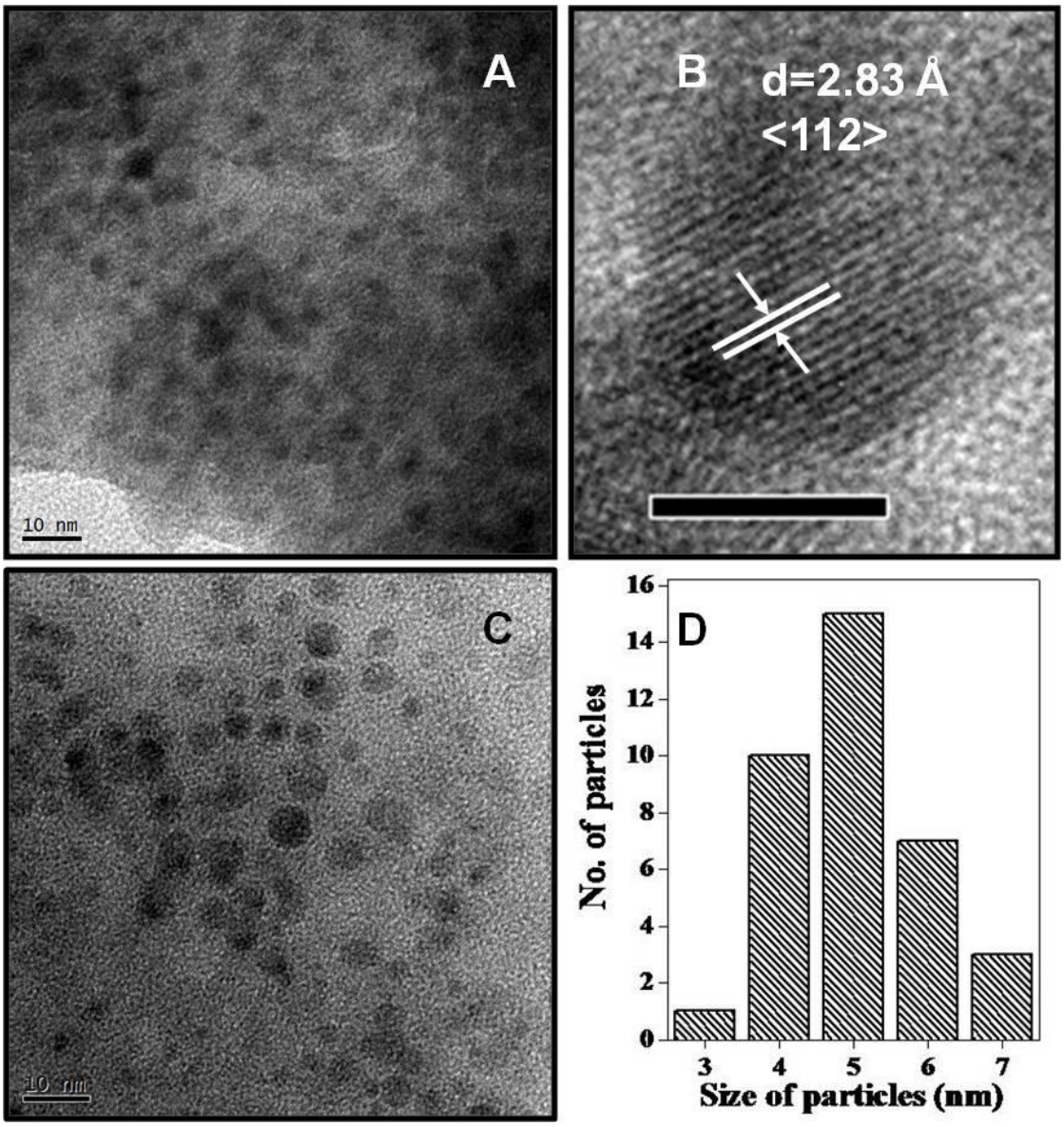

Fig. 3.3: *Transmission electron micrographs of as-synthesized PbS nanoparticles (A & C) TEM images acquired at low resolutions from different areas of the grid (B) HRTEM image of an individual PbS nanoparticle (Scale bar – 5nm) (D) Histogram of size distribution of particles from TEM images*

d. CdS nanoparticles

CdS nanoparticles synthesized using enzyme sulfite reductase in the presence of (γ-Glu-Cys)$_5$-Gly as the template was subjected to TEM analysis. (γ-Glu-Cys)$_5$-Gly templated the synthesis of the smallest CdS nanoparticles with a mean size of 6 nm in diameter. TEM analysis of the sample showed that the as-synthesized nanoparticles are more or less spherical in shape with a size ranging from 5 – 8 nm. Majority of the

nanoparticles have been found to be of 6 nm in size. TEM analysis under higher magnification revealed distinct crystal planes corresponding to CdS crystals with {042} plane clearly visible. Figures 3.4.A, B, C & D represent the TEM analysis of as-synthesized CdS nanoparticles under various magnifications and the corresponding size distribution histogram.

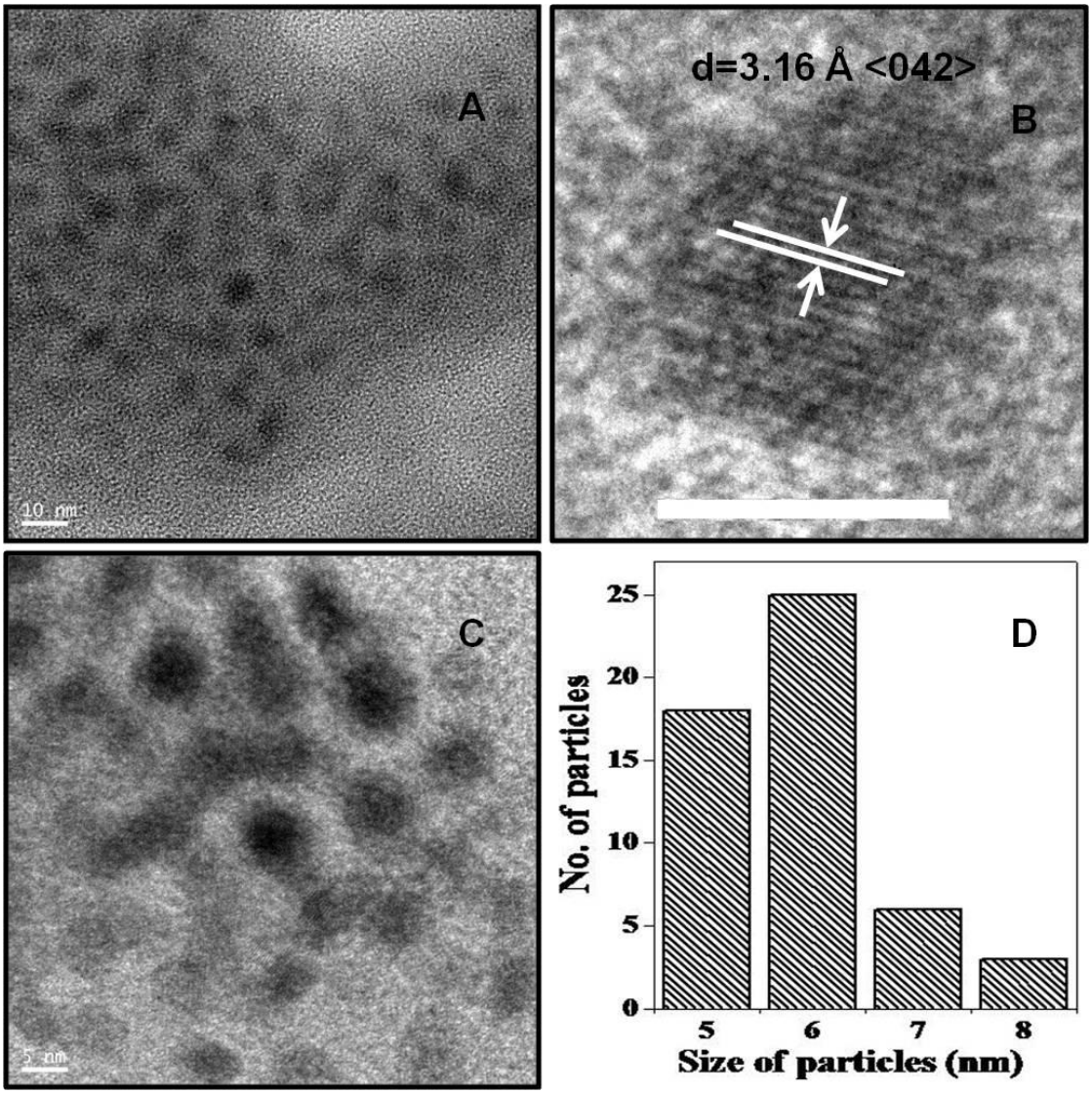

Fig. 3.4: *Transmission electron micrographs of as-synthesized CdS nanoparticles (A & C) TEM images acquired at low resolutions from different areas of the grid (B) HRTEM image of an individual CdS nanoparticle (Scale bar – 5nm) (D) Histogram of size distribution of particles from different TEM images*

e. Ni_7S_6 nanoparticles

Ni_7S_6 nanoparticles synthesized using enzyme sulfite reductase in the presence of (γ-

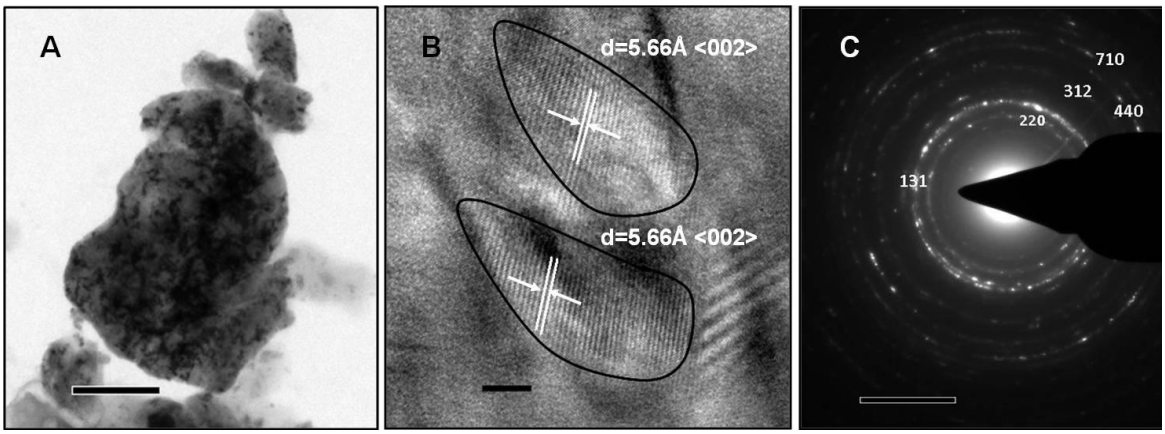

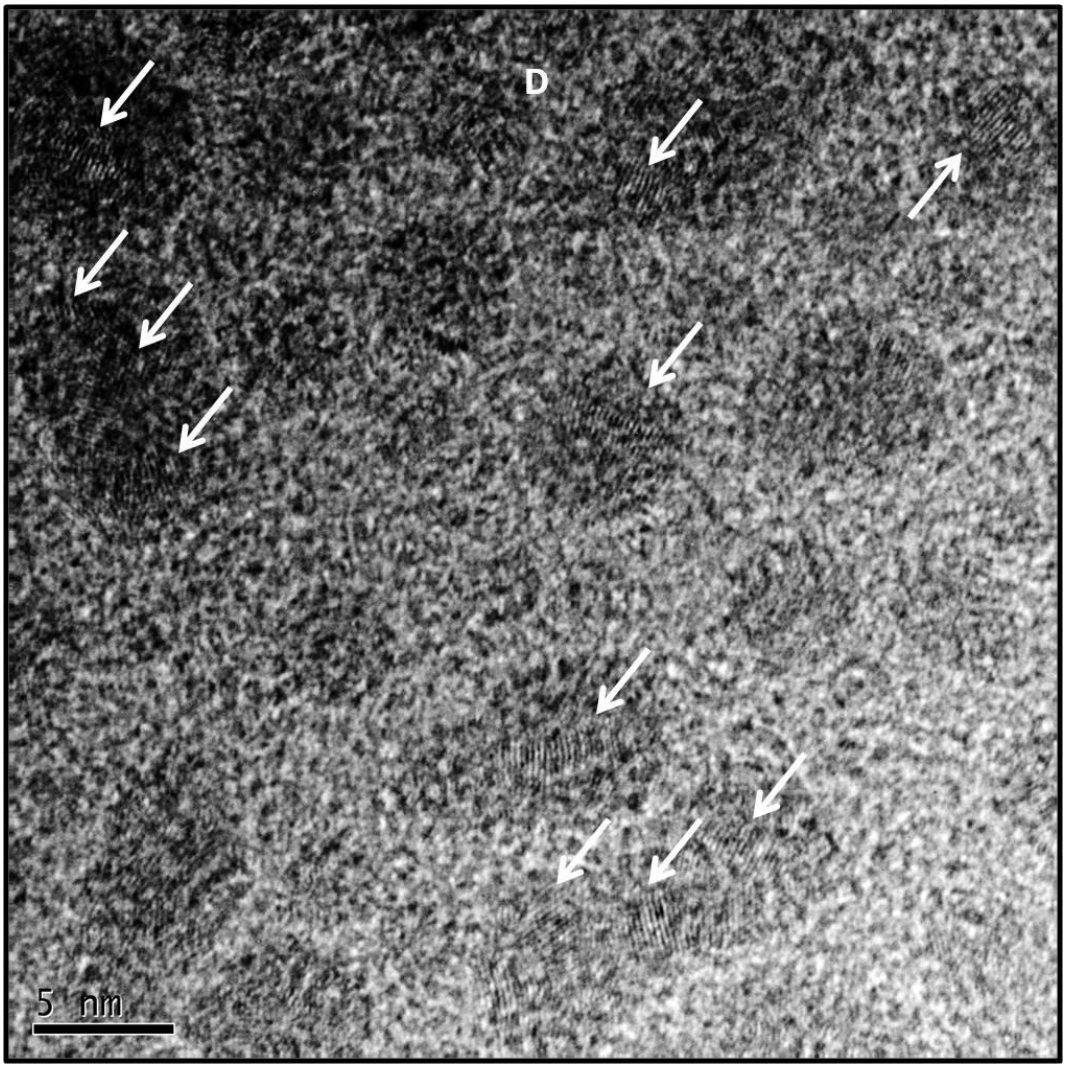

Fig. 3.5: *Transmission electron micrographs of as-synthesized Ni_7S_6 nanoparticles (A) low resolution (Scale bar – 200nm) (B) HR-TEM image of an individual nanoparticle (Scale bar – 5nm) (C) SAED pattern of a single nanoparticle (D) HR-TEM image of nanoparticles*

Glu-Cys)$_3$-Gly as the template was subjected to TEM analysis. (γ-Glu-Cys)$_5$-Gly templated the synthesis of the smallest Ni_7S_6 nanoparticles. The size of Ni_7S_6 nanoparticles were found in the range of 5 – 20 nm in length (Fig. 3.5.A & D). The as-synthesized Ni_7S_6 nanoparticles were elongated in one dimension thereby forming 'tear-drop' shaped nanoparticles with an aspect ratio of 2:5. HR-TEM analysis of the above nanoparticles revealed distinct crystal planes corresponding to the {002} plane of Ni_7S_6 crystal (Fig.3.5.B). SAED analysis confirmed the crystallinity of as-synthesized Ni_7S_6 nanoparticles (Fig.3.5.C).

iv. Optical properties

All the as-synthesized nanoparticles under investigation were further characterized for their optical properties such as absorbance and photoluminescence. Table 3.3 summarizes the absorbance and photoluminescence maxima of the nanoparticles discussed here. The absorbance and emission profiles of all the as-synthesized nanoparticles are given in Fig. 3.6.A - E.

The absorption spectra of the as-prepared nanoparticles in aqueous suspension showed peaks corresponding to the first excitonic transition. All the nanoparticles showed absorbance bands centred in the ultra violet region with the exception of Ni_7S_6 which showed absorbance maxima in the visible range at 407 nm. All the 4 metal sulphide nanoparticles but Ni_7S_6 showed maximum absorbance within a range of 15nm. All the as-synthesized nanoparticles showed a relative blue shift in absorbance as compared to that of the corresponding bulk materials. This phenomenon is characteristic of semiconductor nanocrystals that the absorbance edge shifts to higher energies with corresponding decrease in size. Emission analyses of the above as-synthesized nanoparticles showed that Co_3S_4 and PbS emit in the ultra violet region and the rest viz. CdSe, CdS and Ni_7S_6 in the visible region. The emission profiles of all the as-synthesized nanoparticles showed small stoke's shifts characteristic of nanoparticles. The emission bands observed for all the nanoparticles (CdSe – 454 nm, CdS – 418 nm, Co_3S_4 – 380 nm, PbS – 393 nm, Ni_7S_6 – 473) are attributed to the band gap or near band gap emission resulting from the recombination of electron-hole pairs observed in semiconductor nanocrystals. There are several reports on fluorescent nanoparticles with comparable emission maxima[5-7]. The full-width-half-maximum (FWHM) of emission profile observed for all the as-synthesized nanoparticles are

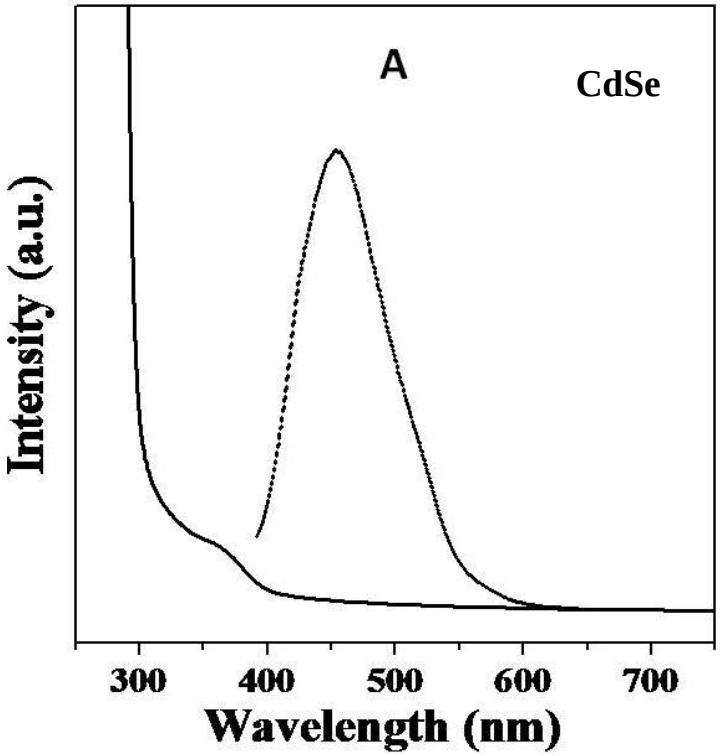

Fig. 3.6: *Absorbance and photoluminescence profile of as-synthesized, A. CdSe nanoparticles (Continuous line – Absorbance, Dotted line – Photoluminescence)*

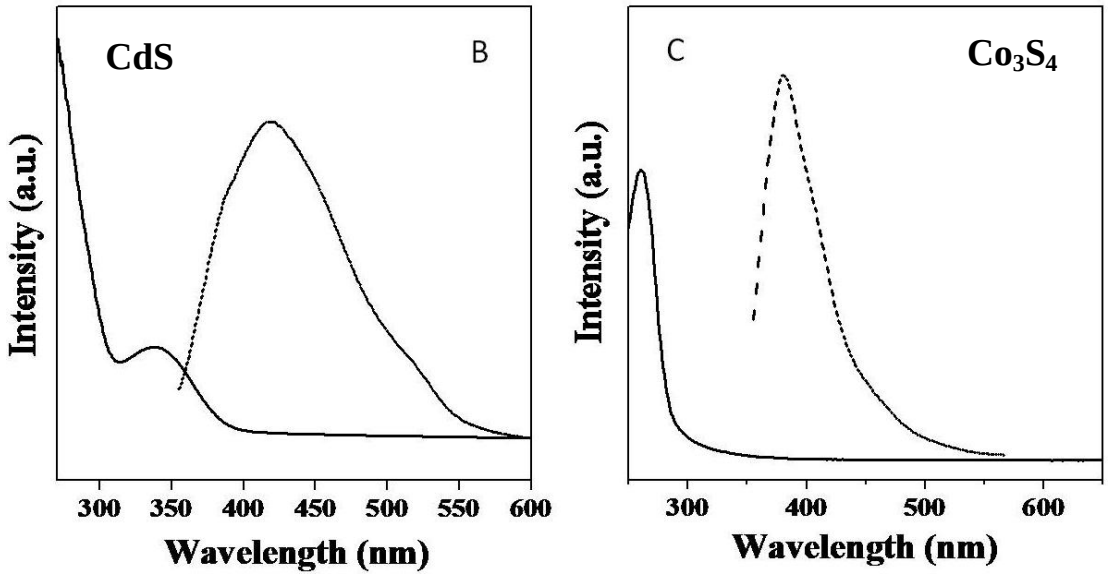

Fig. 3.6: *Absorbance and photoluminescence profile of as-synthesized nanoparticles, B. CdS, C. Co_3S_4, (Continuous Line – Absorbance, Dotted line – Photoluminescence)*

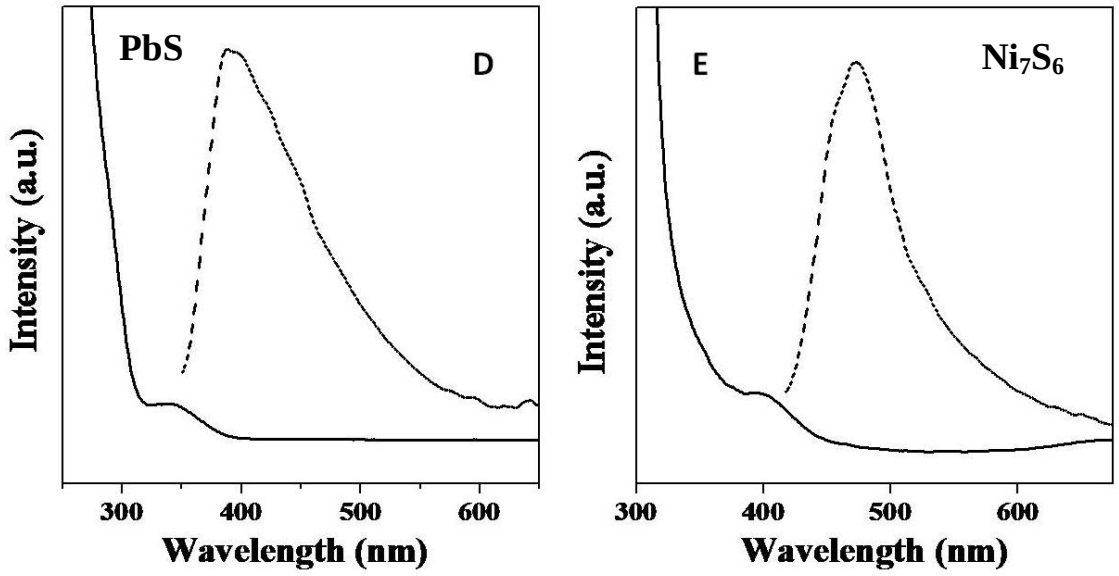

Fig. 3.6: *Absorbance and photoluminescence profile of as-synthesized nanoparticles, D. PbS, E. Ni_7S_6 (Continuous Line – Absorbance, Dotted line – Photoluminescence)*

Nanoparticle	$Absorbance_{max}$	$Emission_{max}$
CdSe	366 nm	454 nm (2.73)
CdS	339 nm	418 nm (2.96)
Co_3S_4	333 nm	380 nm (3.26)
PbS	342 nm	393 nm (3.16)
Ni_7S_6	407 nm	473 nm (2.62)

Table 3.3: *Summary of the absorption and emission maxima of as-synthesized nanoparticles. (The values in brackets represent the corresponding band width achievable for the given emission maximum)*

narrow indicating the narrow size distribution of nanoparticles. This matches well with the size distribution calculated from the TEM analyses. These emission maxima correspond well with the photoluminescence achieved for semiconductor nanocrystals.

The resulting band gap calculated from the emission maxima of all the nanoparticles under study are larger than those observed for bulk materials of identical elemental composition. This property is characteristic feature observed of semiconductor nanocrystals.

v. Determination of crystal structures

All the size controlled as-synthesized nanoparticles currently under study were analysed for their crystal structures. The purity of the as-synthesized materials has been determined by this analysis. Individual nanoparticles suspensions were drop coated on glass substrate and air dried before subjecting them for structural analysis using powder X-Ray diffraction. Fig.3.7 – 11.

X-Ray diffraction profile of CdSe nanocrystals synthesized using nitrate reductase and $(\gamma\text{-Glu-Cys})_5$-Gly is shown in Fig.3.7. The as-synthesized CdSe nanoparticles have been found to possess wurtzite structure. The observed broadening of Bragg's peaks

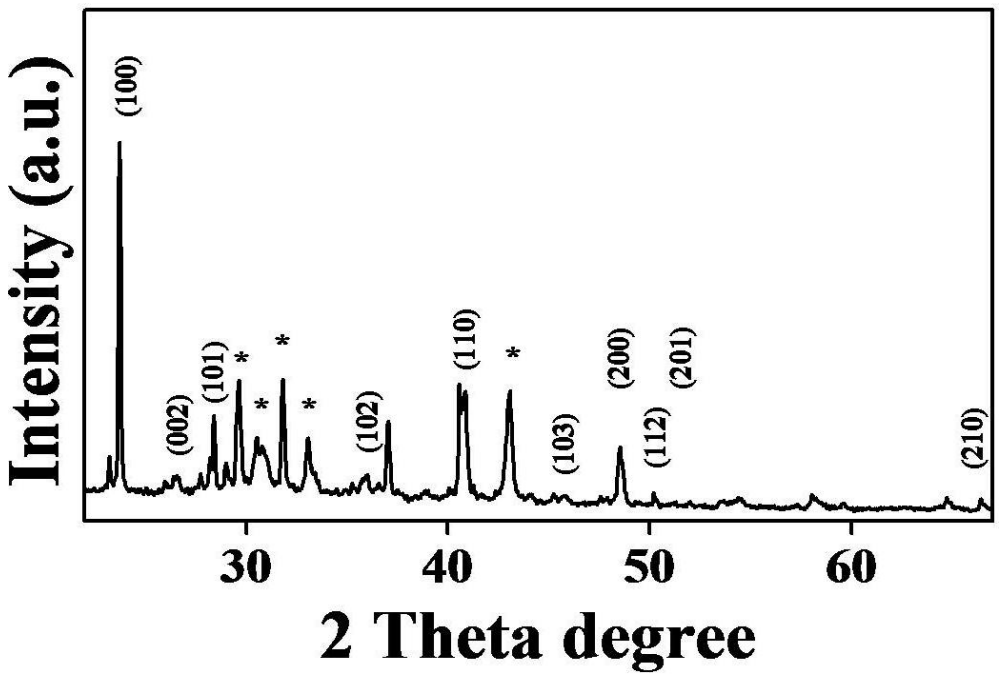

Fig.3.7: *Powder X-Ray diffraction profile of CdSe nanoparticles (CdO peaks are marked with asterisk (*))*

indicates the particles are in nanoscale dimensions. The diffraction measurements indicate the CdSe nanocrystals to be in hexagonal phase with values of a = 4.30 and c = 7.02 and $\alpha = \beta = 90°$ and $\gamma = 120°$. The analysis also revealed the presence of CdO

phases.

The crystal structure of the as-synthesized Co_3S_4 nanoparticles was determined by the powder X-ray diffraction analysis. The principle bragg's reflections were indexed to the (311), (400), (211), (200), (440) and (533) planes which correspond to the linnaeite – cubic Co_3S_4 phase of cobalt sulphide with a preferential orientation

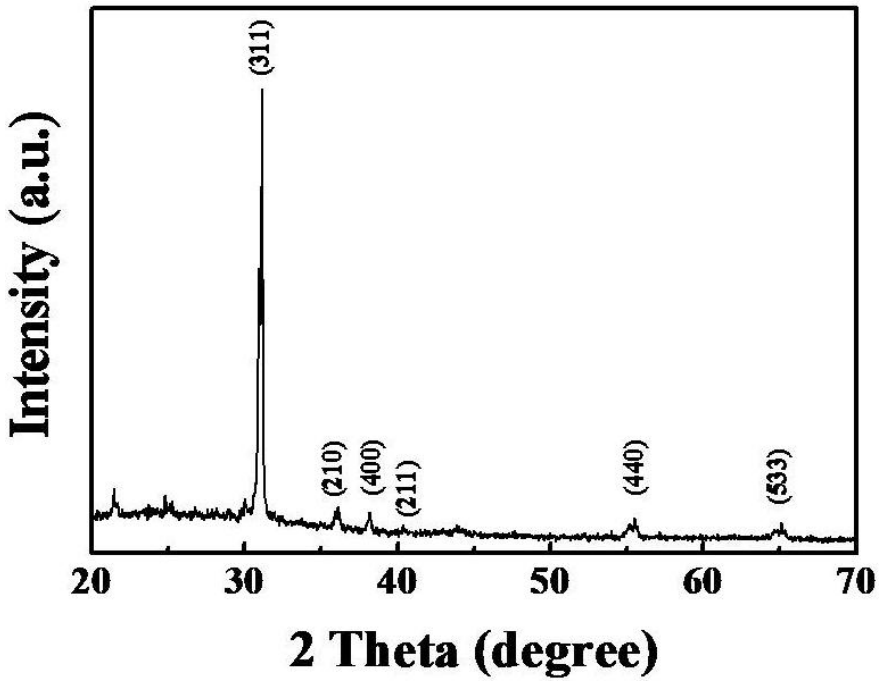

Fig.3.8: *Powder X-Ray diffraction profile of Co_3S_4 nanoparticles*

towards the (311) plane (Fig. 3.8). This characteristic is also evident in the HR-TEM analysis of an individual Co_3S_4 nanoparticle. The absence of other phases indicates that the synthesized cobalt sulphide is devoid of other phases such as that of CoS, CoS_2 and Co_9S_8. The broadening of peaks is characteristics of nanomaterials and indicates crystallinity of the material.

Fig.3.9 represents the XRD profile of PbS nanoparticles synthesized using sulphite reductase and $(\gamma\text{-Glu-Cys})_4$-Gly as the template. The principle bragg's reflections were indexed to the signature peaks corresponding to the crystal structure of tetragonal phase of PbS. The prominent peak corresponding to the <112> plane was also visible in the HR-TEM analysis. The broadening of the peaks indicates that the particles are in nano dimension. XRD profile indicates that the as-synthesized PbS is pure.

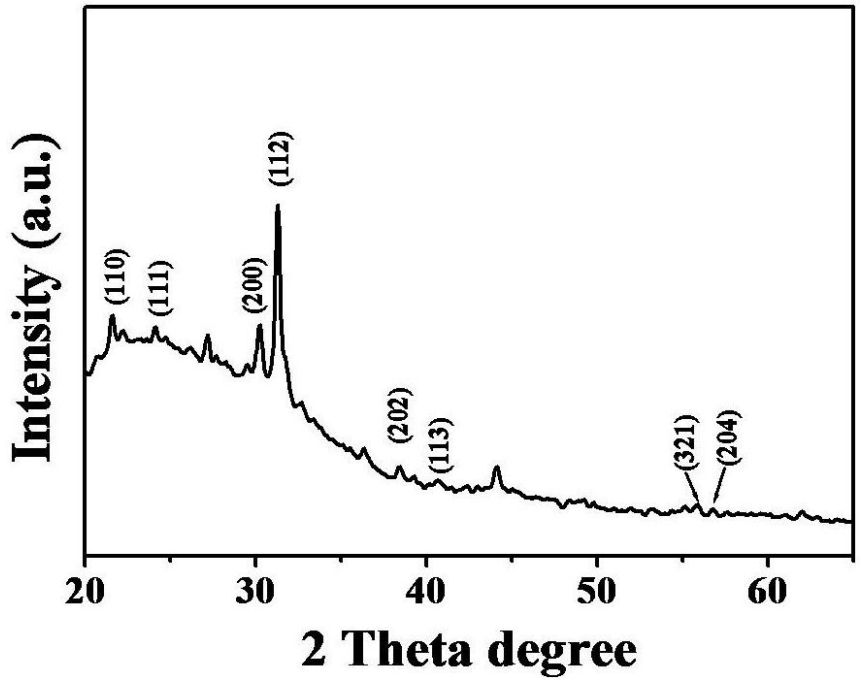

Fig.3.9: *Powder X-Ray diffraction profile of PbS nanoparticles*

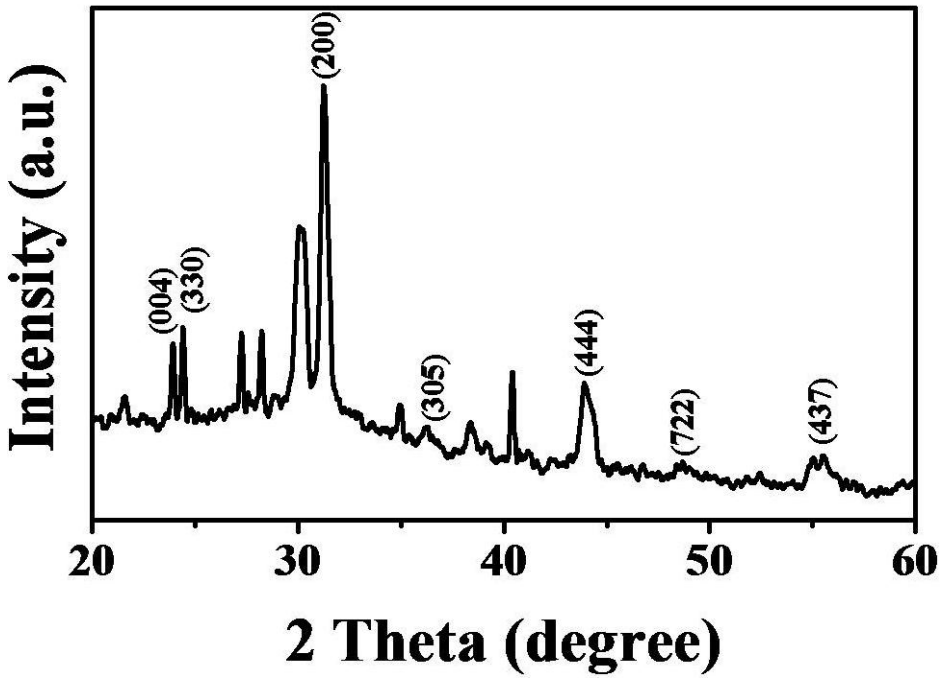

Fig.3.10: *Powder X-Ray diffraction profile of CdS nanoparticles*

Fig.3.10 represents the XRD profile of CdS nanoparticles synthesized using sulphite reductase and $(\gamma\text{-Glu-Cys})_5$-Gly as the template. Principle bragg's reflections were indexed to the CdS crystal reported in literature. The diffraction values show that the

CdS nanocrystals are in orthorhombic phase with values of a = 14.31, b = 14.07 and c = 14.56 and $\alpha = \beta = \gamma$. The peak broadening observed is indicative of the particles in the nano regime.

XRD pattern of the as-synthesized nickel sulphide nanoparticles is shown in Fig. 3.11. The principle bragg's reflections could be indexed to the orthorhombic phase of nickel sulphide. Based on the deduced crystal structure the empirical formula of the material can be calculated to Ni_7S_6. The above analysis shows that the as-synthesized material is a pure phase nickel sulphide without the presence of other phases of nickel sulphide such as NiS, Ni_3S_2, Ni_3S_4, Ni_9S_8, etc.

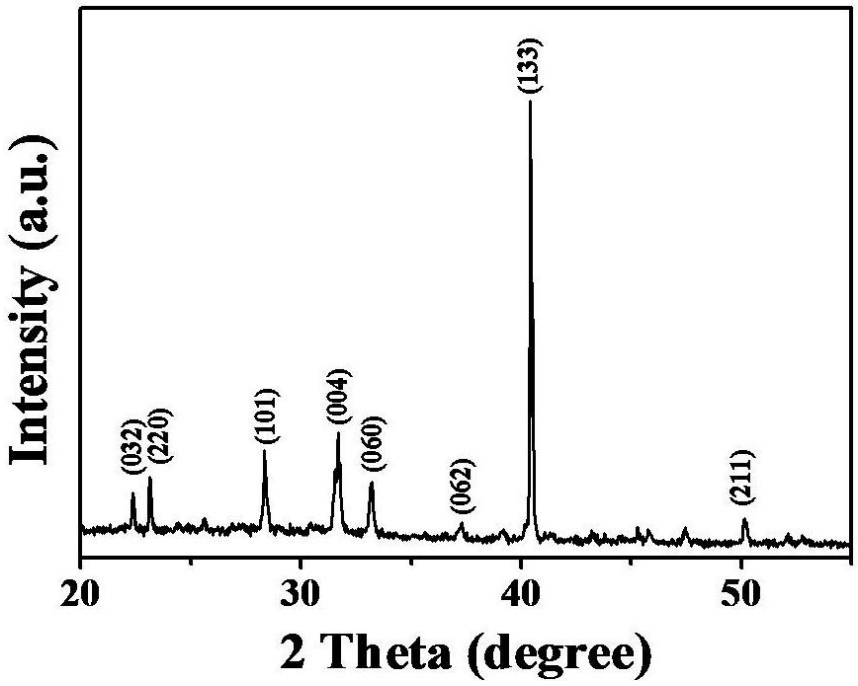

Fig.3.11: *Powder X-Ray diffraction profile of Ni_7S_6 nanoparticles*

vi. X-ray photoelectron spectroscopy analysis

The chemical states of all the as-synthesized nanoparticles were determined by X-Ray photoelectron spectroscopy. Narrow and wide scan XPS were performed on the as-synthesized nanoparticles. Core level binding energies for Cd and Se in the as-synthesized CdSe nanocrystals agree well with the values of the standards. This is due to the fact that the crystal structure of the nanocrystal is the same as the bulk, hence the presence of identical type of bonding. The binding energies of 405.5 and 412.5 eV observed for Cd is due to the decomposition of Cd3d spectrum into $Cd3d_{5/2}$ and $Cd3d_{3/2}$ with a spin orbit splitting factor of ≈7.0 eV (Fig.3.12.A). The Se 3d peak

observed at binding energy of 54.8 eV agrees with the core level binding energy reported for Se (Fig.3.12.B). Fig.3.13 represents the general scan obtained for the as-synthesized CdSe nanoparticles.

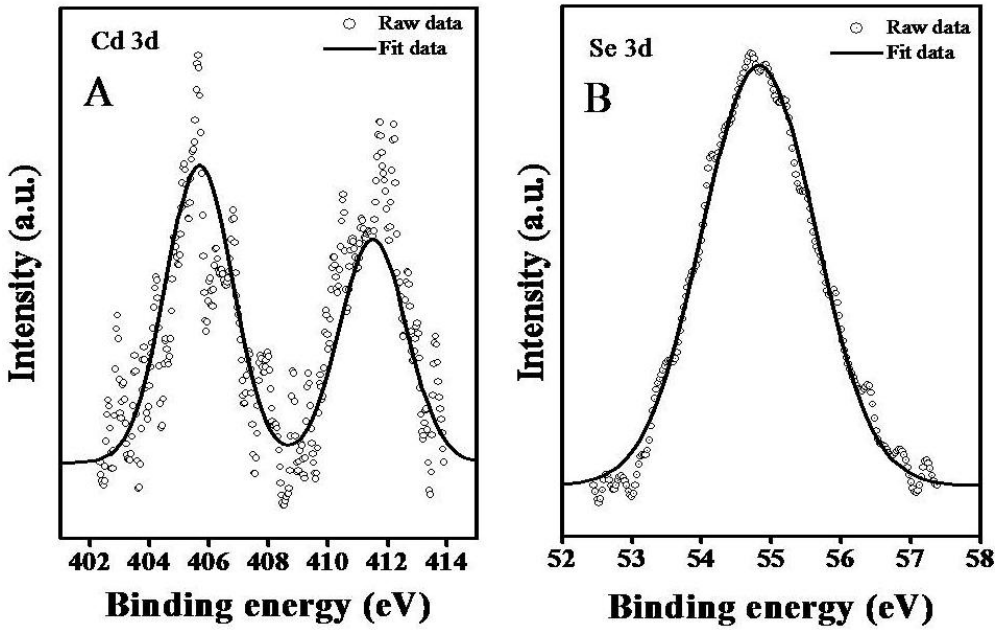

Fig.3.12.A&B: *Core level spectra of Cd 3d and Se3d of as-synthesized CdSe nanocrystals*

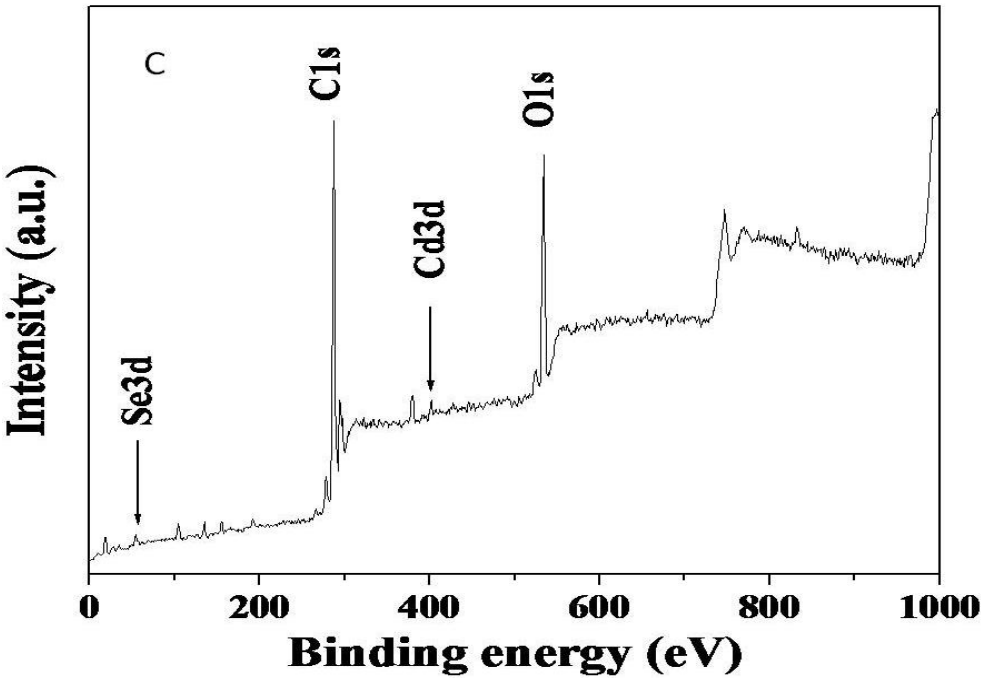

Fig.3.13: *General scan XPS profile of as-synthesized CdSe nanocrystals*

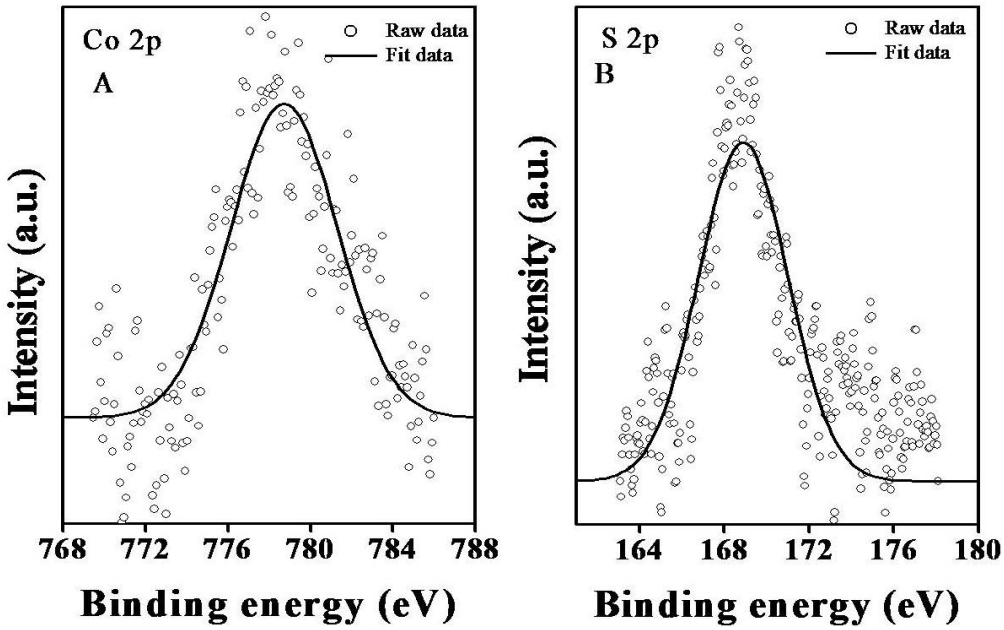

Fig.3.14.A & B: *Co 2p core level spectra and S 2p core level spectra, recorded from as-synthesized Co_3S_4 nanoparticles*

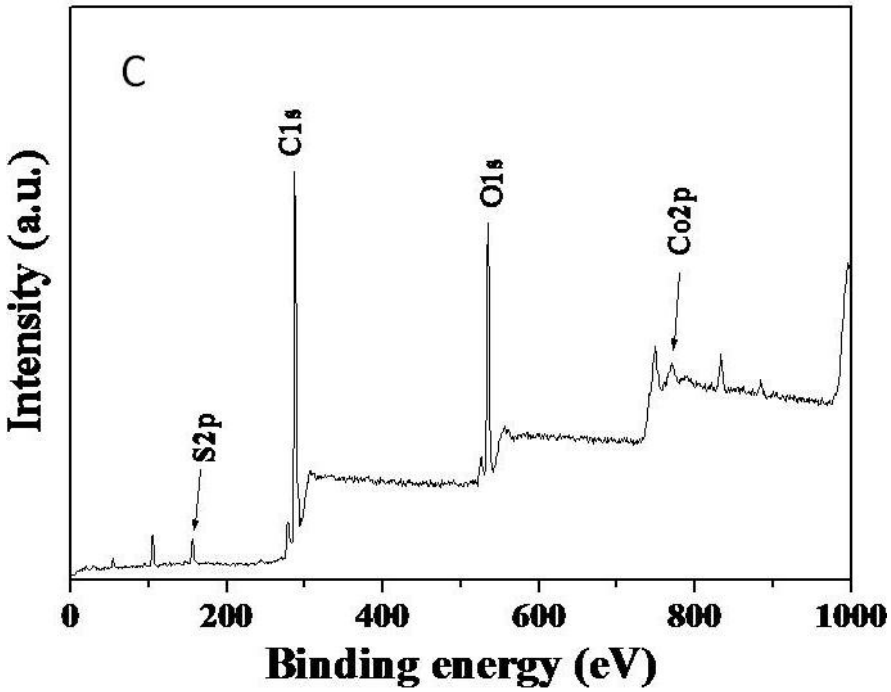

Fig.3.15: *General scan XPS profile of as-synthesized Co_3S_4 nanocrystals*

Fig.3.14 – 15 represent the narrow scan and wide scan XPS profiles of as-synthesized Co_3S_4 nanoparticles. The binding energy could be assigned to the Co-S couple of spin-

orbit splitting component. The S2p peak occurring at 168.8eV is characteristic of Sulfur bound to Cobalt in Co_3S_4 through the formation of Co-S-thiolate linkage (Fig.3.14.B). This may be due to the participation of sulfur contributed by cysteine present in the capping peptide used to control the size of the nanocrystal. The core level binding energies associated with Co and S agree with the results obtained for the synthesized Co_3S_4 nanoparticles. Wide scan XPS profile of as-synthesized Co_3S_4 is presented in Fig.3.15.

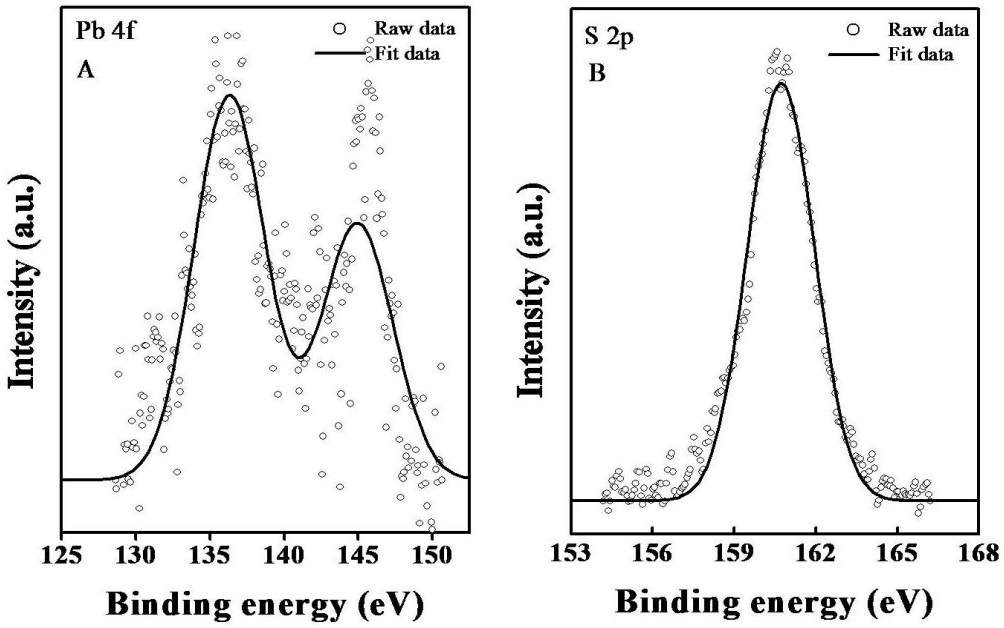

Fig.3.16.A & B: *Pb 4f core level spectra and S 2p core level spectra, recorded from PbS nanoparticle suspension drop coated on a conductive substrate. The two spin-orbit components are shown in the figure*

Fig.3.16.A & B represent the narrow scan XPS profiles of Pb and S of as-synthesized PbS nanoparticles. The XPS scan of PbS resulted in peaks corresponding to binding energies of 136.44eV and 141.88 eV which represents Pb4f and 161.5 eV which is due to S2p1/2 of the Pb-S bond. Wide scan XPS of as-synthesized PbS is given in Fig.3.17.

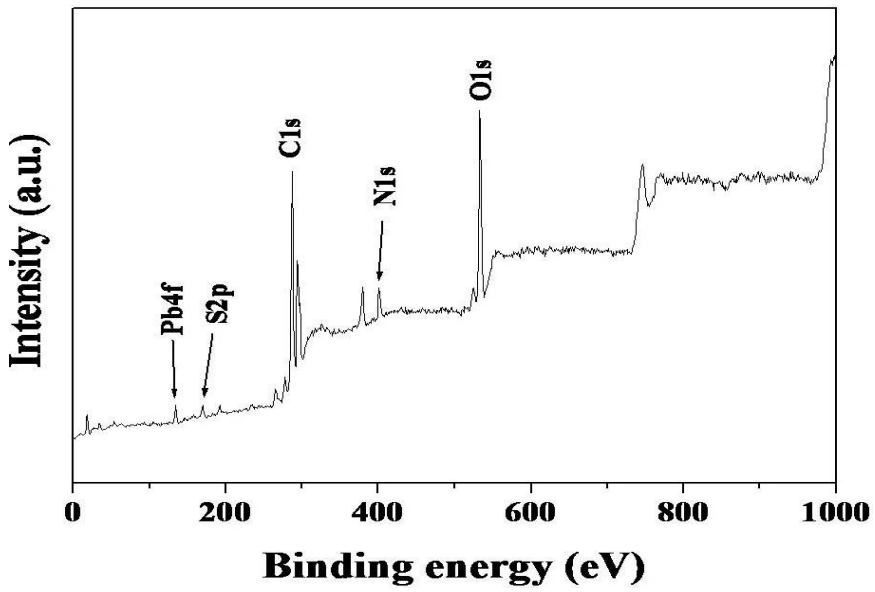

Fig.3.17: *General scan XPS of PbS nanoparticles*

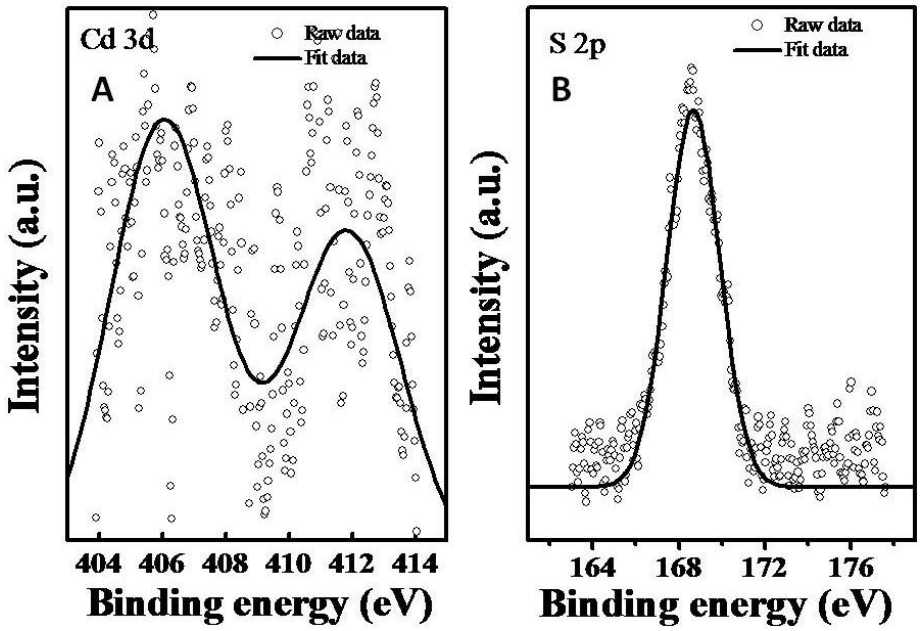

Fig.3.18.A & B: *Cd 3d core level spectra and S 2p core level spectra, recorded from CdS nanoparticles suspension drop coated on a conductive substrate. The two spin-orbit components are shown in the figure*

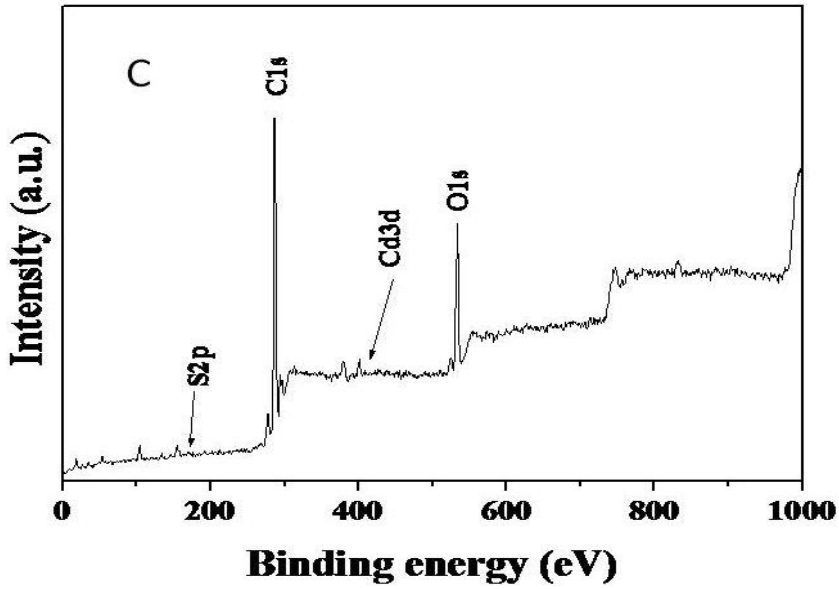

, **Fig.3.19:** *Wide scan XPS of CdS nanoparticles*

Fig.3.18.A & B represent the narrow scan XPS profile of as-synthesized CdS nanoparticles. Cd and S peaks in the X-ray photoelectron spectra are observed at 405.5 eV and 168.8 eV respectively, corresponding well with the expected value for Cd bound to sulfur. The Cd 3d spectrum could be decomposed into two spin-orbit components Cd 3d 5/2 and Cd 3d 3/2 (spin orbit splitting ~ 7.0 eV). The peaks occurred at a binding energy of 405.5 eV and 412.5 eV respectively and are characteristic of metallic Cd (Fig.3.18.A). These results agree with the core level binding energies reported in the literature. The S 2p peak occurring at a binding energy of 168.8 eV is characteristic of metallic S (Fig.3.18.B) and agrees with the core level binding energies reported earlier. Fig.3.19 represents the wide scan XPS profile of as-synthesize CdS nanoparticles.

Fig.3.20.A & B represent the narrow scan XPS profile of as-synthesized Ni_7S_6 nanoparticles. The peaks at 853.0 eV and 861.0 eV correspond to Ni2p and the satellite peak of Ni in Ni_7S_6 respectively which is in agreement with the values reported in literature. The peak at 162.4 eV corresponds to S2p which indicates sulphur to be in metallic state, bound to Nickel. Fig.3.21 represents the wide scan XPS profile of as-synthesized Ni_7S_6 nanoparticles. Table 3.4 summarises the binding energies recorded, of individual elements for all the as-synthesized fluorescent nanoparticles.

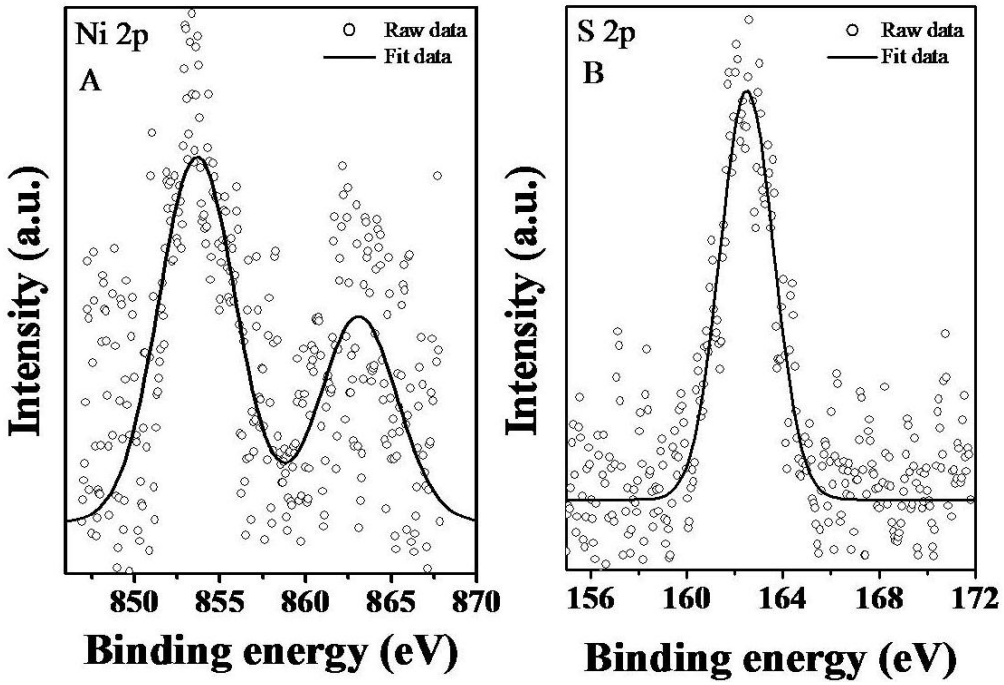

Fig.3.20.A & B: *Ni 2p core level spectra and S 2p core level spectra, recorded from Ni_7S_6 nanoparticles suspension drop coated on a conductive substrate. The main peak at 853 eV and a satellite peak are clearly visible*

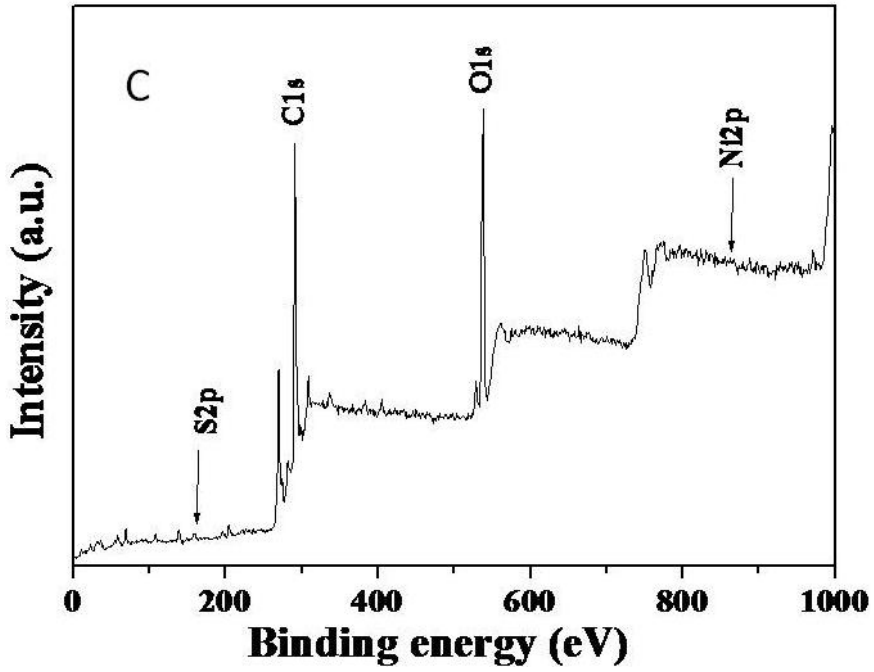

Fig.3.21: *Wide scan XPS of Ni_7S_6 nanoparticles*

Nanoparticle	Observed Binding Energy (eV)	
CdSe	Cd - 405.5, 412.5	Se - 54.8
Co_3S_4	Co - 778.7	S - 168.8
CdS	Cd - 405.5	S - 168.8
PbS	Pb - 136.4, 141.8	S - 161.5
Ni_7S_6	Ni - 853.0, 861.0	S - 162.4

Table 3.4: *Summary of binding energies recorded from XPS analysis of as-synthesized nanoparticles*

vii. Conjugation of nanoparticles with glycopeptides

CdS and CdSe nanoparticles synthesized in vitro using enzymes were evaluated for their potential use as bio-labels. The as-synthesized nanoparticles were precipitated with 1, 4-dioxane to remove the excess proteins and peptides that were used for their synthesis. The number of free carboxyl groups and free amino groups present in the capping peptide associated with the CdS and CdSe nanoparticles were determined. Both the nanoparticles have been found to contain reactive amino groups. But no carboxyl group has been detected associated with both as-synthesized CdS and CdSe nanoparticles.

The conjugation of as-synthesized CdS and CdSe nanoparticles was carried out by using a modified protocol used for the estimation of carboxyl group. The above synthesis of nanoparticle-glycopeptide conjugate was carried out at pH 6.0 by using the free amino group of the capping peptide associated with the nanoparticles, for cross-linking with reactive carboxyl group present on bi/tri-antennary glycopeptides. The reaction utilizes the water-soluble 1- Ethyl-3-(3-dimethylaminopropyl)-carbodi--imide (EDC) to catalyze reactions between nanoparticle-capping peptide amino group and acid group of bi-/tri-antennary glycopeptides. In the above reaction, the concentration of bi-/tri-antennary glycopeptides was kept twice as that of the nanoparticles in order to facilitate the formation of nanoparticle-glycopeptide

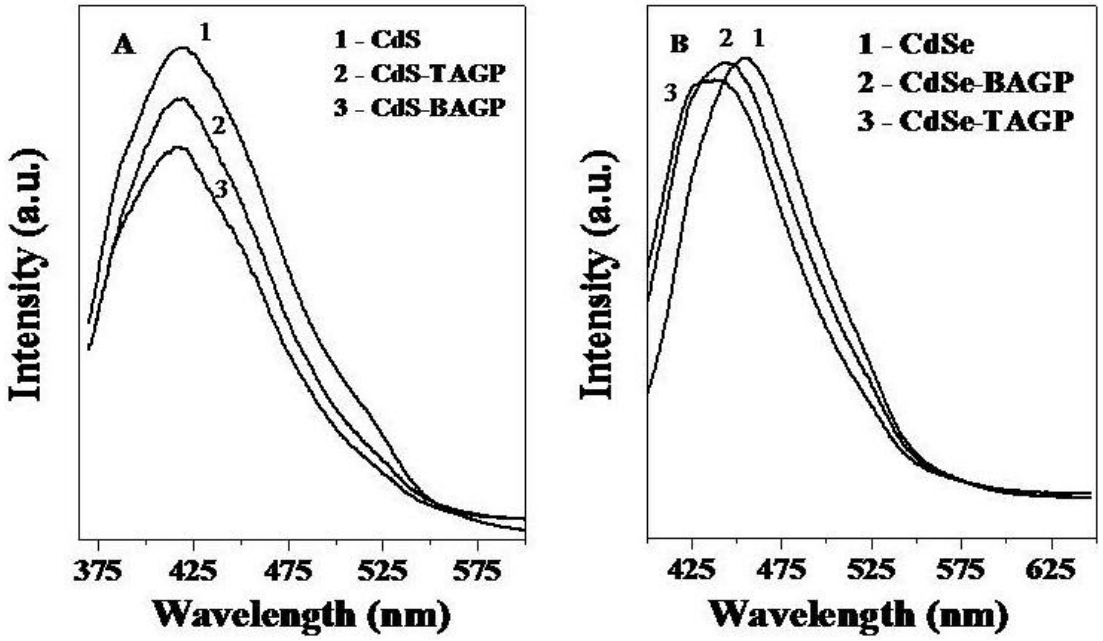

Fig.3.22: *Photoluminescence emission profile of A. CdSe-glycopeptide conjugates, B. CdS- glycopeptides conjugates*

conjugates. When passed through the size exclusion matrix, the elution profile of nanoparticle-bi/tri-antennary glycopeptides conjugates also showed a shift in the retention time as compared to the retention times of unconjugated nanoparticles, bi/tri-antennary glycopeptides. The emission profile of CdSe-glycopeptide conjugates showed a blue-shift (CdSe-bi-antennary glycopeptide – 443 nm and CdSe-tri-antennary glycopeptides – 437 nm) as compared to the naked CdSe nanoparticles (454 nm). Meanwhile, there were no significant shifts in the emission profiles of CdS-glycopeptide conjugates (CdS-bi-antennary glycopeptide – 418 nm and CdS-tri-antennary glycopeptides – 416 nm) even after successful conjugation. Fig.3.21.A & B represent the emission profiles of conjugates of CdSe-glycopeptides and CdS-glycopeptides. The shifts in the elution and emission profiles of the nanoparticle-glycopeptide conjugates indicate the successful formation of CdSe-bi/tri-antennary glycopeptides conjugates. Our group in one of our previous work reported the conjugation of CdS nanoparticles with biomolecules such as plant lectins using an identical protocol[3].

REFERENCES

1. Huang, K; Ehrman, S. H; (2007) *Langmuir* 23, 1419-1426
2. Kumar, S. A.; Ansary, A. A.; Ahmad, A.; Khan, M. I.; (2007) *J. Biomed. Nanotechnol.* **3(2)**, 190-194
3. Ansary, A. A; Kumar, S. A; Krishnasastry, M. V; Abyaneh, M. K; Kulkarni, S. K; Ahmad, A; Khan, M. I; (2007) *J. Biomed. Nanotechnol.* **3**, 406-413
4. Kumar, S. A; Abyaneh, M. K; Gosavi, S. W; Kulkarni, S. K; Ahmad, A; Khan, M. I. (2007) *Biotechnol. Appl. Biochem.* **47(4)**, 191-195
5. Lei, Z; Wei, X; Fan, Y; Liu, Y; Bi, S; (2006) *J. Colloid Interf. Sci.* **304**, 402-407
6. Yang, Y. J; Xiang, B. J; (2005) *J. Cryst. Growth* **284**, 453-458
7. Liu, C; Kwon, Y. K; Heo, J; (2009) *J. Non-cryst. Solids* **355**, 1880-1883

CHAPTER: 4

DISCUSSION

This chapter discusses the various principles and concepts underlying the current investigation of the synthesis of fluorescent nanoparticles, control of size and shape of particles, their characterization and their potential applications. The principle behind the use of reducing enzymes for the synthesis of fluorescent nanoparticles is discussed. Various other factors that influence the synthesis of nanoparticles are also discussed. The possible mechanism underlying the conversion of metal ions into stable fluorescent nanoparticles is also discussed in detail. The ability of synthetic capping peptides to control the morphology of various nanoparticles into different sizes and shapes is discussed.

i. Enzyme mediated synthesis of fluorescent nanoparticles and role of synthetic peptides

a. Role of reducing enzymes

Ideally, under anaerobic conditions, when precursor metal salt(s) ($CdCl_2$ & $SeCl_4$ for CdSe, $CdCl_2$ for CdS, $Co(NO_3)_3$ for Co_3S_4, $Pb(NO_3)_3$ for PbS, $NiCl_2$ for Ni_7S_6) along with substrate and capping peptide is/are incubated in 200mM phosphate buffer at pH 7.2, with reductase enzyme, it results in the synthesis of stable nanoparticles with the capping peptide bound to it. $NaNO_3$ and Na_2SO_3 serve as the substrates for the enzymes, nitrate and sulphite reductases, respectively. Both the enzymes nitrate and sulphite reductases used in the present work have been purified from the extracellular broth of the fungus, *Fusarium oxysoporum*, and require NADPH for their activity. The absence of the enzyme or NADPH or capping peptide or the addition of the denatured enzyme did not result in the synthesis of nanoparticles. This indicates that all the components present in the reaction mixture are necessary for the synthesis of stable nanoparticles currently under investigation viz. CdSe, CdS, Co_3S_4, PbS and Ni_7S_6. There are numerous reports on the synthesis of stable nanoparticles by the reduction of metal ions using a variety of reducing agents[1-5]. Microbes involved in bioremediation and bioleaching reduce metal or metal ores by producing a variety of metal reducing enzyme reductases. Reducing enzymes have also been used in a variety of reactions for their reducing properties. Anil et al have established the use of enzyme nitrate and sulphite reductases for the in vitro syntheses of noble metal nanoparticles[6-7]. Our group reported the use of enzyme sulphite reductase for the in vitro synthesis of CdS nanoparticles[8]. Based on the observation presented above, the synthesis of CdSe

requires the involvement of enzyme in the reduction of Cd^{2+} and Se^{4+} utilizing nitrate as the substrate and NADPH as the cofactor as described in Eq.(1).

$$Cd^{3+} + Se^{4+} + NO_3^- \xrightarrow[NADPH,\ CP_n]{\text{Nitrate reductase}} CdSe + NO_3^- \qquad (1)$$

The synthesis of metal sulphide nanoparticles under investigation such as Co_3S_4, PbS and Ni_7S_6 requires the reduction of precursor metal ion utilizing sulphite as the substrate and NADPH as the cofactor as described in Eq. (2)

$$M^+ + SO_2^- \xrightarrow[NADPH,\ CP_n]{\text{Sulphite reductase}} MS \qquad (2)$$

It has been hypothesized that the synthesis of nanoparticles involves the reduction of precursor ions by the reducing enzymes followed by the binding of synthetic peptides to form stable nanoparticles. There are several reports on the synthesis of fluorescent nanoparticles. CdSe nanoparticles have been synthesized using a variety of routes that include biosynthesis using fungus, co-precipitation, colloidal synthesis, ion implantation, etc[9-12]. Similarly, there are several reports on the synthesis of metal sulphides such as PbS, Co_3S_4, Ni_7S_6 nanoparticles spanning a wide variety of synthetic procedures[13-18]. Production of nanoparticles has gained importance because of the novel properties associated with nanoparticles[19-21]. Synthesis of nanoparticles can be achieved in a variety of methods spanning physical, chemical and biological methods with the former methods involving harsh conditions[22-24]. Hence, biosynthesis of nanoparticles, especially synthesis of nanoparticles under ambient conditions such as near neutral pH, room temperature synthesis in aqueous phase, utilising reducing enzymes could be regarded as an appropriate alternative for the eco-friendly synthesis of nanoparticles.

b. Source of the reducing enzymes

Both the enzymes nitrate and sulphite reductases used in the present work have been purified from the extracellular broth of the fungus, *Fusarium oxysoporum*. The fungus, *Fusarium oxysporum* has been implicated in the syntheses of a number of nanoparticles of a variety of elemental compositions[9,25-28]. This indicates that the fungus, *Fusarium oxysporum* is inherently equipped with versatile biological

machineries capable of over-coming stress in the form of metal ions. Moreover, any living organism possesses the innate ability to evolve and adjust to the surrounding conditions by acquiring the ability to neutralize the stress factors. In addition, fungus being an eukaryote, is a highly advance form of living organism with complex metabolic make-ups that is capable of producing biomolecules in the form of chelating molecules or enzymes that help them in survival against environmental oddities.

c. Role of peptides in the synthesis of fluorescent nanoparticles

Synthetic peptides of general structure $(\gamma\text{-Glu-Cys})_n$-Gly, where n – 2, 3, 4 or 5, were used for the synthesis of fluorescent nanoparticles currently under investigation. All the as-synthesized nanoparticles required the addition of synthetic peptides for the formation of stable nanoparticles. The addition of peptide to the reaction mixture resulted in the synthesis of nanoparticles whereas the absence of peptides did not result in the synthesis of nanoparticles. This indicates that the synthetic peptides are involved in the synthesis of nanoparticles by acting as a template on which the crystallization of nanoparticles occur. Flynn et reported the isolation of specific peptides that bind and nucleate the formation of CdS and ZnS nanocrystals[29]. In another report, Naik et al identified unique sequences of amino acids that bind to silver and cobalt[30]. In addition to the use of peptides as templates, a wide variety of molecules including biomolecules such as nucleotides, proteins, polysaccharides etc have been implicated in the templating of synthesis of nanoparticles[31-37]. Dickerson et al have extensively reviewed the role of peptides and proteins in the synthesis of inorganic materials[38]. In the absence of synthetic peptides, the precursor ions might be reduced by the enzyme but the absence of a binding agent or template might hinder the formation of ordered structures that initiate the formation of nuclei. In addition, Anil et al reported that the removal of bound phytochelatin, a metal binding peptide, from gold nanoparticles resulted in the aggregation of gold nanoparticles[6]. These aggregates lost their surface plasmon resonance that is characteristic of gold nanoparticles indicating that the aggregates no longer possess the characteristics attributed to nanoparticles. Wang et al demonstrated the synthesis of gold nanoparticles and its aggregates using a biomimetic strategy involving a polypeptide sequence designated MS14[39]. Gupta et al reported the use of cationic peptides for the synthesis of poly(acrylic acid) (PAA) nanoparticles[40]. Interestingly, as-synthesized

CdSe and CdS nanoparticles have been found to contain reactive amino groups. The presence of reactive amino groups could be explained only by the presence of synthetic peptides bound to nanoparticles. Another factor that supports the presence of bound peptide to nanoparticles is that all the as-synthesized nanoparticles discussed here are water-dispersible. This property of as-synthesized nanoparticles could be due to the presence of amino group that render these nanoparticles hydrophilic. Qu et al reported the synthesis of water-dispersible iron oxide magnetic nanoparticles by the surface functionalization of nanoparticles using a range of organic molecules[41]. These factors indicate that the synthetic peptides bind to reduced metal ions to form stable nanoparticles. Moreover, these synthetic peptides are also involved in the integrity of synthesized fluorescent nanoparticles. The as-synthesized nanoparticles have been found to be stable even after 24 months post-synthesis.

d. Size control of as-synthesized nanoparticles

The as-synthesized fluorescent nanoparticles were found to be of different sizes. All the nanoparticles under investigation were restricted to different sizes under a given condition. CdSe nanoparticles were restricted to an average of 5nm in the presence of CP_2 while metal sulphides were not size restricted by CP_2. Metal sulphides like PbS and Co_3S_4 were size restricted to a mean size of 5 and 9 nm respectively, in the presence of CP_4 while the other nanoparticles remained unaffected. Similarly, Ni_7S_6 and CdS were size restricted by CP_3 and CP_5 respectively. This indicates that the there is no consensus regarding the size of the synthetic peptides in restricting the size of nanoparticles under study. While CP_4 is involved in the size control of both PbS and Co_3S_4 still the size of the size restricted PbS and Co_3S_4 were not identical. This indicates that the binding of synthetic peptides to form the nanoparticles is a random event. It also explains that synthetic peptides used show altered affinities towards synthesis of different materials. Metal binding proteins and peptides have been reported to be synthesized by organisms to counter heavy metal stress. These metal binding proteins and peptides called Metallotheins and Phytochelatins respectively, show diverse specificity towards a range of metals. These proteins and peptides are being used in bioleaching and bioremediation of ores and wastes, respectively. Nanoparticles have attracted lots of attention due to their size dependent properties. In order to study the properties of specific nanoparticles, it becomes imperative to

Peptide	CdSe	Co_3S_4	PbS	Ni_7S_6	CdS
ECECG	**~5 nm**	~158 nm	~67 nm	~30 nm	~27 nm
ECECECG	~ 78nm	~78 nm	~25 nm	**~ 20 nm**	~32 nm
ECECECECG	~ 218nm	**~9 nm**	**~9 nm**	~ 35 nm	~77 nm
ECECECECECG	~ 278nm	~45 nm	~90 nm	~ 75 nm	**~6 nm**

Table 4.1: *Summary of the size distribution of nanoparticles synthesized using different lengths of synthetic peptides*

produce nanoparticles of uniform sizes such that the sum of properties of all the nanoparticles in a given population reflects the properties associated with an individual nanoparticle. In theory, nanoparticles possessing a standard deviation of up to 5% are regarded as homogenous. Hence, strategies to produce size control of nanoparticles gains importance. Banerjee et al controlled the size of Cu nanotubes and Ni nanocrystals by altering the confirmation of peptides in the template peptide nanotubes[42-43]. In another study, Ramasamy et al tuned the size of Au nanoparticles by radiating Au_{25} quantum clusters anchored to dipeptide nanotubes[44].

e. Influence of size of the synthetic peptides on size control of nanoparticles

The factors that are involved in the restriction of a particular metal ion, the precursor ions in this case, to a specific size are not clear. Since in the case of CdS the longest synthetic peptide, CP_5 brings about the synthesis of 6nm sized nanocrystals while in the case of CdSe 5nm sized particles were produced in the presence of the shortest peptide, CP_2. On the contrary, in the case of other metal sulphides such as PbS, Ni_7S_6 and Co_3S_4 neither CP_2 nor CP_5 produced the size restriction but only medium size peptides were involved in the size restriction. Flynn et al reported that the length and structure of the template peptides influence the synthesis of metal sulphide nanoparticles such as ZnS, PbS and CdS[29].

f. Influence of secondary structure of the synthetic peptides on size control

In order to study the influence of secondary structure of the synthetic peptides on the synthesis and size control of fluorescent nanoparticles, the synthetic peptides CP_4 and CP_5 were subjected to circular dichroism (CD) analysis. The resulting CD spectra were analysed by CD Pro, a data analysis program developed by Sreerama et al[45]. CD analysis revealed that only 1 out of the 4 synthetic peptides viz. CP_5 possesses remarkable secondary structures while CP_4 showed the presence of minimal secondary

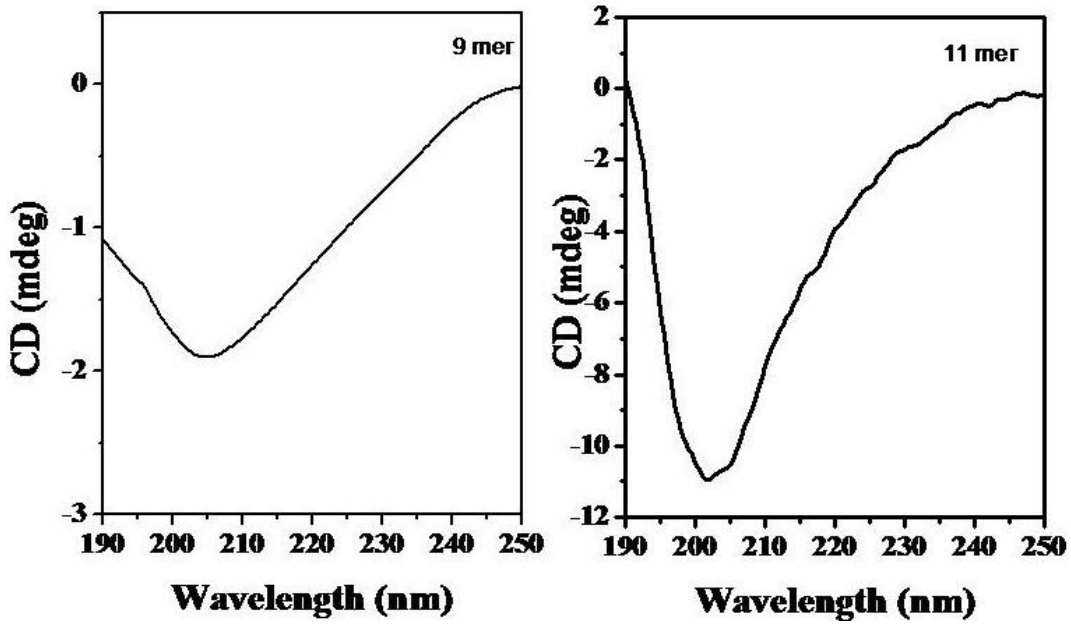

Fig.4.1: *Circular dichroism spectra of CP_4 and CP_5 peptides*

structure. The CD spectra of both CP_5 are represented in fig.4.1. In general, larger linear peptides tend to fold onto themselves to form secondary structures. Analysis of CD spectra of CP_5 using two programs, CDSSTR and CONTINLL revealed that the majority of the secondary structure of CP_5 is composed of unordered structures and β-sheets with a mediocre level of random turns followed by a minimal presence of α-helix. As expected, there is a minimal occurrence of secondary structure in CP_4 due to its shorter length. Table 4.1 summarizes the results of CD analysis of CP_5 using CDSSTR and CONTINLL. Other synthetic peptides owing to their smaller size did not show identifiable secondary structures. Out of the 5 fluorescent nanoparticles under investigation, only CdSe and Ni_7S_6 nanoparticles were size restricted by

medium to smaller sized synthetic peptides that do not possess a prominent secondary structure. On the contrary, majority of the metal sulphides under study were size

	CDSSTR	CONTINLL
α-helix	4.7	5.9
β-sheet	34.2	37.6
Turn	24.5	22.5
Unordered	35.4	34.0

Table 4.1: *Summary of secondary structures of CP_5 calculated using CDSSTR and CONTINLL. The values are indicated as percentage*

restricted by synthetic peptides with a moderate to prominent secondary structures. In case of both PbS and Co_3S_4, size restriction is brought about by CP_4 which possesses minimal secondary structure if not prominent. Meanwhile, CP_5 with a prominent secondary structure was involved in the size control of CdS nanoparticles. This indicates that presence of secondary structure is favourable for the synthesis and size restriction of metal sulphides with the only exception of Ni_7S_6 nanoparticles which were size restricted by CP_3. Flynn et al reported that the length and structure of the template peptides influence the synthesis of metal sulphide nanoparticles such as ZnS, PbS and CdS[29].

g. Shape control of nanoparticles using synthetic peptides

The possible role of synthetic peptides in the shape control of fluorescent nanoparticles under investigation has been studied. TEM images have revealed that all the as-synthesized nanoparticles were in quasi-spherical morphology with the exception of Ni_7S_6 nanoparticles which were found to be in 'tear-drop' morphology. The formation of spherical shapes is favoured due to their uniform surface charge distribution and minimal energy requirement. This explains the formation of spherical nanoparticles in case of CdSe, CdS, PbS and Co_3S_4 which, is favoured. In case of Ni_7S_6, 'tear-drop' shaped nanoparticles with an aspect ratio of 2:5 are formed in the presence of CP_3. This indicates that the synthetic peptide CP_3 binds to Ni_7S_6 in such a

way that the nanoparticles are forced to grow in a particular direction leading to the formation of Ni_7S_6 with 'tear-drop' morphology. There are several studies that investigated the shape control of nanoparticles. Cao et al developed a mild hydrothermal method for the synthesis of flower-like Ni_7S_6 nanoparticles with enhanced catalytic properties[46]. Cheng et al reported the shape controlled synthesis of hexagonal and pyramidal CdS nanoparticles while Nyamen et al reported the synthesis of CdS nanoparticles in the form of rods, bipods and tripods[47-48]. Champion et al reported the syntheses of more than 20 different shapes of polymeric nanoparticles[49]. Kumar et al have reviewed the control of shape in semiconductor nanomaterials[50]. Shape control of nanoparticles is of importance since properties of nanoparticles have been associated with specific shapes. By restricting a nanomaterial to a specific shape, the properties of the nanomaterial can be tuned according to the requirement. Nanomaterials of different shapes have been reported to possess enhanced optical, thermal, electrical and catalytic properties[51]. Song et al prepared spinel cobalt ferrite nanocubes with enhanced magnetic properties[52]. The chemical properties associated with the shape of different nanomaterials have been extensively reviewed by El-Sayed and co-workers[53].

h. Role of amino acids in size and shape control of nanoparticles

The synthetic peptides used as the templates for the synthesis of fluorescent nanoparticles under investigation have a general structure of $(\gamma\text{-Glu-Cys})_n$-Gly, where n – 2, 3, 4 or 5. In other words, the structure of the synthetic peptides is composed of alternating pairs of glutamic acid and cysteine with a glycine at the C-terminus. The number of pairs of glutamic acid and cysteine is varied with the size of the synthetic peptides. The amino acids, Glutamic acid and cysteine are hydrophilic with the former being negatively charged and the later being polar. Glycine is a non-polar amino acid but hydrophobic. The presence of large number of hydrophilic amino acids as compared to the presence of a single glycine residue imparts hydrophilicty to the synthetic peptides. The hydrophilic nature of the synthetic peptides favours the complete dissolution of synthetic peptides increasing the availability. The A7 peptide of sequence CNNPMHQNC that preferentially binds ZnS also consists of hydrophilic amino acids in majority[54]. Similarly, the peptide CTYSRLHLC that recognizes CdS quantum dots also shows a similar trend with respect to hydrophilicity[55]. This might

favour the better interaction of peptides with precursor ions resulting in the synthesis of nanoparticles. Moreover, the presence of repeating unit viz. glutamic acid and cysteine may play a role in the synthesis of nanoparticles. Brown demonstrated that the affinity of gold binding peptides increased with increase in number of repeats of binding units[56].

Peptide	Molecular Mass	Isoelectric point	Charge
ECECG	539.6	3.1	-2.1
ECECECG	771.8	3.0	-3.1
ECECECECG	1004.1	3	-4.2
ECECECECECG	1236.4	2.9	-5.2

Table 4.3: *Summary of properties of synthetic peptides (Charge indicates net charge on peptides at pH 7.2)*

In addition, all the 4 peptides discussed here have been calculated to possess pI in the acidic range. These peptides possess a net negative charge at the working pH i.e. 7.2, of the reaction. Due to presence of negative charge the peptides tend to interact with the positively charged precursor metal cations due to electrostatic attractions thereby favouring the formation of nanoparticles. Table 4.3 presents the properties of synthetic peptides under specific conditions.

i. Hypothetical mechanism of nanoparticle synthesis

Based on the above observation, the enzyme mediated reduction of precursor ions and the subsequent binding of synthetic peptides leading to the formation of stable fluorescent nanoparticle involves an array of different factors that interact closely for the successful formation of nanoparticles. The presence of proton acceptor amino acid Glutamic acid as well as the open structure of the peptide is assumed to be responsible for the formation of nanoparticle in solution. We propose a possible mechanism for the utilization of peptide as the template for the synthesis of nanoparticles. The CP_n peptide, with an acidic pI in solution at pH 7.2 could be regarded as an anionic polyelectrolyte. The precursors completely dissociate in aqueous solution generating the corresponding cations. In neutral or slightly alkaline solution, the peptide CP_n of

acidic pI carries a net negative charge owing to the functional groups present in the sequence, thereby attracting the precursor cations due to electrostatic interactions. This might result in the formation of nuclei. The reduction of the electrostatically bound precursor cations, results in the formation of stable nanocrystals stabilized by the templating peptide CP_n. Fig.4.1 represents the hypothetical scheme of the synthesis of nanoparticles using enzyme reductase in the presence of synthetic peptides. The net negative charge carried by the synthetic peptides might also be responsible for the maintenance of the as-synthesized nanoparticles in the nano-size regime by preventing the agglomeration of nanoparticles due to repulsion by like charges.

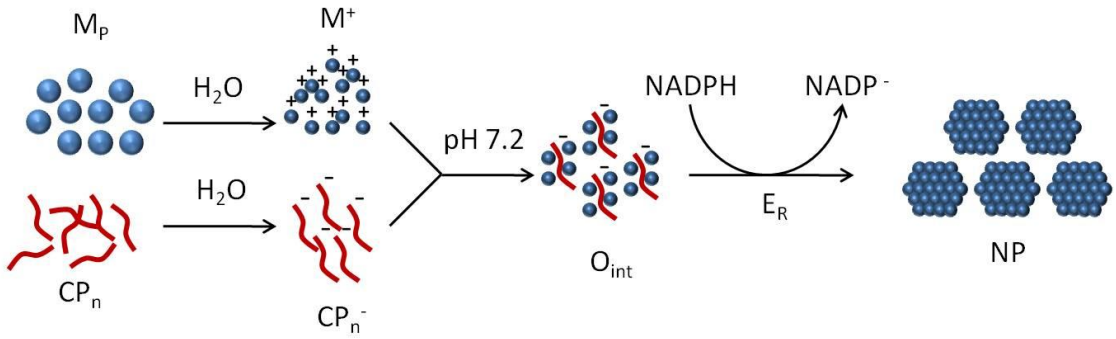

Fig.4.1: *Schematic representation of the enzyme mediated bio-synthesis of nanoparticles in the presence of synthetic peptides (M_P – Metal precursor(s), M^+ - Metal cations, CP_n – synthetic peptides, CP_n^- - negatively charged synthetic peptides, O_{int} – Nucleus (intermediate), E_R – Reductase enzyme, NP – Stable nanoparticles)*

ii. Characterization of as-synthesized fluorescent nanoparticles

All the as-synthesized fluorescent nanoparticles were characterized in order to confirm the properties characteristics of nanoparticles. The nanoparticles were characterized for their morphological, optical, structural and chemical properties. The deviation of properties in nanomaterials with respect to their bulk counterparts is discussed in detail.

a. Morphological characteristics

The morphological properties of the as-synthesized nanoparticles have been studied using Transmission electron microscopy. All the nanoparticles under investigation

were found to be discrete with a quasi-spherical morphology. The particles were found to be in the nanometer scale with the crystal planes clearly visible. The crystal planes could be indexed to the crystal structures of corresponding materials.

b. Optical properties

The optical properties of the as-synthesized nanomaterials were studied using absorption and photoluminescence spectroscopy. The absorption spectra, of the as-prepared nanoparticles in aqueous solution, show a peak corresponding to the first excitonic transition. All the as-synthesized nanoparticles showed absorbance band centred in the ultra violet region of the spectrum with the exception of Ni_7S_6 which showed absorption maxima at 407nm. This is in close agreement with the quantum size effect that in direct gap semi-conductors, there is a shift in the optical absorption edge to higher energies with decrease in size. Relatively small stoke's shifts were

Nanoparticle	$Absorbance_{max}$	$Emission_{max}$	$Bulk_{Bandgap}$
CdSe	366 nm	454 nm (2.73)	2.24 eV
CdS	339 nm	418 nm (2.96)	2.96 eV
Co_3S_4	333 nm	380 nm (3.26)	0.78 eV
PbS	342 nm	393 nm (3.16)	0.37 eV
Ni_7S_6	407 nm	473 nm (2.62)	0.8 eV

Table 4.4: *Comparison of optical properties of as-synthesized nanoparticles with that of bulk materials (The values in parentheses indicate band gaps corresponding to observed* $Emission_{max}$*)*

observed for all the nanoparticles. The emission band observed for the nanoparticles is attributed to the band gap or near band gap emission resulting from the recombination of electron-hole pairs in the nanoparticles with a larger band gap. The band gaps associated with the observed optical properties have been found to be much larger as compared to that of the bulk materials. These properties are characteristic features of semiconductor nanomaterials. Several studies report the synthesis of nanoparticles with comparable optical properties as observed[57-61]. Table 4.4 compares the observed

optical properties of as-synthesized nanoparticles with that of the corresponding bulk materials. The relatively narrow half widths of emission peaks indicate that the size distributions of nanoparticles are not highly variable. Nanoparticles that show absorption and emission maxima in the visible range of the spectrum have their own importance as bio-labels. As-synthesized CdS (418nm) and CdSe (454nm) show emission maxima in the visible range while Ni_7S_6 nanoparticles show both, absorption (407nm) as well emission (473nm) maxima in the visible range.

c. Structural properties

X-Ray diffraction measurements confirm the synthesis of all the fluorescent nanoparticles. The crystal structures deduced match with the standards available in literature. The broadening of peak indicates that the as-synthesized nanoparticles are in nano-dimensions. All the fluorescent nanoparticles synthesized show purity of phase confirmed by the absence of other phases except for as-synthesized CdSe nanoparticles. The peaks could be indexed to CdO phase of the nanoparticles. The formation of CdO phase might be due to the uncontrolled reaction that takes place in the presence of atmospheric oxygen in the reaction mixture. Another possibility might be the reaction of CdSe with oxygen atoms to form CdO due to the highly reactive nature of surface Cd atoms in nanoparticles. CdSe nanoparticles have been found to possess wurtzite structure. The crystal structure of Co_3S_4 indicated the formation of Linnaeite – cubic phase of Co_3S_4. The as-synthesized cobalt sulphide is devoid of other phases such as that of CoS, CoS_2 and Co_9S_8 that confirms the purity of the as-synthesized nanoparticles. The above analysis shows that the as-synthesized Ni_7S_6 is a pure phase nickel sulphide without the presence of other phases of nickel sulphide such as NiS, Ni_3S_2, Ni_3S_4, Ni_9S_8, etc. CdS and PbS have been found to be in tetragonal and orthorhombic phases, respectively of the corresponding materials. XRD analyses also confirm that the as-synthesized nanoparticles are crystalline in nature.

d. Chemical properties

The chemical properties of as-synthesized fluorescent nanoparticles were studied using X-ray photoelectron spectroscopy. The binding energies associated with individual atoms of the as-synthesized nanoparticles were in agreement with the standards. Wide scan XPS profiles of the as-synthesized nanoparticles indicated the

presence of carbon, oxygen and nitrogen. The presence of carbon could be due to the atmospheric carbon or from the amino acids of the bound capping peptides. The presence of nitrogen might be from the atmospheric nitrogen or from amino acids of the bound capping peptides. The presence of oxygen could be due to absorption and chemisorptions of oxygen compounds and also of water and atmospheric oxygen.

In case of Co_3S_4, the S2p peak occurring at 168.8eV is characteristic of Sulphur bound to Cobalt in Co_3S_4 through the formation of Co-S-thiolate linkage (Fig.3.14.B). This may be due to the participation of sulfur contributed by cysteine present in the capping peptide bound to the nanocrystal.

iii. Conjugation of nanoparticles with glycopeptides

The conjugation of as-synthesized nanoparticles was attempted in order to demonstrate the utility of as-synthesized fluorescent nanoparticles as bio-labels. As-synthesized CdS and CdSe nanoparticles have been chosen for conjugation because of their wide utility as bio-labels[62]. The presence of functional groups such as free amino groups might be explained by the presence of bound synthetic peptides. Conjugation of CdS and CdSe nanoparticles were accomplished by the formation of a covalent linkage in the form of amide bond, between the free amino groups attached to the nanoparticles with that of the carboxyl group present on the glycopeptides viz. bi-/tri-antennary glycopeptides. The reaction utilizes the water-soluble 1- Ethyl-3-(3-dimethylaminopropyl)-carbodi--imide (EDC) to catalyze reactions between nanoparticle-capping peptide amino group and acid group of bi-/tri-antennary glycopeptides. Bartczak reported the conjugation of peptides to gold nanoparticles[63]. Another study reports the covalent conjugation of gold nanoparticles to DNA templates[64]. The concentrations of glycopeptides and nanoparticles were altered in such a way that the reaction maximises the formation of nanoparticle-glycopeptide conjugates while minimizing formation of other by-products such as polymers of nanoparticles or glycopeptides. The presence of glycopeptides as well as fluorescence in purified conjugates confirmed the synthesis of conjugates. Blue shifts in the emission maxima of CdSe-glycopeptides (CdSe-BAGP – 443nm & CdSe-TAGP – 437) with respect to bare CdSe (454nm) have been observed. This might be due to the covalent attachment of nanoparticles. But in case CdS-glycopeptides conjugate, barely any shift in the fluorescence has been observed. Fluorescent nanoparticles have found

great utility as bio-labels because of several advantages they provide over conventional organic labels. Narrow emission spectra characteristic of fluorescent nanoparticles allow multiwavelength labelling with nanoparticles of different colours with little spectral overlap. Their resistance to bleaching, possession of broad excitation spectrum and tunability project them as a good alternative to organic labels. Kloepfer et al demonstrated the use of quantum dots to identify microbes based on their strain and metabolism[65]. Similarly, quantum dots have been reported to be used as bio-labels in plants, medicine, cell biology, diagnostics, etc[66-69].

References

1. Huang, K; Ehrman, S. H; (2007) *Langmuir*, **23**, 1419-1426
2. Panda, B. R; Chattopadhyay, A; (2007) *J. Nanosci. Nanotechnol.* **7**, 1911-1915
3. Qiu-li, Z; Zhi-mao, Y; Bing-jun, D; Xin-zhe, L; Ying-juan, G; (2010) *Trans. Nonferrous Met. Soc. China* **20**, 240-244
4. Cheng-Min, S; Chao, H; Tian-Zhong, Y, Cong-Wen, X; Shu-Tang, C; Hao, D; Hung-Jun, G; (2008) *Chin. Phys. Lett.* **25**, 1479-1481
5. Bai, L; Wan, H; Street, S. C; (2009) *Colloid. Surface. A* **349**, 23-28
6. Kumar, S. A; Kazemian, M; Gosavi, S. W; Kulkarni, S; Parischa, R; Ahmad, A; Khan, M. I; (2007) *Biotechnol. Appl. Bioc.* **47**, 191-195
7. Kumar, S. A; Kazemian, M; Gosavi, S. W; Kulkarni, S; Parischa, R; Ahmad, A; Khan, M. I; (2007) *Biotech. Lett.* **29**, 439-445
8. Ansary, A. A; Kumar, S. A; Krishnasastry, M. V; Abyaneh, M. K; Kulkarni, S. K; Ahmad, A; Khan, M. I; (2007) *J. Biomed. Nanotechnol.* **3**, 406-413
9. Kumar, S. A; Ansary, A. A; Ahmad, A; Khan, M. I; (2007) *J. Biomed. Nanotechnol.* **3(2)**, 190-194
10. Ueno, Y; Kaigawa, H; Ohashi, T; Suguira, T; Minoura, H; (1987) *Sol. Energ. Mat.* **15(6)**, 421-430
11. Vasiliev, R. B; Dorofeev, S. G; Dirin, D. N; Belov, D. A; Kuznetsova, T. A; (2004) *Mendeleev Commun.* **14(4)**, 169-171
12. Hipp, W; Karl, H; Grobans, I; Stritzker, B; (2003) *Mater. Sci. Engg. B* **101(1-3)**, 318-323
13. Akhtar, J; Malik, M. A; O'Brien, P; Helliwell, M; (2010) *J. Mater. Chem.* **20**, 6116-6124
14. Akhtar, J; Malik, M. A; O'Brien, P; Wijayantha, K. G. U; Dharmadasa, R; Hardman, S. J. O; Graham, D. M; Spencer, B. F; Stubbs, S. K; Flavell, W. R; Binks, D. J; Sirotti, F; Kazzi, M. E; Silly, M; (2010) *J. Mater. Chem.* **20**, 2336-2344
15. Yin, Y; Erdonmez, C. K; Cabot, A; Hughes, S; Alivisatos, A. P; (2006) *Adv. Funct. Mater.* **16(11)**, 1389-1399
16. Chen, X; Zhang, Z; Qiu, Z; Shi, C; Li, X; (2007) J. Colloid Interfac. Sci. **308(1)**, 271-275

17. Tilly, D. J; Jefferson, D. A; (2002) *J. Phys. Chem. B* **106(42)**, 10895-10901
18. O'Brien, P; Waters, J; (2006) *Chem. Vap. Deposition* **(12)**, 620-626
19. Schlamp, M. C; Peng, X. G; Alivisatos, A. P; (1997) *J. Appl. Phys.* **82**, 5837-5842
20. Mattoussi, H; Radzilowski, L. H; Dabbousi, B. O; Thomas, E. L; Bawendi, M. G; Rubner, M. F; (1998) *J. Appl. Phys.* 83, 7965-7974
21. Schreuder, M. A; Xiao, K; Ivanov, I. N; Weiss, S. M; Rosenthal, S. J; (2010) *Nano. Lett.* 10(2), 573-576
22. Baranchikov, A. Y; Ivanov, V. K; Tretyakov, Y. D; (2007) *Russian. Chem. Rev.* **76(2)**, 133–151
23. Savastenko, N; Volpp, H. R; Gerlach, O; Strehlau, W; (2008) *J. Nanopart. Res.* **10(2)**, 277–287
24. Barau, A; Budarin, V; Caragheorgheopol, A; Luque, R; Macquarrie, D. J; Prelle, A; Teodorescu, V. S; Zaharescu, M; (2008) *Catal. Lett.* **124(3-4)**, 204–214
25. Bansal, V; Rautaray, D; Ahmad, A; Sastry, M; (2004) *J. Mater. Chem.* **14**, 3303-3305
26. Durán, N; Marcato, P. D; Alves, O. L; De Souza, G. I. H; Esposito, E; (2005) *J. Nanobiotechnology* 3(8)
27. Ahmad, A; Mukherjee, P; Senapathi, S; Mandal, D; Khan, M. I; Kumar, R; Sastry, M; (2002) *J. Am. Chem. Soc.* **124**, 12108-12109
28. Mukherjee, P; Senapati, S; Mandal, D; Ahmad, A; Khan, M. I; Kumar, R; Sastry, M; (2002) *Chem. Biochem***, 3(5)**, 461-463
29. Flynn, C. E; Mao, C; Hayhurst, A; Williams, J. L; Georgiou, G; Iversona, B; Belcher, A. M; (2003) *J. Mater. Chem.* **13**, 2414-2421
30. Naik, R. R; Jone, S. E; Murray, C. J; McAuliffe, J. C; Vaia, R. A; Stone, M. O; (2004) *Adv. Funct. Mater.* **14(1)**, 25-30
31. Wade, T. L; Wegrowe, J. –E; (2005) *Eur. Phys. J. Appl. Phys.* **29**, 3-22
32. Liu, Q; Guo, M; Nie, Z; Yuan, J; Tan, J; Yao, S; (2008) Langmuir **24**, 1595-1599
33. Hinds, S; Taft, B. J; Levina, L; Sukhovatin, V; Dooley, C. J; Roy, M. D; MacNeil, D. D; Sargent, E. H; Kelley, S. O; (2006) *J. Am. Chem. Soc.* **128**, 64-

65

34. Levina, L; Sukhovatkin, V, Musikhin, S; Cauchi, S; Nisman, R; Bazett-Jones, D. P; Sargent, E. H; (2005) *Adv. Mater.* **17**, 1854-1857
35. Zhang, F; Wong, S. S; (2010) *ACS Nano* **4(1)**, 99-112
36. Chena, T; Wonga, Y; Zhengb, W; Huang, Y. B. L; (2008) Colloid. Surf. B **67**, 26-31
37. Huang, J; Liu, Z; liu, X; He, C; Chow, S. Y; Pan, J; (2005) *Langmuir* 21, 699-704
38. Dickerson, M. B; Sandhage, K. H; Naik, R. R; (2008) *Chem. Rev.* **108**, 4935-4978
39. Wang, Z; Chen, J; Yang, P; Yang, W; (2007) *Appl. Organometal. Chem.* **21**, 645-651
40. Gupta, K, Ganguli, M; Pasha, S; Maiti, S; (2006) *Biophys. Chem.* 119, 303-306
41. Qu, H; Caruntu, D; Liu, H; O'Connor, C. J; (2011) *Langmuir* **27**, 2271-2278
42. Banerjee, I, A; Yu, L; Matsui, H; (2003) *Proc. Natl. Acad. Sci.* **100(25)**, 14678-14682
43. Yu, L; Banerjee, I. A; Shima, M; Rajan, K; Matsui, H; (2004) *Adv. Mater.* **16(8)**, 709-712
44. Ramasamy, P; Guha, S; Shibu, E. S; Sreeprasad, T. S; Bag, S; Banerjee, A; Pradeep, T; (2009) *J. Mater. Chem.* **19**, 8456-8462
45. Sreerama, N; Woody, R. W. (2000) *Anal. Biochem.* **287**, 252-260
46. Cao, F; Liu, R; Zhou, L; Song, S; Lei, Y; Shi, W; Zhang, H; (2010) *J. Mater. Chem.* **20**, 1078-1085
47. Cheng, Y; Wang, Y; Bao, F; Chen, D; (2006) *J. Phys. Chem. B*, **110**, 9448-9451
48. Nyamen, L. D; Pullabhotla, V. R. S; Nejo, A. A; Ndifon, P; Revaprasadu, N; (2011) *New J. Chem.* **35**, 1133-1139
49. Champion, J. A; Katare, Y. K; Mitragotri, S; (2007) *P. Natl. Acad. Sci. USA* **104(29)**, 11901-11904
50. Kumar, S; Nann, T; (2006) *Small* **2(3)**, 316-329
51. Narayanan, R; El-Sayed, M. A; (2004) *J. Phys. Chem. B* **108(18)**, 5726-5733

52. Song, Q; Zhang, Z. J; (2004) *J. Am. Chem. Soc.* **126(19)**, 6164-6168

53. Burda, C; Chen, X; Narayanan, R; El-Sayed, M. A; (2005) *Chem. Rev.* **105**, 1025-1102

54. Lee, S; Mao, C; Flynn, C. E; Belcher, A. M; (2002) *Science* **296**, 892-895

55. *Peelle, B. R; Krauland, E. M; Wittrup, K. D; Belcher, A. M; (2005) Acta Biomater. **1(2)**, 145-154*

56. Brown, S; (1997) *Nat. Biotechnol.* **15**, 269-272

57. Lei, Z; Wei, X; Fan, Y; Liu, Y; Bi, S; (2006) *J. Colloid Interf. Sci.* **304**, 402-407

58. Firth, A. V; Haggata, S. W; Khanna, P. K; Williams, S. J; Allen, J. W; Magennis, S. W; Samuel, D. W; Cole-Hamilton, D. J; (2004) *J. Lumin.* **109**, 163-172

59. Yang, Y. J; Xiang, B. J; (2005) *J. Cryst. Growth* **284**, 453-458

60. Shen, H; Chen, L; Chen, S; (2009) *J. Inorg. Organomet. Polym.* **19**, 374-381

61. Bao, S; Li, Y; Li, C. M; Bao, Q; Lu, Q; Guo, J; (2008) *Cryst. Growth Des.* **8(10)**, 3745-3749

62. Santos, B.S; Farias, P. M. A; Menezes, F. D; Brasil Jr, A. G; Fontes, A; Romao, L; Amaral, J. O; Moura-Neto, V; Tenorio, D. P. L. A; Cesar, C. L; Barbosa, L. C; Ferreira, R; (2008) *Appl. Surf. Sci.* **255(3)**, 790-792

63. Bartczak, D; Kanaras, A. G; (2011) *Langmuir* **(In press)**

64. Stevenson, K. A; Muralidharan, G; Maya, L; Wells, J. C; Barhen, J; Thundat, T; (2002) *J. Nanosci. Nanotechnol.* **2(3-4)**, 397-404

65. Kloepfer, J. A; Mielke, R. E; Wong, M. S; Nealson, K. H; Stucky, G; Nadeau, J. L; (2003) *Appl. Environ. Microbiol.* **69(7)**, 4205-4213

66. Nair, R; Poulose, A. C; Nagaoka, Y; Yoshida, Y; Maekawa, T; Kumar, D. S; (2011) *J. Fluoresc.* (In press)

67. Xu, G; Yong, K. T; Roy, I; Kopwitthaya, A; (2010) *J. Biomed. Nanotechnol.* **6(6)**, 641-647

68. Xue, M; Wang, X; Wang, H; Tang, B; (2011) *Talanta* **83(5)**, 1680-1686

69. Farias, P. M; Santos, B. S; Fontes, A; (2009) *Methods Mol. Biol.* **544**, 407-419

CHAPTER: 5

SUMMARY AND CONCLUSION

This chapter summarizes all the results obtained during the course of the investigation. The significance, scope and future prospects of the work are also discussed. Some of the possible approaches to improve the current strategy are also discussed.

i. Enzyme mediated synthesis and control of geometry of fluorescent nanoparticles:

The work presented here reports the syntheses of fluorescent nanoparticles such as CdSe, Co_3S_4, PbS, and Ni_7S_6 utilizing enzymes purified from the extra-cellular broth of fungus, *Fusarium oxysporum*. Nitrate reductase was used for the synthesis of CdSe while metal sulphide nanoparticles were synthesized using Sulphite reductase. Both the enzymes require NADPH as the co-factor for their activity. All the nanoparticles required one of the synthetic peptides of general structure $(\gamma\text{-Glu-Cys})_n\text{-Gly}$, where n – 2, 3, 4 or 5 for their synthesis which in turn bind to the nanoparticles thereby preventing the nanoparticles from aggregation. The mechanism of synthesis of fluorescent nanoparticles has been hypothesized. The syntheses of the nanoparticles involve the reduction of precursor cations that subsequently gets bound by capping peptides which in turn restricts the as-synthesized nanoparticles into specific sizes and shapes. The size and shape of the as-synthesized nanoparticles were dependent on the length and structure of the synthetic peptides.

a. CdSe nanoparticles:

- CdSe nanoparticles were synthesized using enzyme NADPH-dependent nitrate reductase that utilizes sodium nitrate as the substrate. $CdCl_2$ and $SeCl_4$ served as the precursors
- The synthesis requires synthetic peptides of general structure $(\gamma\text{-Glu-Cys})_n\text{-Gly}$, where n – 2, 3, 4 or 5
- Synthetic peptides of structure, $(\gamma\text{-Glu-Cys})_2\text{-Gly}$ were able to template the synthesis of quasi-spherical CdSe nanoparticles in the size range of 3.9 – 9.0 nm with an average size of 5.5nm
- The as-synthesized CdSe nanoparticles were crystalline and were in wurtzite form of CdSe as deduced from X-Ray diffraction studies
- The CdSe nanoparticles showed absorbance and emission maxima of 366nm and 454nm respectively

- The chemical properties of as-synthesized CdSe nanoparticles matched with the standards
- The CdSe nanoparticles have been found to contain reactive amino group

b. Metal sulphide nanoparticles:

- Metal sulphide nanoparticles such as Co_3S_4, PbS and Ni_7S_6 nanoparticles have been synthesized in vitro using enzyme sulphite reductase that utilized sodium sulphite as the substrate
- $CoCl_2$, $PbCl_2$ and $Ni(NO_3)_3$ served as the precursor salts for Co_3S_4, PbS and Ni_7S_6 nanoparticles respectively
- The particle sizes of CdS, Co_3S_4, PbS and Ni_7S_6 nanoparticles were controlled by utilizing the synthetic peptides of varying sizes
- PbS nanoparticles were size controlled to quasi-spherical particles in the range of 3-7nm using $(\gamma\text{-Glu-Cys})_4$-Gly
- Co_3S_4 nanoparticles were size controlled synthesized to spherical particles in the presence of $(\gamma\text{-Glu-Cys})_4$-Gly
- CdS nanoparticles were controlled to particles in the size range of 5-8nm in the presence of $(\gamma\text{-Glu-Cys})_5$-Gly
- Synthesis of Ni_7S_6 nanoparticles in the presence of $(\gamma\text{-Glu-Cys})_3$-Gly yielded 'tear-drop' shaped nanoparticles
- All the as-synthesized metal sulphide nanoparticles were characterized for their structural properties (CdS - orthorhombic, Co_3S_4 – linnaeite (cubic), PbS – tetragonal, Ni_7S_6 - orthorhombic)
- Absorbance properties of all the nanoparticles showed blue shifts characteristics of nanoparticles of corresponding bulk materials (CdS – 339nm, Co_3S_4 – 333nm, PbS – 342nm, Ni_7S_6 – 407nm)
- Emission spectra of all the nanoparticles showed maxima characteristics of large band gap semiconductors (CdS – 418nm, Co_3S_4 – 380nm, PbS – 393nm, Ni_7S_6 – 473nm)
- X-ray photoelectron spectroscopic analyses confirmed the presence of corresponding elements in the as-synthesized nanoparticles

c. Conjugation of nanoparticles with glycopeptides:

- CdS and CdSe nanoparticles synthesized using enzymes were conjugated with bi-/tri-antennary glycopeptides using a modified EDC mediated coupling method
- The nanoparticles-glycopeptide conjugates were purified using size exclusion chromatography
- The emission maxima of CdSe-glycopeptides conjugates (CdSe-bi-antennary glycopeptide – 443 nm and CdSe-tri-antennary glycopeptides – 437 nm) showed blue-shifts with respect to the bare CdSe nanoparticles (454nm). But little or no shift (1-2nm) is observed in the case of CdS-glycopeptides conjugates

ii. Significance of the current investigation

Nanomaterials have attracted lots of attention because of the novel properties associated with the decrease in size of the material. In order to realise the full potential of nanomaterials with tailor-made properties needs to be produced. Controlled production of nanomaterials involves a wide range of techniques that can be classified into three basic approaches viz. physical, chemical and biological methods. Physical and chemical methods are characterized by high efficiency and specificity. On the other hand, both of these approaches require sophisticated instrumentations, involve harsh conditions such as high temperature and pressure, utilise toxic chemicals and produce toxic wastes. Hence, the need for alternative synthetic approaches that over-comes these draw-backs without compromising the end-products is imperative. The use of biological entities such as microbes that function under ambient conditions has been considered a good alternative for the current methods of controlled synthesis of nanomaterials. But their inherent complexity of the synthetic machinery and/or the factors responsible over-shadows their ability to replace ‘harsh’ synthetic methods. Hence, enzyme mediated synthesis of nanomaterials gains importance. Enzyme mediated synthesis of nanomaterials works on similar principles of the physical and chemical methods but function under ambient conditions. In general, reductase enzymes involved in the synthesis of nanomaterials reduces the precursor(s) resulting in the synthesis of nanomaterials. The careful selection of template molecules produces the end-products of defined shapes and sizes.

Enzyme mediated controlled synthesis of nanomaterials possess the following advantages:

- ✓ Require ambient conditions – majority of the enzymes require ambient temperature and pressure
- ✓ Show high specificity – enzymes are substrates specific
- ✓ Economical and scalable – enzymes can be produced in large scale
- ✓ Versatile – the capping molecules can be replaced with any potential molecule

iii. Scope and future prospects

Enzyme mediated synthesis of nanomaterials has developed as a potential alternative strategy for hazardous synthetic methods. Currently, this method experiences short-comings that need to be rectified before utilising it for large scale applications. Molecular biological approaches to enhance and/or alter the efficiency and specificity of enzymes might have a positive impact on the utility of this method. Elucidation of mechanism of synthesis of nanomaterials using enzymes and the role of synthetic molecules including peptides would open up lots of opportunities for this method in the production of nanomaterials of complex shapes and sizes and with precise properties suited for various applications. An interdisciplinary approach spanning in-vitro, in-vivo and in-silico approaches would provide us with great deal of information to tap the full potential of this novel method. The study of surface properties of the biogenic nanomaterials (synthesized using enzymes and bound by capping peptide) would expand the utility of bio-synthesized nanomaterials. The utility of this method is currently confined to metals, metal sulphides and some oxides. The use of this method for the production of other oxides, nitrides and carbides would be exciting.

The use of fluorescent nanoparticles attached to individual biomolecules as tracers would help in the better understanding of the molecular processes underlying various biological processes. This might expand the opportunities available in the field of diagnostics, treatment and follow up of various medical complications.

ANNEXURE – I

List of publications

1. Extracellular Biosynthesis of CdSe quantum dots by the fungus, *Fusarium oxysporum* S. Anil Kumar, **Abu Ayoobul Ansary**, Absar Ahmad, M. I. Khan, **J. Biomed. Nanotechnol.** 3, 190-194 (**2007**)

2. CdS Quantum dots: In vitro synthesis, characterization and conjugation to plant lectins, **Abu Ayoobul Ansary**, S. Anil Kumar, Majid K. Abyaneh, Sulabha K. Kulkarni, M. V. Krishnasastry, Absar Ahmad and M. I. Khan, **J. Biomed. Nanotechnol.** 3, 406-413 (**2007**)

3. Carbon nanotube-modified sodium dodecyl sulfate–polyacrylamide gel electrophoresis for molecular weight determination of proteins, Meera Parthasarathy, Joyashish Debgupta, Bhalchandra Kakade, **Abu A. Ansary**, M. Islam Khan, Vijayamohanan K. Pillai, **Anal. Biochem.** 409 (2), 230–235 (**2011**)

4. In vitro enzyme mediated synthesis of metal sulfide nanoparticles: Control of particle size of CdS, Ni_7S_6, PbS, Co_3S_4 nanoparticles using synthetic peptides, **Abu A. Ansary**, Muhammed I. Khan, Sushama M. Gaikwad, **Sci. Adv. Mater.** (Accepted)

5. In vitro enzyme mediated synthesis of CdSe quantum dots: control of dot size using synthetic peptides. **Abu A. Ansary**, Muhammed I. Khan, Sushama M. Gaikwad (Manuscript under review)

ANNEXURE – II

Presentations

1. **Poster** presented at the **Eighth International conference on nanostructured materials** (Nano 2006). Indian Institute of Science, Bangalore, India, 20-25 August, 2006. "*In vitro* synthesis of different metal nanoparticles using the purified enzymes and proteins from *Fusarium oxysporum"*. S. Anil Kumar, **Abu Ayoobul Ansary**, Absar Ahmad and M. I. Khan

2. **Oral presentation** at International Interdisciplinary Science Conference, 2010, held at Jamia Millia Islamia, New Delhi, India, from Dec 3-5. "In vitro enzyme mediated syntheses of CdSe and metal sulfide quantum dots: Control of dot size using synthetic peptide", **Abu A. Ansary**, Sushama M. Gaikwad, Muhammed I. Khan